UNIVERSITA' DEGLI STUDI DI PADOVA

DIPARTIMENTO DI INGEGNERIA INDUSTRIALE

CORSO DI LAUREA MAGISTRALE IN INGEGNERIA ENERGETICA

YEARLY ENERGY ANALYSIS OF CO_2 REFRIGERATION SYSTEMS

Relatore: **prof. Davide Del Col**

Correlatore: **prof. Brian Elmegaard**

res. Martin Ryhl Kærn

eng. Kristian Fredslund

Alessio De Min

1084145

ANNO ACCADEMICO 2015-2016

To Mum and Dad

"There is a crank down in Apalachicola, Florida,
that thinks he can make ice by his machine
as good as God Almighty".

New York Globe, 1844.

Abstract

The present thesis was prepared at the Section of Thermal Energy, Department of Mechanical Engineering, Technical University of Denmark (DTU), during the Erasmus exchange program. During the last decades the refrigeration industry was involved in the increasing concern about the environmental aspect. Synthetic refrigerant like CFCs and HCFCs have been banned already from most of the industrialized countries because of the ozone depletion potential and the greenhouse effect. Since 2008 the European Union has started to phase out also HFCs. The necessity to replace these refrigerants has led research into other sustainable alternatives like natural refrigerants. Among these, carbon dioxide seems to be the most promising solution. The main disadvantage of CO_2 is its low critical point. This means that when the environment temperature is high the cycle has to work in transcritical operation, with higher losses and consequently lower performances. The purpose of this project is to study different solutions that can improve the COP of the system during the transcritical operation and see which one performs better from the yearly analysis point of view. The solutions taken into consideration are four: parallel compression, mechanical subcooling, cascade system and the use of an ejector to recover expansion work. In the first part of the project these systems are studied under fixed design conditions. In the second part the yearly analysis is performed using the off-design model of the cycles for two different Italian cities: Milan and Naples. At the end all the results are compared with a R404A cycle. The results show that the most promising solution is the cycle using the ejector combined with the parallel compression. This system is able to save 12.0% and 14.8% of energy during a year of operation in Milan and Naples respectively. The normal parallel compression cycle achieves good performances too, saving 8.8% and 11.0% of energy in the two cities, the mechanical subcooling follows with 7.6% and 10.1%.

Keywords: Refrigeration systems; Natural refrigerant; Carbon dioxide; CO_2; R744; Parallel compression; Mechanical subcooling; Cascade system; Ejector; Yearly energy analysis.

Sommario

La seguente tesi è stata preparata al Dipartimento di Ingegneria Meccanica della Denmark Technical University (DTU) grazie al programma di scambio Erasmus.
Durante gli ultimi decenni l'industria del freddo è stata scossa dal punto di vista normativo a causa della scoperta del danno ambientale che i fluidi sintetici possono arrecare al nostro pianeta se rilasciati in atmosfera. I refrigeranti come i CFC e gli HCFC sono già stati banditi dal commercio in gran parte dei paesi industrializzati a causa del loro potenziale di distruzione dell'ozono e dell'effetto serra. Dal 2008 l'Unione Europea ha emanato una serie di normative in modo da iniziare ad escludere dal mercato anche gli HFC. La necessità di sostituire questi refrigeranti sintetici ha condotto la ricerca a puntare il mirino su altre soluzioni più sostenibili come i refrigeranti naturali. Questa categoria comprende diversi fluidi tra i quali l'acqua, l'anidride carbonica, l'ammoniaca e gli idrocarburi. La CO_2 tra tutti sembra essere il fluido più promettente: è presente nell'atmosfera, è ininfiammabile, atossica, non provoca la distruzione dello strato di ozono, il suo coefficiente di effetto serra è minimo ed ha elevati rendimenti quando la temperatura esterna è inferiore a 25°C circa. Lo svantaggio principale della CO_2 è la bassa temperatura critica, il che significa che quando la temperatura esterna è alta il ciclo deve lavorare in condizioni transcritiche, con maggiori perdite durante il processo di *gas cooling* ed il processo di laminazione. L'obbiettivo di questo progetto è studiare diverse soluzioni che siano in grado di aumentare il COP del sistema durante il funzionamento in condizioni transcritiche e vedere quale tra queste è in grado di raggiungere il più alto grado di risparmio energetico sotto il punto di vista di un analisi annuale. Le soluzioni prese in considerazione sono quattro: la compressione parallela, con economizzatore e con sottoraffreddamento integrato, il sottoraffreddamento meccanico, il sistema a cascata e l'uso di un eiettore per recuperare il lavoro perso durante l'espansione, con e senza compressione parallela. I sistemi studiati sono dunque sei più il ciclo base. Nella prima parte della tesi i cicli sono modellati e studiati sotto condizioni di design fissate, in modo da poter ottimizzare i principali parametri e fare un primo confronto tra i vari sistemi. Nella seconda parte le ottimizzazioni effettuate sono utilizzate per scrivere i modelli in off-design con condizioni al contorno più specifiche. Come già accennato, il principale problema dei cicli utilizzanti CO_2 come fluido refrigerante è il basso rendimento quando operano ad alte temperature. L'analisi energetica annuale è dunque effettuata per due diverse città italiane: Milano, posta al nord e quindi con un clima più freddo, e Napoli, che si trova al sud ed ha una temperatura media più elevata. Per calcolare i risultati è stato utilizzato il *Test Reference Year (TRY)*, l'analisi è dunque su base oraria (8760 valori). Riguardo il carico frigorifero è stato preso in considerazione un supermercato di taglia

media con carico di picco pari a 100 kW.
I risultati mostrano che la soluzione migliore è il ciclo con eiettore combinato con la compressione parallela che, comparato con il ciclo base, permette di risparmiare il 12,0% e il 14,8% di energia nell'arco di un anno, a Milano e Napoli rispettivamente. La compressione parallela semplice raggiunge anch'essa buoni risultati con un risparmio del 8,8% e del 11,0%, seguita dal sottoraffreddamento meccanico con 7,6% e 10,1%. Il ciclo semplice con eiettore non raggiunge buoni risultati a causa di alcune restrizioni che non permettono di utilizzare il dispositivo se la temperatura è inferiore ai 25°C. Il sistema a cascata è sicuramente quello che raggiunge i COP più elevati quando si opera ad alte temperature, perde tutto il suo vantaggio però quando la temperatura esterna è inferiore ai 20°C. Siccome un impianto installato sia a Milano che Napoli lavora per molte ore durante l'anno al di sotto di questo valore, il sistema a cascata non è competitivo; lo potrebbe diventare nel caso in cui la temperatura di evaporazione vanga abbassata.
Nell'ultimo capitolo della tesi è riportato il confronto tra i sistemi ad anidride carbonica studiati e un ciclo base che utilizza R404A come fluido refrigerante. Viste le diverse caratteristiche di scambio termico dei due fluidi, che portano gli scambiatori di calore a lavorare con Δt differenti è stata eseguita un'analisi di sensibilità variando, per il ciclo a R404A, la temperatura di evaporazione e la differenza di temperatura tra aria e fluido al condensatore. I risultati mostrano che anche nelle condizioni più sfavorevoli il ciclo con eiettore e compressione parallela è in grado di utilizzare meno energia del ciclo a R404A durante il corso dell'anno. Le due appendici della tesi, A e B, riportano rispettivamente i testi dei modelli compilati con EES (Engineer Equation Solver) e due schemi per ogni sistema, uno che mostra il sistema mentre opera in condizioni subcritiche e l'altro in condizioni transcritiche, riportandone i parametri più importanti.

Parole chiave: Sistemi di refrigerazione; Refrigerante naturale; Anidride carbonica; CO_2; R744; Compressione parallela; Sottoraffreddamento meccanico; Sistema a cascata; Eiettore; Analisi energetica annuale.

Contents

Nomenclature

Abbreviations

2SG	Two suction groups
BS	Base cycle
CFC	Chlorofluorocarbon
CO2	Carbon dioxide
EERC	Ejector expansion refrigeration cycle
EES	Engineering Equation Solver
GWP	Global Warming Potential
HCFC	Hydrochlorofluorocarbon
HFC	Hydrofluorocarbon
HFO	Hydrofluoroolefin
IIR	International Insitute of Refrigeration
MS	Mechanical subcooling
ODP	Ozone Depletion Potential
PCE	Parallel compression economization
TEWI	Total Equivalent Warming Impact
TRY	Test Reference Year
VCRC	Vapour compression refrigeration cycle

Variables

COP	coefficient of performance	[-]
c_p	specific heat at constant pressure	[J/kgK]
Δt	temperature difference	[°C]
Δp	pressure difference	[bar]
Δh	specific enthalpy difference	[J/kg]
h	specific enthalpy	[J/kg]
$\dot{m}$	mass flow rate	[kg/s]
η	efficiency	[-]
p	pressure	[bar]
P	power	[W]
φ	mass ratio(sec. compressor ej. cycle)	[-]
q	specific heat	[J/kg]
r	mass ratio	[-]
s	specific entropy	[J/kgK]
t	temperature	[°C]
w	specific work	[J/kg]
x	quality	[-]
y	mass fraction	[-]

Subscripts

0	cooling effect
amb	ambient
av	average
c	compressor
CO2	CO_2 cycle
cond	condensation
d, diff	diffuser
dis	discharge
eco	economizer
ej	ejector
ev	evaporation
gc	gas cooler
in	inlet
is	isentropic
lift	lift
liq	liquid
m	mass or motive nozzle
main	main cycle
max	maximum
mix	mixing section
opt	optimal
out	outlet
r	real
s	suction nozzle
t	theoretical
sec	secondary cycle
sub	subcooling or subcooling cycle
sc	subcooler
tot	total
var	variation

1 Introduction

1.1 Background

During the last century the world energy consumption has been grown rapidly and is projected to keep increasing in the next decades. Nowadays the amount of energy used by the entire population is estimated around 12000 Mtep every year. Several studies have tried to figure out if this growth have an asymptote, but all of them have different results. Indeed different factors effect the energy consumption, like the population, the economy, the life behaviour and it is particularly challenging understand how these factors will alter the results. Nevertheless the world energy use is prospected to increase by 56% during the next 30 years [1], which is due, like mentioned above, to the quickly population growth and the rising of developing countries. Refrigeration industry is responsible for the 10-20% of the total consumption as estimate from the International Institute of Refrigeration [2]. Moreover it has been discovered that the chlorine substances used as refrigerant are very dangerous for the environment. For this reason during the last decades the refrigeration sector was forced to face some radical changes. CFCs (chlorofluorocarbons), invented in the 1930 by Thomas Midgley and then widely used as refrigerants because of the high performance that they can achieve, were discovered to be incredibly harmful for our planet in the middle of the 1980s. They are the main responsible for the ozone depletion phenomena and they also have an high global warming potential (GWP). GWP is an index that relates of a greenhouse gas to the CO_2 emission over 100 years period (for this reason CO_2 has unitary GWP). CFCs were replaced by HCFCs (hydrochlorofluorocarbons). Anyway this category still causes ozone depletion because of the atoms of chlorine inside the molecules and still increases the green house effect when released in the atmosphere. CFCs and HCFCs have been banned from all the industrialized countries that signed the Montreal Protocol (1987) and the subsequent updates [3]. These refrigerants are almost off the market nowadays and only their "brothers", the HFCs (hydrofluorocarbons), are trying to survive. Not having chlorine atoms they are not dangerous for the ozone layer but they still have an high GWP. The HFC refrigerants that were once excepted to be acceptable permanent replacement fluids are now target of political actions due to their impact to the climate change. They are included in the greenhouse gasses covered by the Kyoto Protocol(1997) and from 2008 the

European Union started to phase them out. The cold industry is now more than ever looking for new sustainable solutions able to replace the old refrigerants once for all. The solutions are two: using new chemical compounds, like HFOs (hydrofluoroolefins), with the risk that they will be banned in few years too, or focus the effort in natural refrigerants. Thus there is an increasing interest in technology based on the ecological natural refrigerants like air, water, noble gases, ammonia, hydrocarbon and carbon dioxide. Among all of these, carbon dioxide is the only non-flammable and non-toxic fluid that can operate in a vapour-compression cycle below 0°C. In the last 3 decades, for the reasons reported above, carbon dioxide (CO_2, R744) has been rediscovered and the interest about it of the cold industry is keep growing. As reported by Sharma et al., based on U.S. supermarkets, leakages of refrigerants are estimated between 3% and 35% of the charge [4]. The wide range is due to the fact that new and old equipment have very different performances. A leak of "traditional" refrigerant has a great impact on the environment, for this reason the direct impact is becoming more important every day. It is worth to remember that a refrigeration cycle has also an indirect impact. This secondary effect take into account the emissions of greenhouse gases during the production of the electricity needed by the cooling system in one year of operation. The TEWI index (Total Equivalent Warming Impact) includes both these two effect and is used for the environmental impact analysis of the refrigeration systems. Carbon dioxide has no ozone depletion potential and unitary global warming potential, it is safe, cheap and available as secondary product of many industrial processes. It also has very good properties for refrigeration applications. However, CO_2 has low critical temperature and its operating pressure is higher than traditional refrigerants. This means that the cycle could work for many hours during a year as transcritical, with more losses and consequently lower efficiency (see section 1.4). The purpose of this project is to study some possible solutions able to increase the performances of the basic 1-stage vapour compression CO_2 refrigeration cycle during a year of operation, focusing the effort on improve the system especially when it is working in hot climates condition. The improved system considered are four: parallel compression, mechanical subcooling, cascade system and the use of an ejector to recover the expansion work. After a brief introduction about history and proprieties of carbon dioxide as refrigerant, the above mentioned systems will be modelled and studied. In the first part all the different cycles are presented under fixed design conditions in order to understand their behaviour when applied in hot climate conditions. Some assumptions will be made to simplified the analysis. The second part is the main part of the project and it is about the yearly analysis of the systems. The design conditions study of a certain cycle give important hints about its behaviour under specific boundaries. Anyway a refrigeration system can face very different working conditions along one year of operation. In order to follow these changing, off design models will be made with more accurate assumptions. In the end a comparison with a R404A refrigeration cycle will be presented. The models of each cycle have been made with the software EES (Engineering Equation Solver)[5]. This software bases its CO_2 calculations on the fundamental equation of state provided by Span and Wagner [6]. The models used for the yearly analysis are proposed in Appendix A. Appendix B shows how the most important variables of the studied cycles change passing from a subcrtitical working condition to a supercritical one.

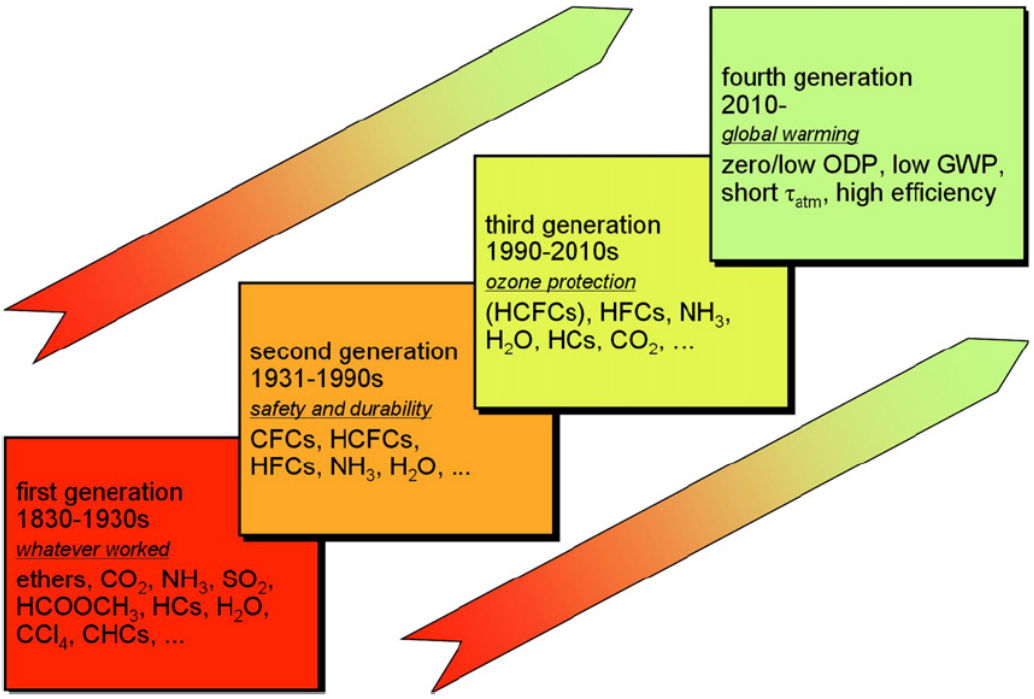

Figure 1.1 – Refrigerants progression [8].

1.2 History of CO_2

Using as guideline the study of Pearson [7] a brief history of CO_2 is here presented. Before that fig.1.1, proposed by Calm [8], is reported in order to have a simply overview on the history of the cold industry. It gives an interesting idea of the refrigerants used along the years, dividing them in four generations.

Carbon dioxide has been discovered in the 18^{th} century. During his experiment on magnesium carbonate, the Scottish physician James Black came to the discovery of CO_2. Anyway Black was not interested in refrigeration. It seems that the first person proposing a closed cycle for refrigeration has been Oliver Evans in 1805, but only 30 years later, in 1834, Evans's friend Jacob Persing was granted the British patent for his ethyl ether machine. Ethyl ether was the first refrigeration fluid proposed because readily manufactured and already uses as solvent in other application. After some trial with air and the discovery of the absorption refrigeration cycle carbon dioxide finally make a breakthrough in 1866, thanks to the work of the American Thaddeus Lowe that solve the problem of the compression of CO_2 adapting an hydrogen compressor used to fill military balloon for carbon dioxide. He was able to create ice using a close loop but he never patented his idea. In those years other refrigerants were more appreciated and the use of CO_2 in refrigeration systems was delayed because of the problem of the high working pressures. Carbon dioxide became a good option starting from 1887

when Raydt, Linde and Windhausen rediscovered it and started building the first cycles. From 1887 onwards, CO_2 gained favour as a refrigerant for marine applications due to the safety that it ensures. Ammonia was still the leading refrigerant for stationary application. From the beginning of the 20^{th} century ammonia started to generate some safety concerns, so the companies started to think different solutions to make the systems safer. One of these solution was proposed by the Frick Company in 1932. They started installing cascade systems with ammonia for the high temperature loop and CO_2 for the low temperature loop. Using a cascade system permitted also to avoid the CO_2 cycle to work in transcritical mode. Nevertheless carbon dioxide was not able to reverse the leadership of ammonia because of its higher efficiencies. From the middle of the 20th century carbon dioxide was completely abandoned due to the appearance of the CFCs in the market. In few years these synthetic fluids removed all the other refrigerants from the cold industry. They had the efficiency and flexibility of ammonia with the safety of carbon dioxide. Moreover in those years new compressors running at higher speed were developed, making the systems smaller, cheaper and easier to maintain. CO_2 is having only now a real change to reach a leadership position in the market. In fact from the end of the 20th century the cold industry had to face the problem of the environmental impact of the synthetic refrigerants and had to look to new, or old, environmental friendly solutions. The pioneer of the reappraisal of carbon dioxide was Gustav Lorentzen ([9],[10]), that in 1990 published a patent application for a transcritical cycle using CO_2 for automotive application [11]. He started also organizing the IIR conferences about new environmental friendly refrigerants. All the papers and the works presented at these conferences pulled the carbon dioxide reborn as refrigerant.

1.3 Properties of CO_2

Nowadays the proprieties of the carbon dioxide are well known and they are quite different from the conventional refrigerants. In this section the most important features of CO_2 are presented and commented using as base the paper of Kim et al. [12]. Carbon dioxide is colorless and odorless gas presents in the atmosphere with a concentration of about 0.04% by volume. This natural chemical compound is composed by a carbon atom covalent double bonded to two oxygen atoms. CO_2 is then a natural refrigerant, non-flammable, non-toxic, with no ozone depletion potential and negligible global warming potential. This features are important because made it a very safe fluid. Fig.1.2 shows the phase diagram of CO_2. Critical temperature and pressure are respectively 31.1°C and 73.8 bar and the saturation pressure at 0°C is 35 bar. These working pressures are much higher than those for the conventional refrigerants. Above the critical temperature is not possible to transfer heat to the ambient by condensation as in a traditional vapour compression cycle, but it has to be used a gas cooler. In this case the heat transfer process occurs in the supercritical region where pressure and temperature are not coupled and the pressure can be regulated independently in order to optimize the working condition of the system. Fig.1.3 and fig.1.4 present the t-s and the p-h diagram respectively. Fig.1.5 show the vapour pressure curve of CO_2 compared

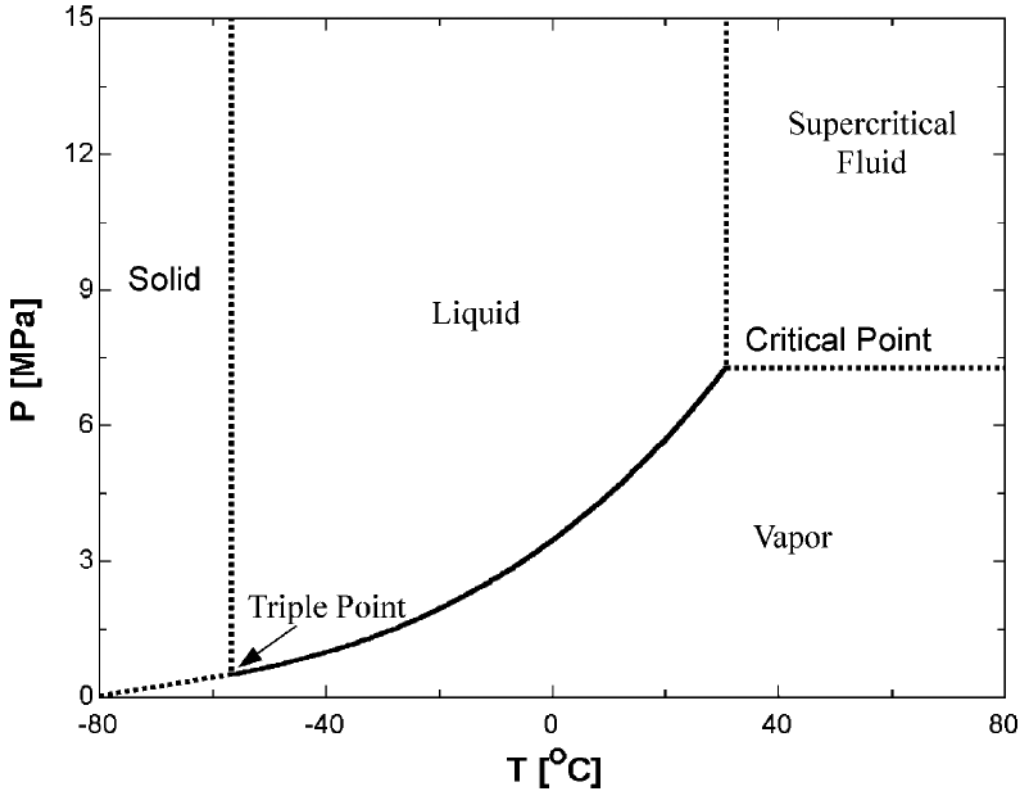

Figure 1.2 – Phase diagram of CO_2 [12].

to other fluids. It is possible to see that the vapour pressure of CO_2 is much higher than the other refrigerants and so the steepness of the curve. This means that the temperature change associated with a pressure drop in the evaporator is smaller compared with the other fluids. Carbon dioxide presents also an higher volumetric refrigeration capacity compared to the traditional refrigerants as shown in fig.1.6. This is due to the high vapour density, as the volumetric refrigeration capacity is defined as the product between the latent heat of evaporation and the vapour density. Fig.1.7 and fig.1.8 present the density of CO_2 as function of temperature and the ratio of liquid to vapour density for different fluids. From the first figure is possible to observe that the density of CO_2 changes quickly close to the critical point (this behaviour could be observed also for the other proprieties [12]). The second one shows that the density ratio of CO_2 is smaller than the other refrigerants, this means a more homogeneous two phase flow. This factor is important since it determines the flow pattern and consequently the heat transfer coefficient [13]. Also the thermal conductivity of CO_2 is better compared to other refrigerants. Citing Kim et al. [12]: *" In summary the thermodynamic and transport properties of CO_2 seem to be favourable in terms of heat transfer and pressure drop, compared to other typical refrigerants".*

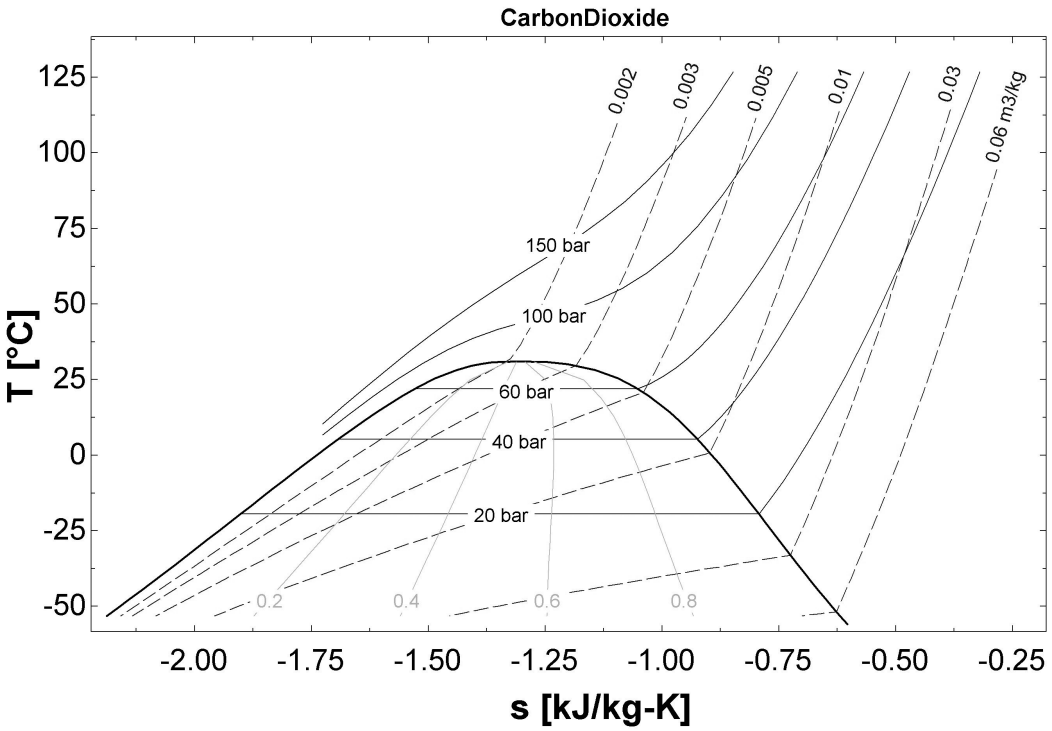

Figure 1.3 – Temperature-entropy diagram of CO_2.

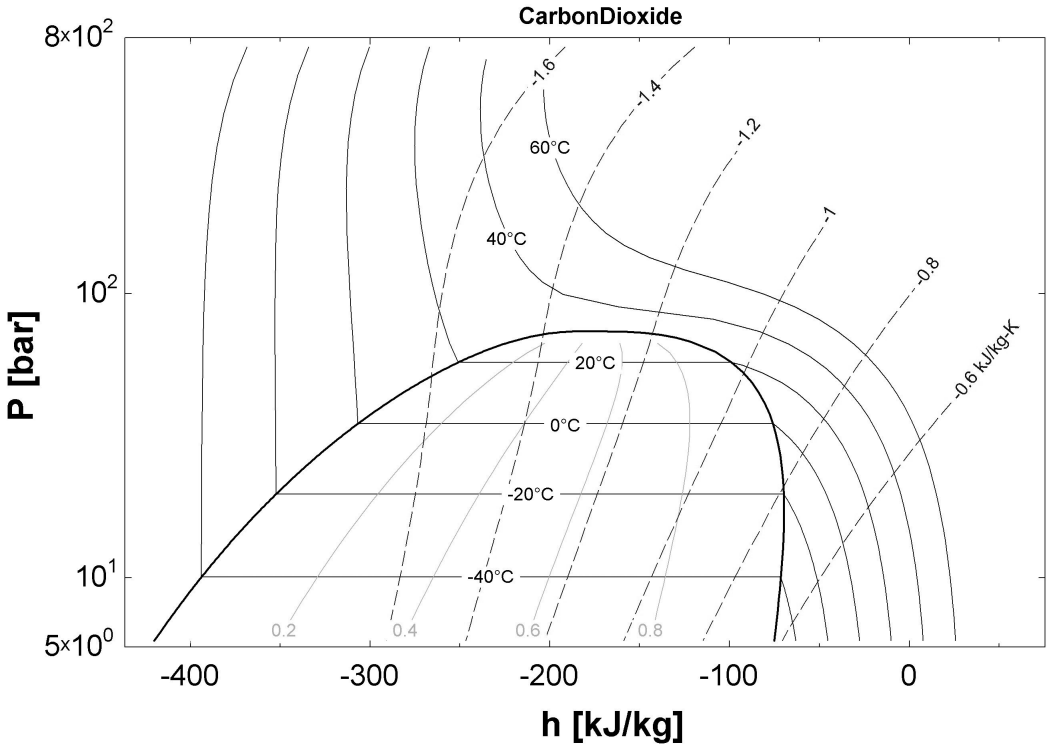

Figure 1.4 – Pressure-enthalpy diagram of CO_2.

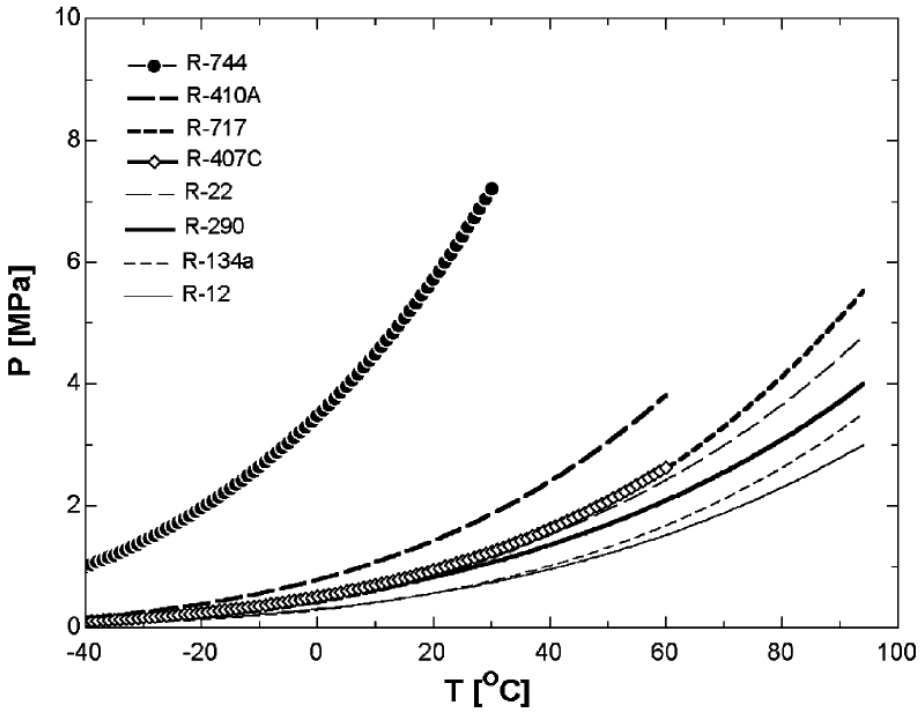

Figure 1.5 – Vapour pressure for different refrigerants [12].

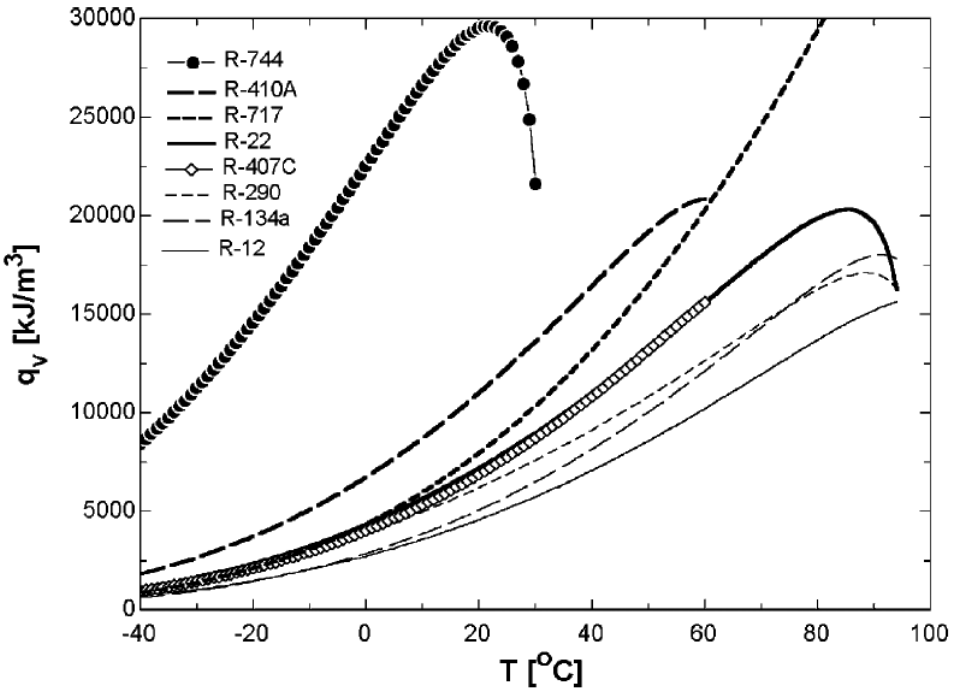

Figure 1.6 – Volumetric refrigeration capacity for different refrigerants [12].

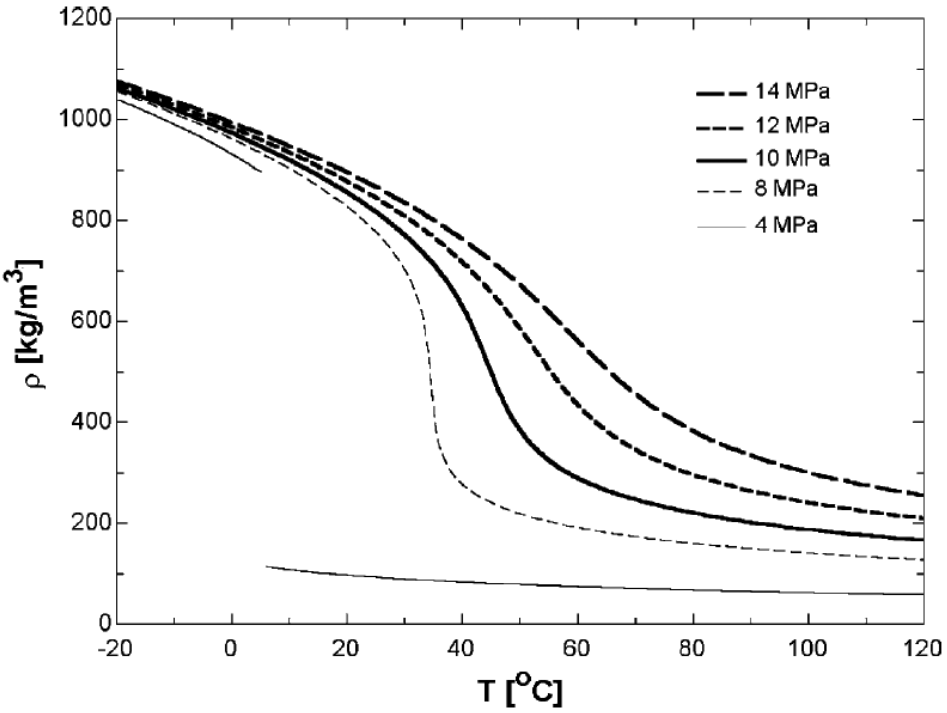

Figure 1.7 – Density of CO_2 as function of temperature for different pressure levels [12].

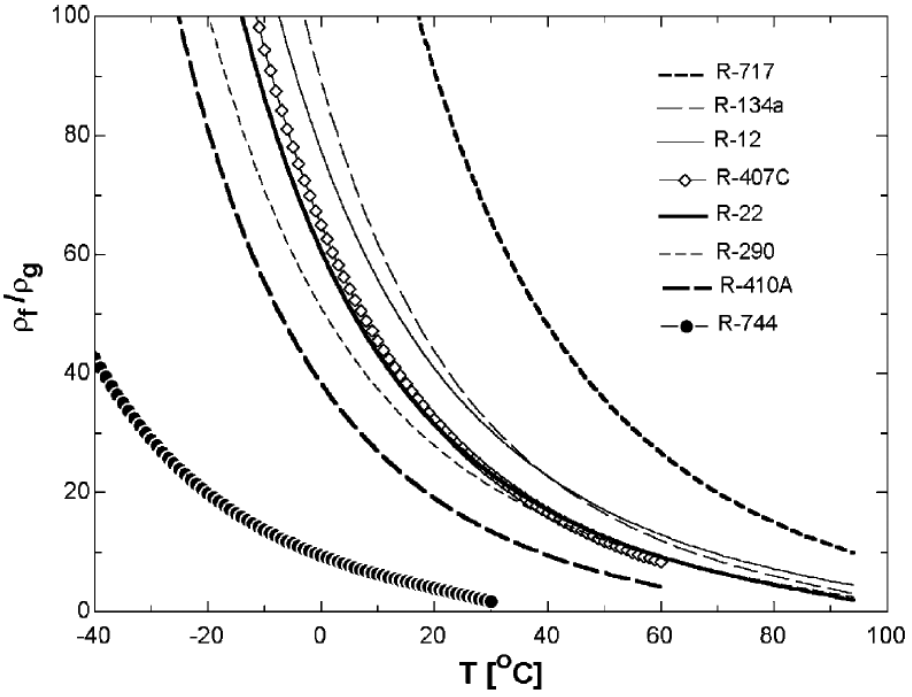

Figure 1.8 – Ratio of liquid to vapour density at saturation for different refrigerants [12].

1.4 CO_2 as refrigerant

The carbon dioxide 1-stage vapour compression cycle is nowadays well known in all his features and components and it is widely used, mostly in northern Europe where the climate conditions are favourable. The studies in the last years focused on how to improve the performance of this system also when operating in hot climates. As seen in the previous section the more remarkable property of CO_2 compared to the conventional refrigerants is the low critical temperature. For this reason the heat rejection will in most cases take place in supercritical region. This cause an higher discharge pressure and it makes the cycle working as transcritical. Transcritical operation means that the evaporation temperature is below the critical point, while the heat rejection temperatures are over it. Some peculiarities of transcritical cycles are here discussed.

1.4.1 Transcritical operation

Fig.1.9 shows the p-h diagram of a CO_2 transcritical cycle. During operation at high ambient temperature the CO_2 systems will work in transcritical conditions. In this case the heat rejection at the high-side pressure will not take place in a condenser, but in a gas cooler at supercritical pressure, therefore above the critical point where no saturation conditions exist and temperature and pressure are independent. The main consequence of this is the existence of an optimal gas cooler pressure. At fixed evaporative temperature, in conventional systems the compressor work and consequently the COP depend on the discharge pressure: higher the discharge pressure lower the performance. The behaviour is quite different in a transcritical cycle. Looking at fig.1.9 is possible to see that varying the discharge pressure has two different effects: increase the specific refrigerating capacity (q_0) and increase the the specific compressor work (w). The COP is defined as the ratio of q_0 on w. Consequently, increasing the discharge pressure, the COP reaches a maximum when the added capacity no longer compensates for the additional work of compression. In the next chapters this optimal pressure will be calculated for all the different systems, however due to the different operation mode, the value will be different in each case. Regarding the losses, like reported by Kim et al.: *"the transcritical cycle suffers from a larger thermodynamic losses than an 'ordinary' cycle with condensation"*[12]. This is due to the higher average temperature of heat rejection and the larger throttling loss. The high average temperature is explained by the use of a gas-cooler instead of a condenser. The throttling loss depends on the ratio $c_{p,liq}/e$. CO_2 specific heat is high and the evaporation enthalpy is low working near the critical point, then the throttling loss become large. Fig.1.10 shows the additional thermodynamic losses of the CO_2 cycle compared with the R134a one, assuming equal minimum rejecting temperature and equal evaporating temperature.

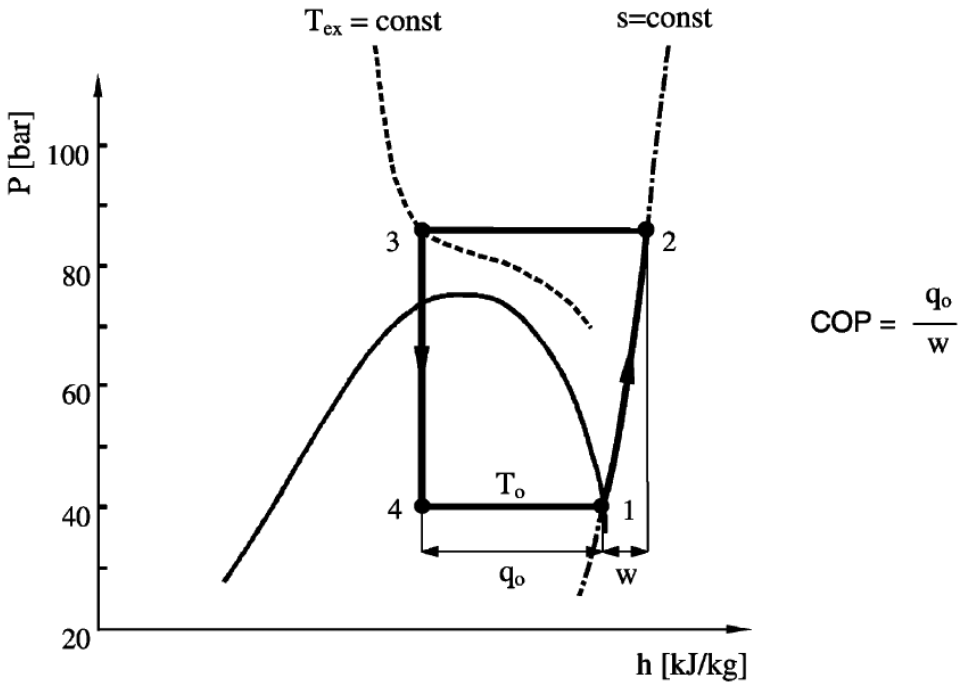

Figure 1.9 – Transcrtitical cycle: p-h diagram [12].

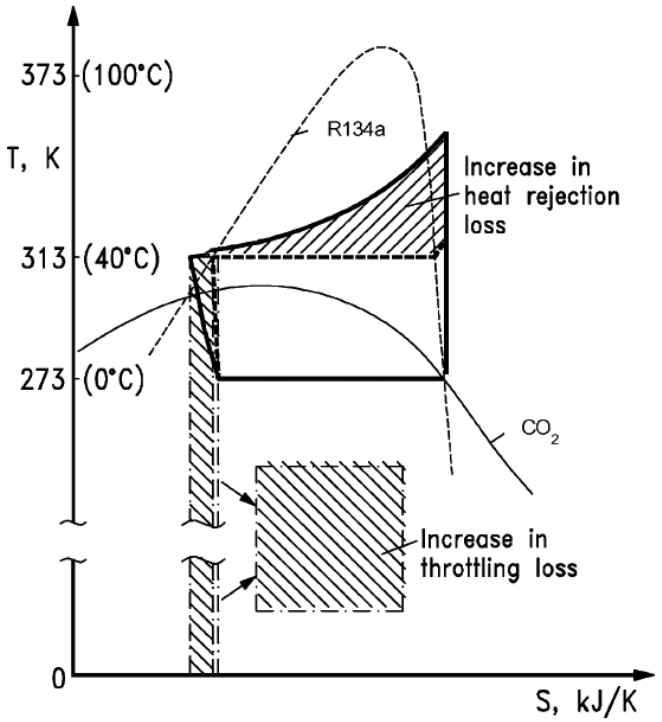

Figure 1.10 – Comparison of thermodynamic cycles for R134a and CO_2 [12].

2 Design conditions

In this section different solutions are presented and then compared in order to understand which one has the better performance during transcritical operation. As a reference for the comparison the base CO_2 cycle is used. The purpose is to improve the performance of this system, especially when working with high ambient temperature. The four proposed solutions are: parallel compression, mechanical subcooling, cascade system and the use of an ejector to recover the expansion work. In the parallel compression two different designs will be studied, the simple one with an economization and a second one with the subcooling integrated. For the ejector cycle after using the normal one, a different solution with two suction groups will be studied. Three different fluids will be used for the mechanical subcooling and for the secondary loop of the cascade system, the fluids are: R404A, R134a and propane. After the presentation of the boundary conditions needed for the modelling, all the cycles will be presented with their features and some specific results will be discussed. In the next chapter the overall results will be presented and the comparison of all of them will be made with the same outdoor conditions. The models of each cycle have been made with the software EES (Engineering Equation Solver, [5]) and are reported in Appendix A. The results presented come from different simulations and have been collected in separate sheets where it has been possible to postprocess them.

2.1 Boundary conditions

The different cycles are modelled in the same way in order to compare them. With this aim some boundary conditions are required. These conditions are presented below, the assumptions are made specifically for the design conditions modelling of the systems, with the purpose of comparing different system for the same conditions. The entire systems have been modelled based on mass and energy balance of every single component. The following assumptions have been made for the analysis:

- Steady-state processes.

- Isenthalpic expansion.
- Pressure drop and heat losses are neglected.
- Constant isentropic efficiency for the compressor is assumed to be 0.6 for all the cycles and all the conditions.
- The processes in the heat exchangers are considered isobaric.
- The evaporation temperature is set to -2°C, however some simulations with different value will be made in order to understand how this value effect the performance of the cycle.
- The ambient temperature is set to 42.5°C. This choice has been made with the purpose of simulating very hot ambient conditions; reason for this is to use the Italian climate as the worst-case scenario. This temperature will be used to compare the cycle in the next chapter, while in this one the behavior of the system will be studied also for different conditions. In order to model the cycle for the off-design, it is necessary to understand how to optimize the specific parameters of the systems also for different ambient temperature.
- The gas cooler is assumed as air-cooled and the outlet temperature is set to be 5°C higher than the ambient temperature.
- The fluid state at the outlet of the evaporator is considered saturated vapor.
- Superheat before the compressor is neglected.
- Separation and mixing process are isobaric.
- Fan power is neglected because it was assumed to be equal for all the systems.
- The cooling capacity is fixed to 100kW for all the cycles and all the operative conditions. The choice is quite random and is useful only to compare the cycles with the same value. For example Girotto et al. used for the same analysis a value of 120kW [14], while Sawalha et al. used an higher value, i.e. 230kW [15]. In this first part of the project the cooling capacity is supposed to be constant also if the ambient temperature is varying. This is not a real assumption, because the lower the ambient temperature is the lower the dispersion and consequently the cooling capacity. A more accurate load profile will be used for the yearly analysis with the aim to model a system as close as possible to a real one.

Other assumptions will be made in the next chapters when required specifically to each system. Every section will be divided in three parts: the description of the system, the system analysis and in the end the results preceded by a table that summarized the assumptions made for every cycle.

2.2 Base CO_2 refrigeration cycle

In this chapter the base CO_2 transcritical cycle will be presented and discussed. When using the term base cycle the meaning is the 1-stage vapour-compression refrigeration cycle. This cycle is the simpler cycle and it will be used as a reference to the comparison for all the other systems. Before the presentation of the results and the comparison, all the different systems will be presented in order to understand all the specific features.

2.2.1 Description of the system

The 1-stage vapour compression refrigeration cycle is made up from four main components, where four different transformations happen. Fig.2.1 shows the layout of the system, the components are respectively the compressor in the right, the gas cooler in the top, the throttling valve in the left and the evaporator in the bottom. In all these components a different process takes place. The evaporator make possible the heat exchange with the low temperature heat sink, the ambient that have to be maintained at a certain temperature, and the gas cooler with the high temperature heat sink, the external environment. Compressor and throttling valve maintain an high pressure side and a low pressure side. The evaporator is a container or a pipe system where the CO_2 vaporizes at low pressure and temperature, this temperature has to be below the temperature of the air in the refrigerated space. The latent heat necessary for this aim is thus taken from this space. Fig.2.2 shows the logp-h diagram according with Fig.2.1. It is possible to see at the outlet of the evaporator (state 1) that the fluid is saturated vapor, usually the vapor will continue to absorb heat from the surrounding and become slightly superheated before leaving the heat exchangers, but to make the model simpler the superheat is considered nil. The fluid enters the compressor and reaches state 2 at the high-pressure side, the compression is supposed to be non-isentropic. The high pressure is not a function of the temperature like in the subcritical cycle therefore it will be possible to optimize it to reach the best performance. From state 2 the fluid is cooled in the gas-cooler (state 2-3), from there the fluid will expand in the throttling valve (state 3-4). The expansion process combined with the high temperature heat exchange are the main source of losses in the transcritical cycle. Moreover, working in transcritical mode means work at high pressures and then lower compressor efficiency, so also the compression process could be improved. The purpose of the modified cycles that will be presented is to reduce these losses. In the end, after the expansion device, the fluid enters the evaporator (state 3).

For the base cycle the performance of the system are simply given as:

$$COP = \frac{(h_1 - h_4)}{(h_2 - h_1)} \tag{2.1}$$

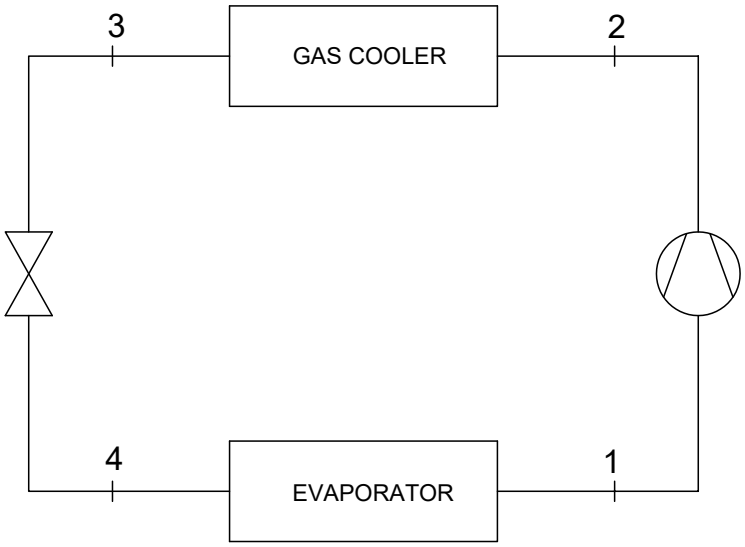

Figure 2.1 – Layout of the base CO_2 cycle.

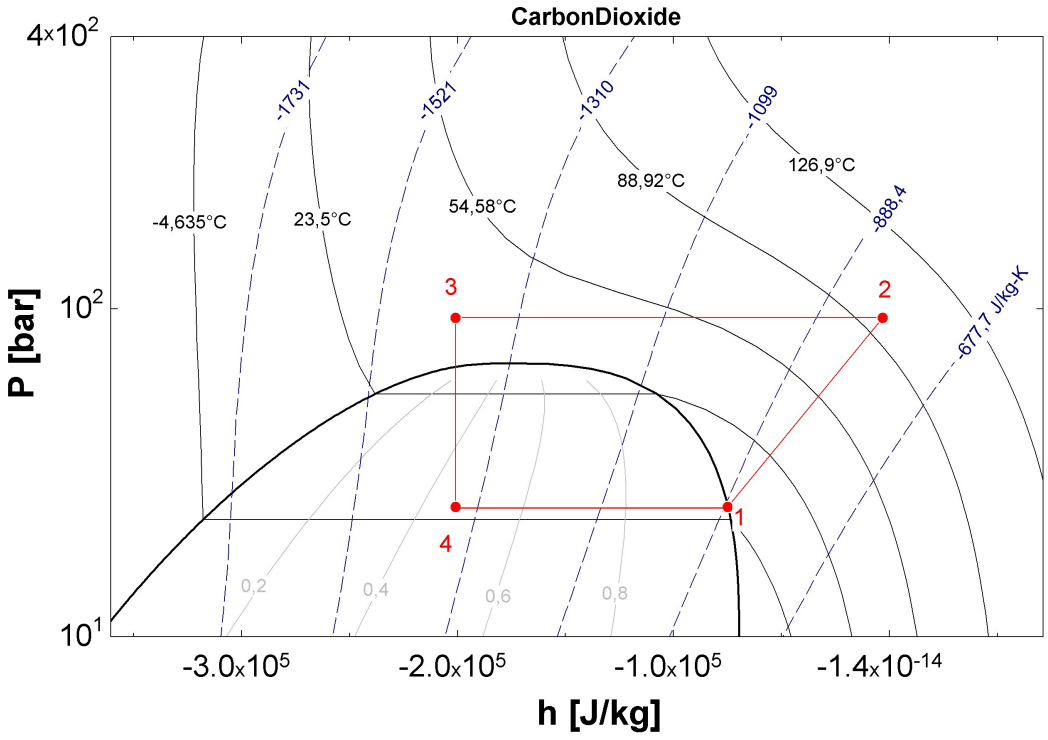

Figure 2.2 – logp-h diagram of the base CO_2 cycle.

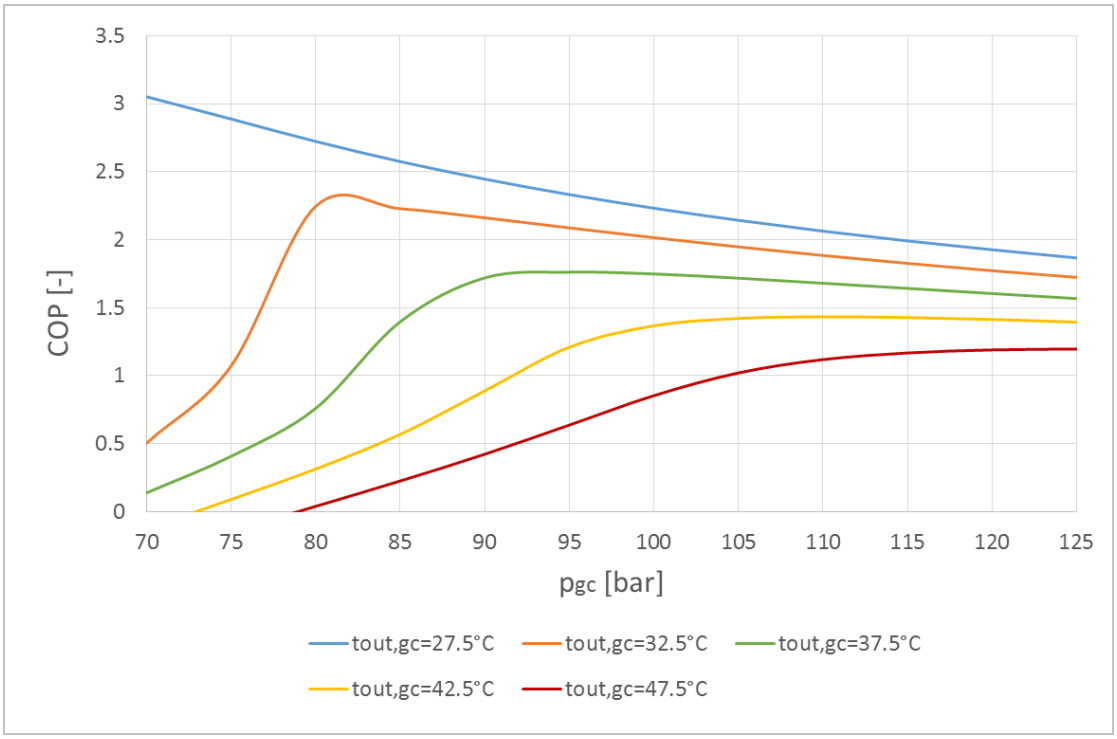

Figure 2.3 – COP vs gas-cooler pressure for different gas-cooler outlet temperatures (t_{ev}=-2°C).

2.2.2 System analysis

As mentioned in the beginning of this chapter all the cycle will be studied with the same boundary conditions. Despite what the differences are in the systems, it is necessary to understand how it is possible to achieve the best performance for each of them. Considering the base cycle the only parameter that has to be optimized is the gas-cooler pressure. Before the optimization, it is worth to see how the COP varies in function of this pressure. Fig.2.3 shows the COP in function of the gas-cooler pressure for different gas-cooler outlet temperature. It is possible to see that for every outlet temperature there is an optimal pressure in the way to maximize the COP. This optimal pressure increase when the gas-cooler outlet temperature increases, then when the ambient temperature increases.

Using the EES min/max function it has been possible to find the optimal pressure for the different working conditions. Fig.2.4 shows the pressure as function of the gas-cooler outlet temperature, while the evaporative temperature is kept constant at -2°C. As expected the optimal pressure increase with the temperature. Fig.2.5 shows instead the pressure as function of the evaporative temperature, while the ambient temperature is kept constant at 42.5°C, this means that the gas-cooler outlet temperature is 47.5°C. In this case the lower the evaporative temperature the higher the optimal gas-cooler pressure.

The results that have been obtained are compared with the correlation for the optimal heat

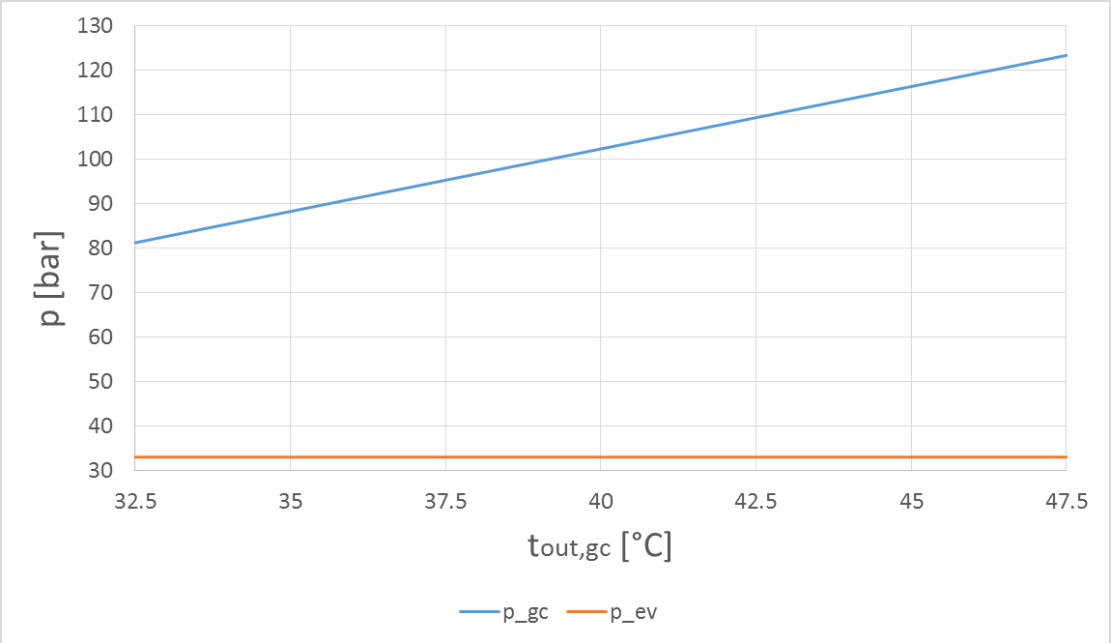

Figure 2.4 – Optimal gas-cooler pressure in function of the gas-cooler outlet temperature (t_{ev}=-2°C).

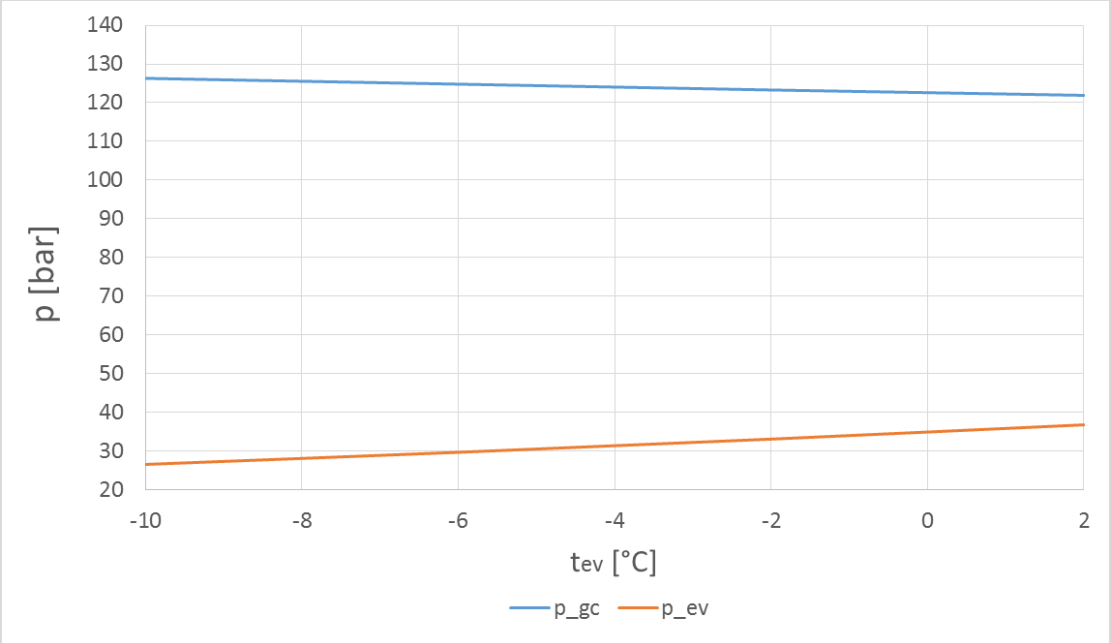

Figure 2.5 – Optimal gas-cooler pressure in function of the evaporation temperature (t_{amb}=-42.5°C).

rejection pressure proposed by Liao et al. [16], another correlation is proposed by Ge et al.[17]. The equation is expressed in terms of evaporation temperature and gas-cooler outlet temperature and is here reported, the temperatures are in °C and the pressure is in bar.

$$p_{gc,opt} = (2.778 - 0.0157 \cdot t_{ev}) \cdot t_{gc,out} + (0.381 \cdot t_{ev} - 9.34) \tag{2.2}$$

The results found using this equation and the results obtained with the EES min/max function are exactly the same.

2.2.3 Results

Before presenting the results, the assumptions that have been made are summarized in the following table.

Evaporative temperature	-2°C
Gas-cooler pressure	optimized
Gas-cooler approach temperature difference	5°C
Subcooling and superheating	0°C
Compressor isentropic efficiency	0.6
Fan power	neglected
Cooling capacity	100 kW

Tables 2.1 and 2.2 show the main parameters of the cycle for different working conditions.

t_{ev}	t_{amb}	$t_{out,gc}$	$p_{opt,gc}$	COP	Pc
°C	°C	°C	bar	-	kW
-2	27.5	32.5	81.2	2.252	44.4
	32.5	37.5	95.25	1.761	56.8
	37.5	42.5	109.3	1.433	69.8
	42.5	47.5	123.3	1.195	83.7

Table 2.1 – Base cycle results: different ambient temperature.

t_{amb}	$t_{out,gc}$	t_{ev}	$p_{opt,gc}$	COP	Pc
°C	°C	°C	bar	-	kW
42.5	47.5	2	121.9	1.31	76.3
		-2	123.3	1.195	83.7
		-6	124.8	1.092	91.6
		-10	126.3	1.001	99.9

Table 2.2 – Base cycle results: different evaporation temperature.

2.3 Parallel compressor economization

A large number of cycle modification are possible to improve the COP of vapour compression refrigeration system. The main purpose of the modified cycle is to reduce the losses due to the throttling process. Parallel compression economization system (PCE) is one of the promising improvement techniques of vapour compression refrigeration cycle [18], where refrigerant vapour is compressed to supercritical discharge pressure in two separate streams, one coming from the evaporator and one coming from the separator or economizer. The main difference from the base cycle is the introduction of the separator, which makes it possible for the division of the throttling process into two stages. The effect of the separator is beneficial for the system because it prevents the flash vapour to enter into the evaporator, this mean a reduction of the compressor work and an increase of the refrigerant enthalpy difference in the evaporator due to the less refrigerant quality at the inlet of it, but also the need of a secondary compressor. In this section an optimization of the transcritical CO_2 cycle with PCE is carried out, it is important to know that in this case there are two parameters that can be optimized, the gas-cooler pressure and the economizer or intermediate pressure.

2.3.1 Description of the system

The flow diagram and the corresponding p-h diagram are showed in Fig.2.6 and Fig.2.7 respectively. After the gas-cooler (state 3) the fluid is expanded in the first expansion valve from gas-cooler pressure to economizer pressure. The two-phase fluid (state 4) is then separated in the economizer. The saturated liquid (state 5) is expanded again in the second expansion valve from the intermediate pressure to the evaporator pressure (state 5-6) and then sent in the evaporator to provide the cooling effect (state 6-1). The saturated vapour from the evaporator and the separator are then compressed with two different compressors to the states 2 and 8 respectively. After the compression the two different flows are mixed (state 9) and sent in the gas cooler where the rejection of the heat to the hot tank is achieved (state 9-3).

For unit total mass flow rate, the mass flow rate through the secondary compressor and the main compressor are x_4 and $1-x_4$ respectively, where x_4 is a function of pressure and specific enthalpy at state 4. The refrigerating effect of the evaporator is:

$$q_{ev} = (1-x_4)\cdot(h_1 - h_6) \tag{2.3}$$

The specific work input to the compressors:

$$w_c = (1-x_4)\cdot(h_2 - h1) + x_4\cdot(h_8 - h7) \tag{2.4}$$

In the end the performance of the system is given as:

$$COP = \frac{q_{ev}}{w_c} \tag{2.5}$$

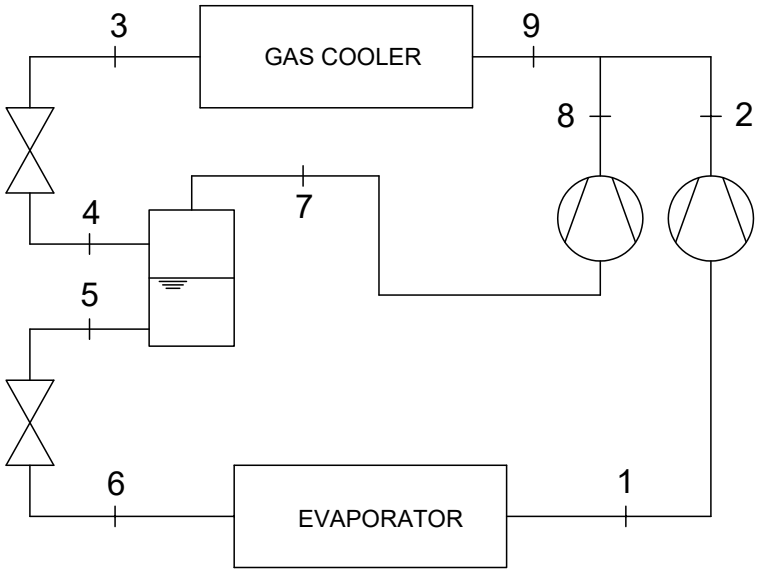

Figure 2.6 – Layout of the refrigeration cycle with parallel compression economization.

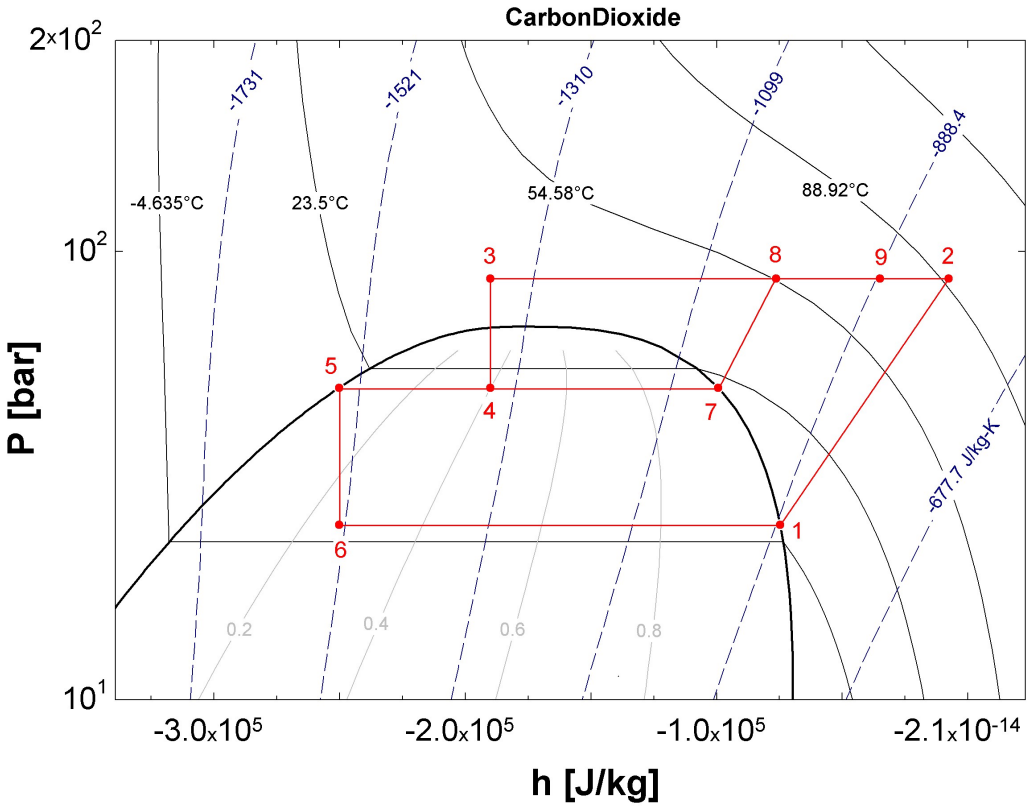

Figure 2.7 – logp-h diagram of the refrigeration cycle with parallel compression economization.

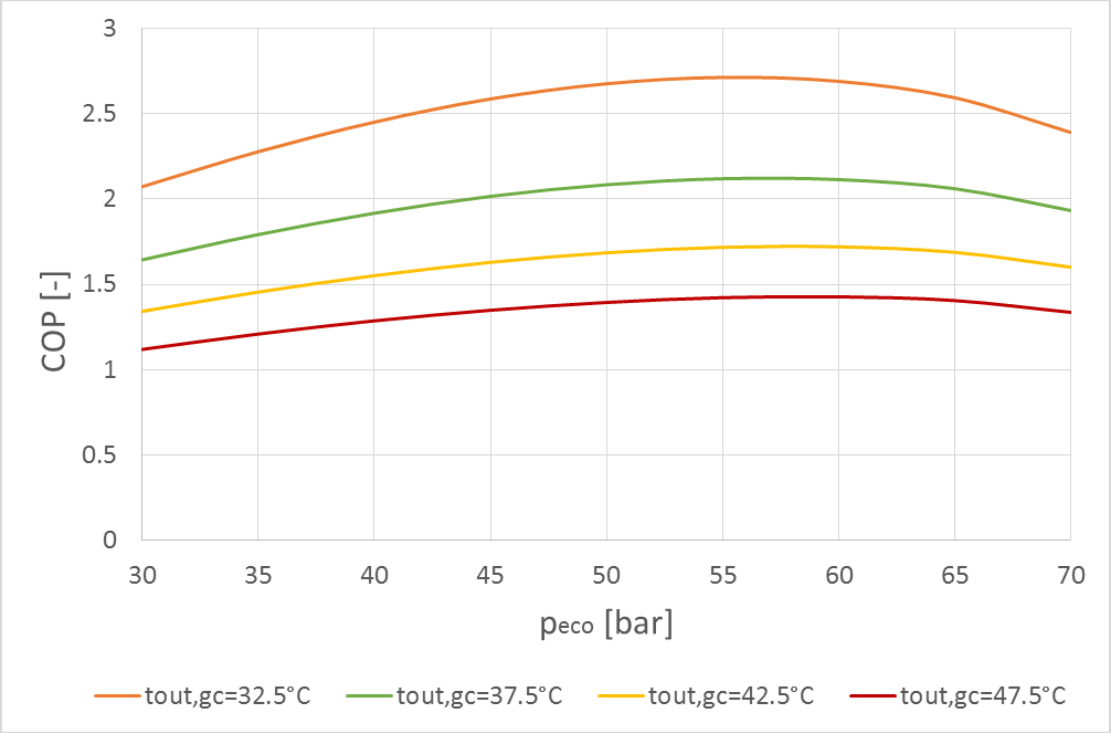

Figure 2.8 – COP vs economizer pressure for different gas-cooler outlet temperature (t_{ev}=-2°C).

2.3.2 System analysis

The operating condition of the system are the same as assumed for the base cycle according with the boundary conditions listed in chapter 2.1. It is also important to remember that separation and mixing processes are considered isobaric and adiabatic. As said in the previous section the PCE cycle works between three level of pressure: the evaporative pressure, the economizer pressure and the gas-cooler pressure. The first one is fixed by the evaporative temperature, while the intermediate pressure is an influential parameter to find the best performance along with the gas-cooler pressure. It is then necessary to optimize these two pressures simultaneously [19].

Fig. 2.8 shows the COP in function of the economizer pressure for different gas-cooler outlet temperature. It is possible to see that for each temperature there is a certain pressure where COP attains the maximum value. The same result has been reached also by Sarkar and Agrawal: *"existence of the optimum economizer pressure is mainly on account of the changing slope of the saturation curve"*[19]. Increasing the economizer pressure means to increase the quality at the inlet of the evaporator, then both the compressor work and the refrigeration effect decrease. On the other hand they increase when the economizer pressure is lower. According to Sarkar [18] it is possible to find the optimal condition when the compressor work is minimum and the effect on the cooling capacity is negligible. Using the EES min/max function with two degrees of freedom has been possible to find the optimal gas-cooler pressure and the optimal

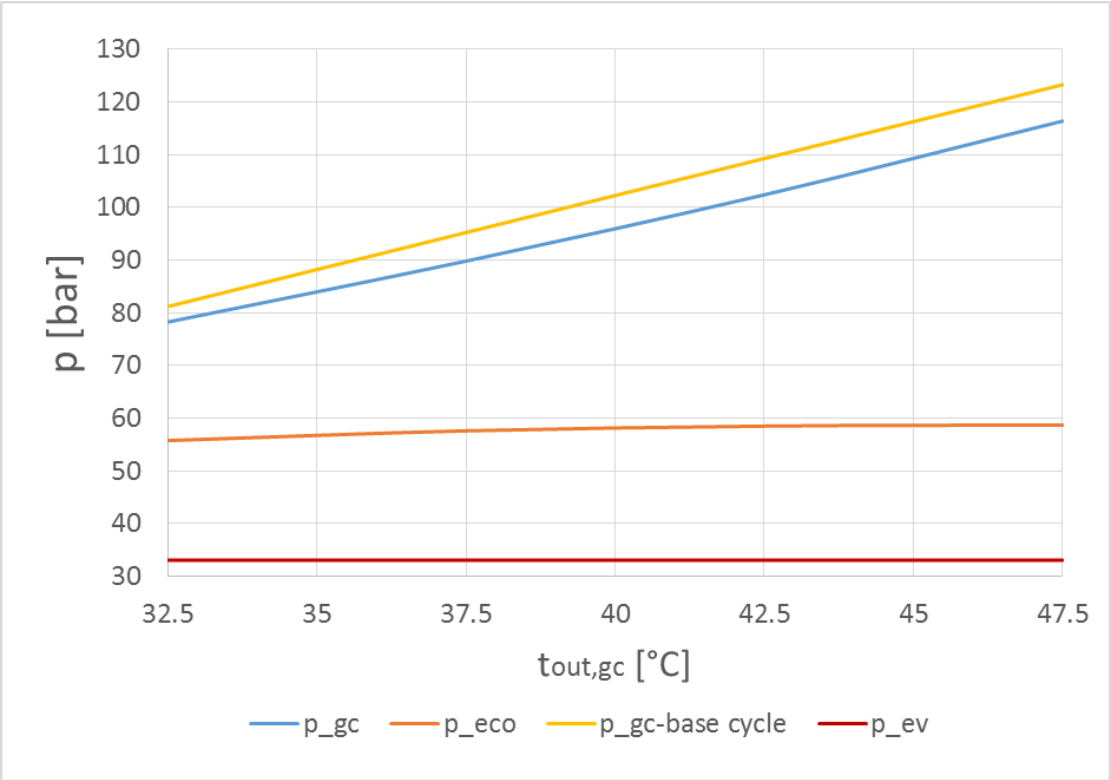

Figure 2.9 – Gas-cooler and economizer pressure vs gas-cooler outlet temperature (t_{ev}=-2°C).

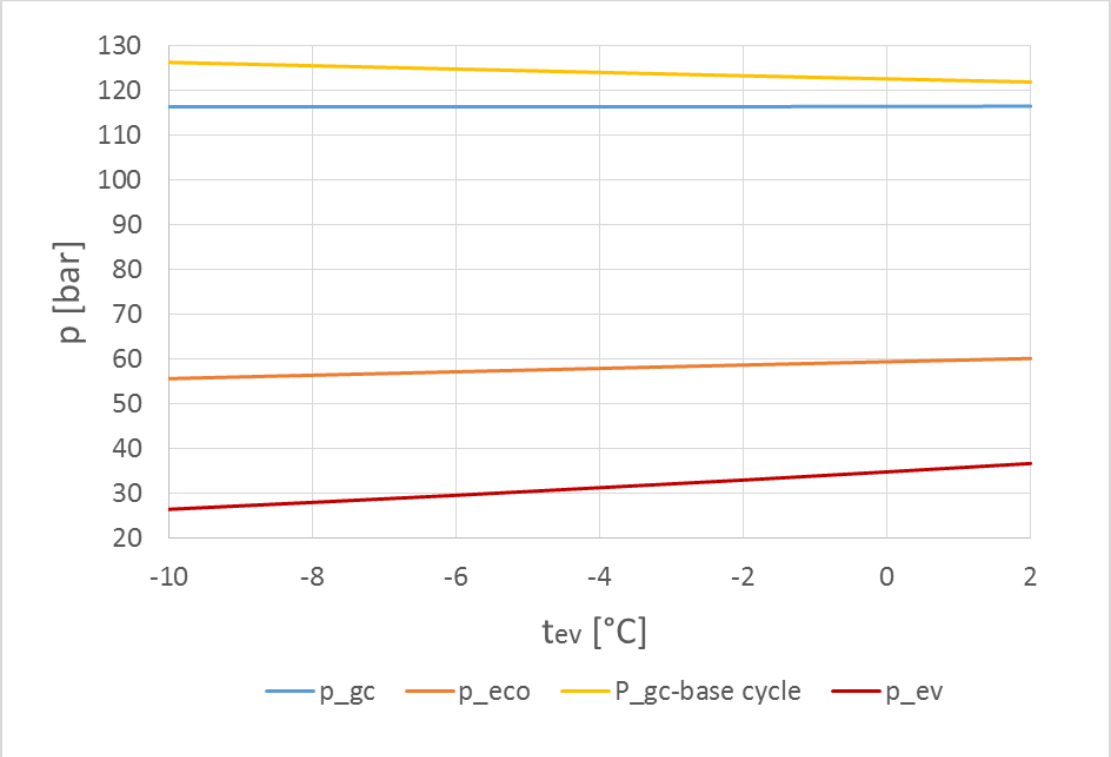

Figure 2.10 – Gas-cooler and economizer pressure vs evaporative temperature (t_{amb}=42.5°C).

economizer pressure in the same time for different working conditions. Fig.2.9 shows the gas-cooler and the economizer pressure against the gas-cooler outlet temperature, the results are also compared with the optimal gas-cooler pressure of the base cycle (yellow line). The graph shows that the gas-cooler pressure for the base cycle is always higher in comparison to the PCE cycle, this means that the parallel compressor economization is a useful technique to increase the performance as well as decreasing the gas-cooler outlet pressure and the discharge temperature. Fig.2.10 shows how the same pressures vary against the evaporative temperature (ambient temperature set to 42.5°C). It is possible to see that the gas-cooler pressure variation is almost nil, while the economizer pressure is decreasing going down with the evaporative temperature.

2.3.3 Results

Before presenting the results, the assumptions that have been made are summarized in the following table.

Evaporative temperature	-2°C
Gas-cooler pressure	optimized
Gas-cooler approach temperature difference	5°C
Economizer pressure	optimized
Subcooling and superheating	0°C
Compressor isentropic efficiency	0.6
Fan power	neglected
Cooling capacity	100 kW

Tables 2.3 and 2.4 show the main parameters of the cycle for different working conditions.

t_{ev}	t_{amb}	$t_{out,gc}$	$p_{opt,gc}$	$p_{opt,eco}$	COP	Pc
°C	°C	°C	bar	bar	-	kW
-2	27.5	32.5	78.26	55.75	2.714	36.8
	32.5	37.5	89.82	57.6	2.126	47.0
	37.5	42.5	102.4	58.5	1.724	58.0
	42.5	47.5	116.4	58.71	1.428	70.0

Table 2.3 – PCE results: different ambient temperature.

t_{amb}	$t_{out,gc}$	t_{ev}	$p_{opt,gc}$	$p_{opt,eco}$	COP	Pc
°C	°C	°C	bar	bar	-	kW
42.5	47.5	2	116.5	60.17	1.535	65.1
		-2	116.4	58.71	1.428	70.0
		-6	116.4	57.2	1.331	75.1
		-10	116.4	55.67	1.242	80.5

Table 2.4 – PCE results: different evaporation temperature.

2.4 Parallel compressor economization with recooler

The performance of the base CO_2 refrigeration system can be significantly improved by further cooling the refrigerant after the gas-cooler. Parallel compressor economization cycle with recooler, also called parallel compression cycle with integrated subcooling, is one of the possibilities to achieve this goal. Thermodynamics of this cycle has been study for the first time by Zubair in 1989 [20] and improved in the 1994 [21]. Later Khan et al. carried out an overview on this system and studied the thermodynamic behaviour also under the second law of the thermodynamic standpoint [22]. In all these studies it has been found that the system performance improved when operating in situations when the gap between the gas-cooler and the evaporating pressure is large, so in hot climate conditions. The major components of the system are two compressors, two expansion valves, gas-cooler, evaporator, separator and a recooler or subcooler. The components are almost the same of the PCE system, except for the subcooler, from the literature it is possible to find this system as a modification of the one seen in the last section [18].

2.4.1 Description of the system

Representation of the flow diagram and the corresponding p-h diagram are showed in Fig.2.11 and Fig.2.12 respectively. The exit transcritical vapour from the gas-cooler (state 3) is re-cooled (state 3-8) by the secondary stream (state 4-5), which is at a lower temperature and pressure due to the first expansion valve (state 3-4), which is located before the recooler. The flow leaving the recooler is then expanded in the second throttling valve (state 8-9) before entering the evaporator (state 9-1) where the cooling effect is performed. It is assumed that the exit state of the cooling flow is saturated vapour (state 5) this state can be maintained by a proper splitting of the refrigerant flow at the outlet of the gas-cooler. The saturated vapour from the evaporator and the recooler are then compressed with two different compressors to states 2 and 6 respectively. They are then mixed (state 7) before entering the gas-cooler where the heat is rejected to the ambient (state 7-3).

The model written with EES is based on the efficiency of the recooler, which is taken as 0.7, given as:

$$\eta_{sc} = \frac{t_3 - t_8}{t_3 - t_4} \tag{2.6}$$

Eq.2.7 and eq.2.8 are respectively energy conservation and the mass conservation for the recooler:

$$\dot{m}_{sc} \cdot (h_5 - h_4) = \dot{m}_{ev} \cdot (h_3 - h_8) \tag{2.7}$$

$$\dot{m}_{tot} = \dot{m}_{sc} + \dot{m}_{ev} \tag{2.8}$$

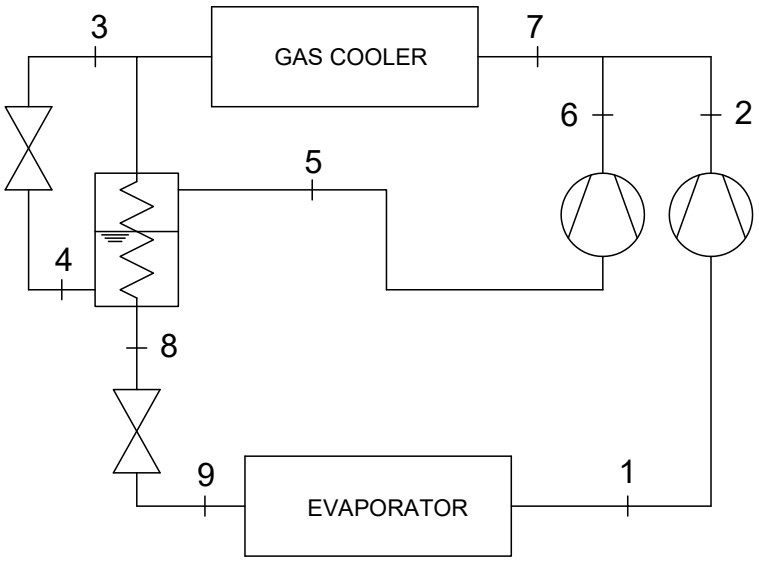

Figure 2.11 – Layout of the refrigeration cycle with parallel compression economization with recooler.

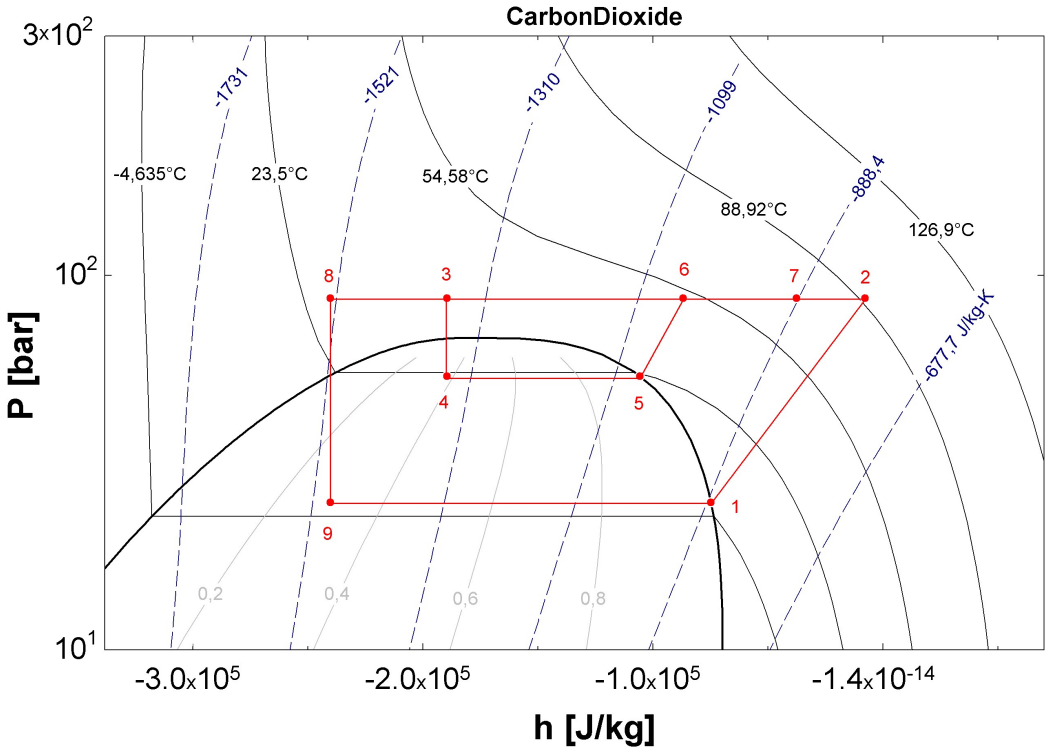

Figure 2.12 – logp-h diagram of the refrigeration cycle with parallel compression economization with recooler.

Dividing the two mass flow rate for the unit total mass flow rate it's possible to find the mass fraction trough the subcooler and through the evaporator, given as:

$$y_{sc} = \frac{\dot{m}_{sc}}{\dot{m}_{tot}} \tag{2.9}$$

$$y_{ev} = \frac{\dot{m}_{ev}}{\dot{m}_{tot}} \tag{2.10}$$

Then the performance of the system is given as:

$$COP = \frac{y_{ev} \cdot (h_1 - h_9)}{y_{ev} \cdot (h_2 - h_1) + y_{sc} \cdot (h_6 - h_5)} \tag{2.11}$$

2.4.2 System analysis

The layout of the parallel compressor economization system with integrated subcooling is similar to the layout of the simple PCE, for this reason similar results are expected. Using the same operating condition given in the chapter 2.1 it is possible to study this system and then compare the result with PCE. The assumed ambient temperature forces the system to transcritical operation, besides the system work between three level of pressure like the PCE system, therefore as done for this cycle both the intermediate pressure and the gas-cooler pressure have been optimized simultaneously.

Fig.2.13 shows the gas-cooler and the economizer pressure against the gas-cooler outlet temperature and fig.2.14 shows how the same pressures vary against the evaporative temperature (ambient temperature is set to 42.5°C). The results are also compared with the optimal gas-cooler pressure of the base cycle (yellow line). As expected the graphs are similar to the two seen for the PCE and the same considerations are valid. In order to understand which one of the two systems is better, the performance of the parallel compressor economization system with integrated subcooling has been studied varying the subcooler efficiency and then compared with the PCE system.

Fig.2.15 shows the COP against the efficiency of the subcooler (red line) for the PCE system with recooler. As expected the COP increases if the efficiency increases. However the interesting thing about the graph is the comparison with the PCE system. The orange line represents the COP of the PCE system at the same condition, t_{amb}=42.5°C and t_{ev}=-2°C, of the system with the subcooler. The two lines cross at $\eta_{sc} = 7.2$, this mean that the PCE system with subcooling has better performance than the normal one only if the efficiency of the recooler is higher than 7.2. This fact could be explain thinking about the heat exchanger: the PCE system with subcooling add a new component to the system, the recooler. This means a more complexity of the cycle and a further heat exchange, therefore if the heat exchange has good performance, the COP is better than the normal cycle, otherwise the losses in the heat exchange compromise also the

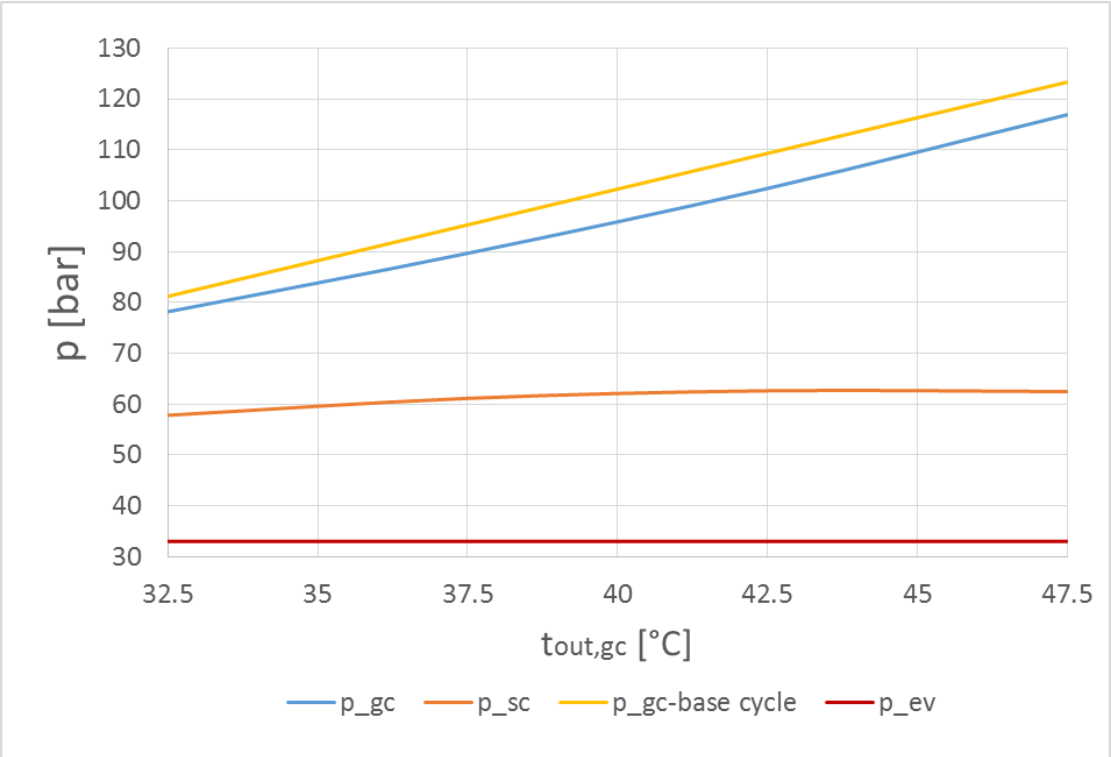

Figure 2.13 – Gas-cooler and economizer pressure vs gas-cooler outlet temperature (t_{ev}=-2°C).

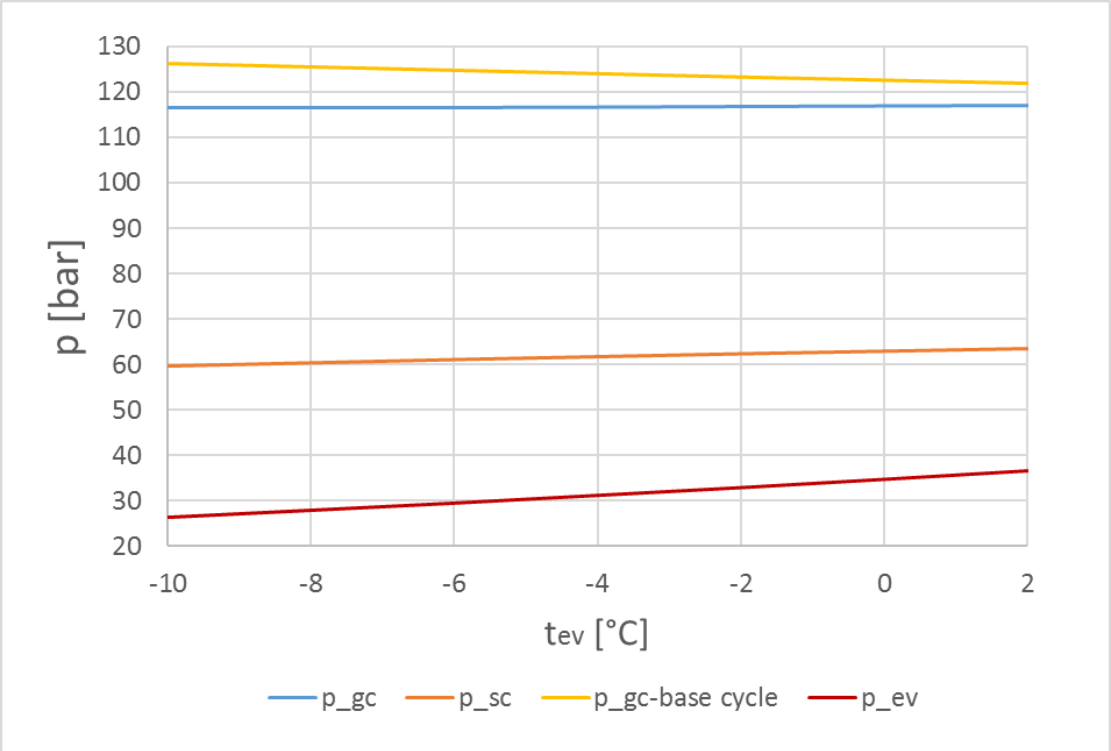

Figure 2.14 – Gas-cooler and economizer pressure vs evaporative temperature (t_{amb}=42.5°C).

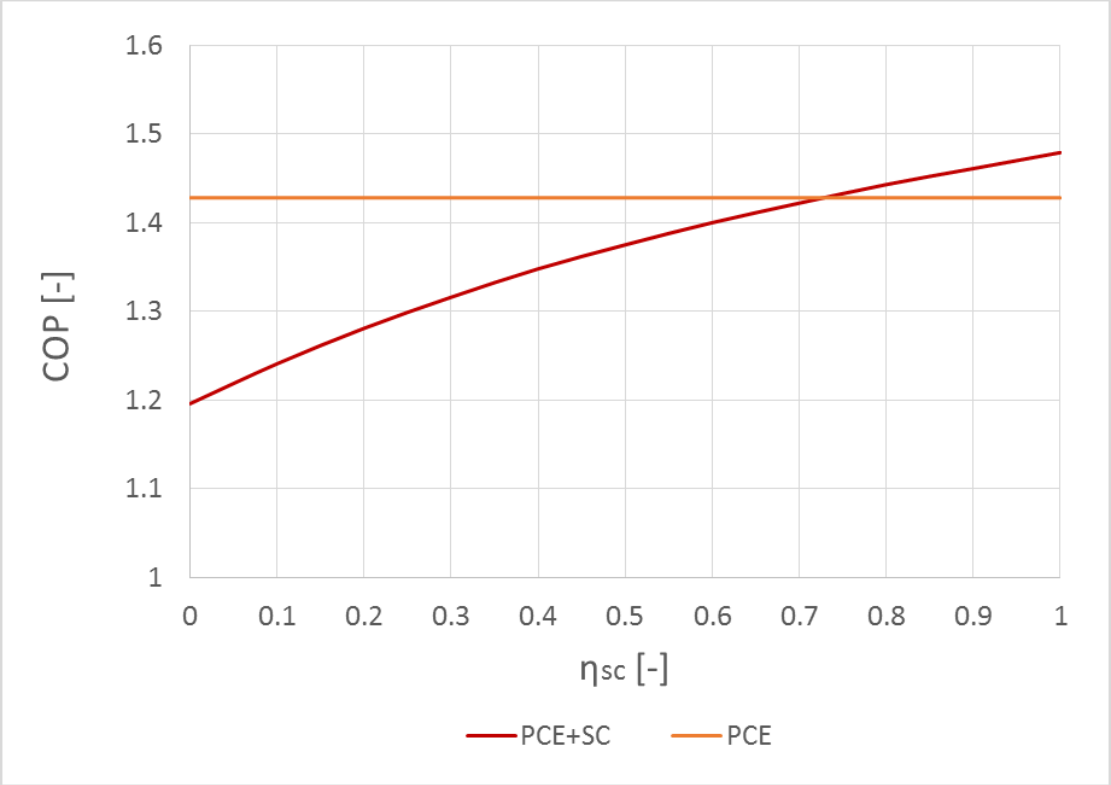

Figure 2.15 – COP vs η_{sc}, comparison with the PCE cycle.

performance of the entire system.

2.4.3 Results

Before presenting the results, the assumptions that have been made are summarized in the following table.

Evaporative temperature	-2°C
Gas-cooler pressure	optimized
Gas-cooler approach temperature difference	5°C
Recooler pressure	optimized
Recooler efficiency	0.7
Subcooling and superheating	0°C
Compressor isentropic efficiency	0.6
Fan power	neglected
Cooling capacity	100 kW

Tables 2.5 and 2.6 show the main parameters of the cycle for different working conditions.

t_{ev}	t_{amb}	$t_{out,gc}$	$p_{opt,gc}$	$p_{opt,sub}$	COP	Pc
°C	°C	°C	bar	bar	-	kW
-2	27.5	32.5	78.18	57.83	2.679	37.3
	32.5	37.5	89.67	61.15	2.11	47.4
	37.5	42.5	102.4	62.64	1.717	58.2
	42.5	47.5	116.9	62.48	1.422	70.3

Table 2.5 – PCE with subcooling results: different ambient temperature.

t_{amb}	$t_{out,gc}$	t_{ev}	$p_{opt,gc}$	$p_{opt,sub}$	COP	Pc
°C	°C	°C	bar	bar	-	kW
42.5	47.5	2	117.1	63.6	1.534	65.2
		-2	116.9	62.48	1.422	70.3
		-6	116.7	61.2	1.32	75.8
		-10	116.7	59.77	1.227	81.5

Table 2.6 – PCE with subcooling results: different evaporation temperature.

2.5 Refrigeration system with mechanical subcooling

As said in the previous section the performance of the base CO_2 refrigeration system can be significantly improved by further cooling the refrigerant after the gas-cooler. The subcooling allows the refrigerant to enter the evaporator with low quality, thus increasing the specific cooling capacity of the plant and for the transcritical systems also reducing the optimal heat rejection pressure. However these improvement come with a price, as reported by Thorton et al.:*"The amount of subcooling provided to the main cycle must equal the heat addition to the subcooling cycle evaporator. The heat addition to the subcooling cycle must be rejected in the subcooling cycle condenser/gas cooler at the cost of the work of the subcooling cycle compressor"*[23]. The mechanical subcooling, that can be called dedicated mechanical subcooling, is only one of the possible subcooling technologies (in the previous section 2.4 the integrated mechanical subcooling has been studied) and the literature is full of promising results. The mechanical subcooling was investigated under the first thermodynamic law standpoint by Thornton et al. in 1994 [23], a more precise analysis has been carried out later by Khan [24]. The system is made by two different cycles: the main one, with CO_2, where the cooling effect is achieved and the secondary one, necessary to subcool the carbon dioxide after the gas cooler. The components of the first one are the same as for the base CO_2 refrigeration system with the addition of the subcooler, which is also the evaporator of the secondary cycle. In this study three different refrigerants have been used to run the subcooling cycle: R404A, R134a and propane.

2.5.1 Description of the system

The layout of the system and the corresponding p-h diagram for the CO_2 main cycle are showed in Fig.2.16 and Fig.2.17 respectively. The main cycle is a 1-stage transcritical vapor cycle with the addition of the subcooler after the gas-cooler, where the refrigerant is further cooled (state 4-5) rejecting the heat to the secondary flow. The secondary fluid absorbs the heat from the CO_2 while evaporating (state 9-6). Both cycles perform the heat rejection, in the condenser of the subcooling cycle and in the gas-cooler of the primary cycle, to the same hot sink, the ambient temperature.

In order to write the model with EES it is necessary to add some specific boundary conditions. Regarding the primary cycle, as done for the other cycles, to obtain the gas-cooler outlet temperature (state 3) an approach of 5°C temperature difference from the ambient temperature has been chosen. The subcooler outlet temperature (state 4) is obtained considering a determinate temperature difference in the heat exchanger (Δt_{sub}). For the secondary cycle have been considered only fluids working in subcritical conditions. The condensing pressure is chosen considering a temperature difference from the environment of 8°C. The conditions of the refrigerant at the outlet of the condenser and the evaporator are respectively saturated liquid and saturated vapor. The isentropic efficiency of the compressor is assumed to be 0.6 and constant (more precise condition will be taken into consideration in the second

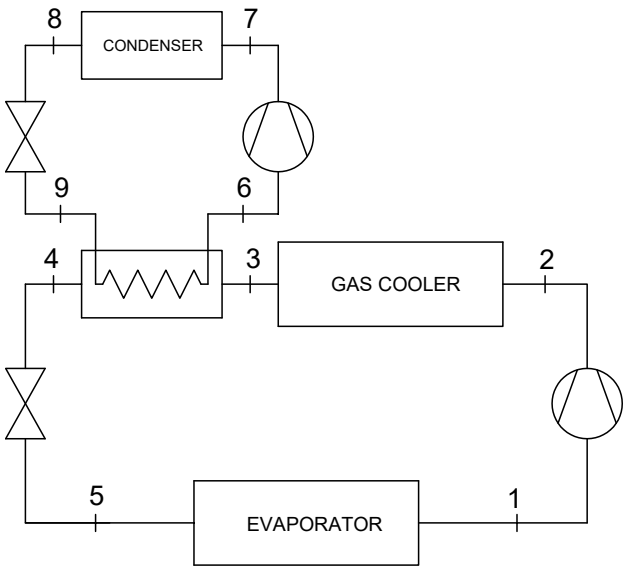

Figure 2.16 – Layout of refrigeration cycle with mechanical subcooling.

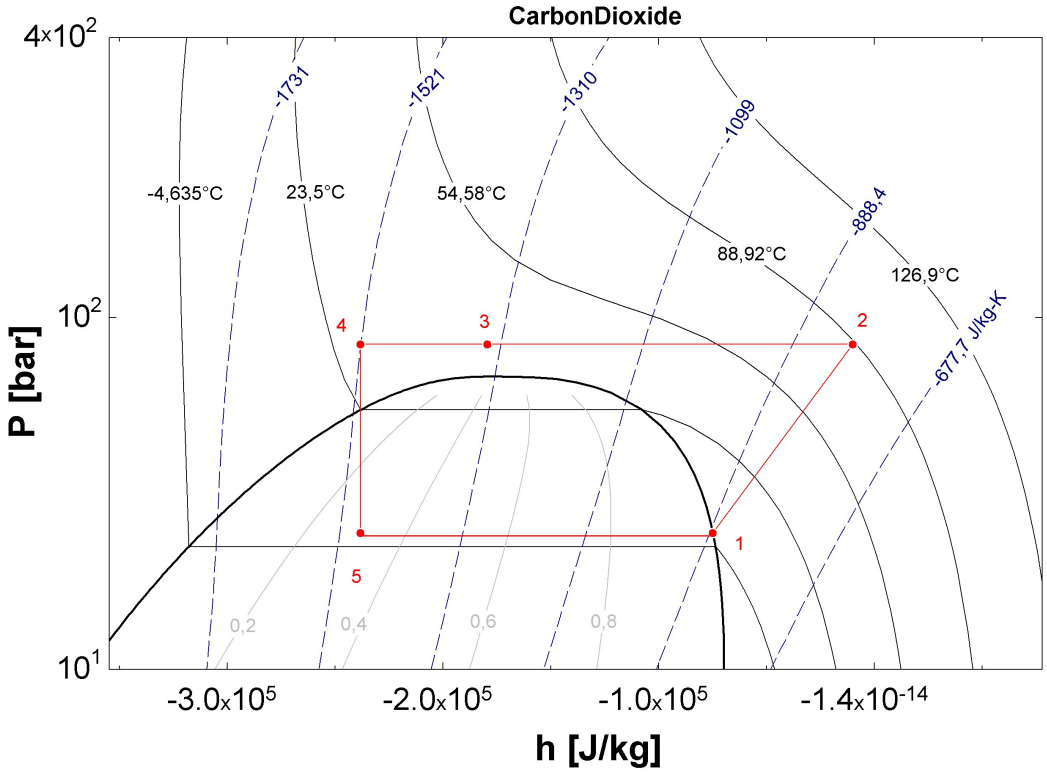

Figure 2.17 – logp-h diagram of the refrigeration system with mechanical subcooling, main cycle.

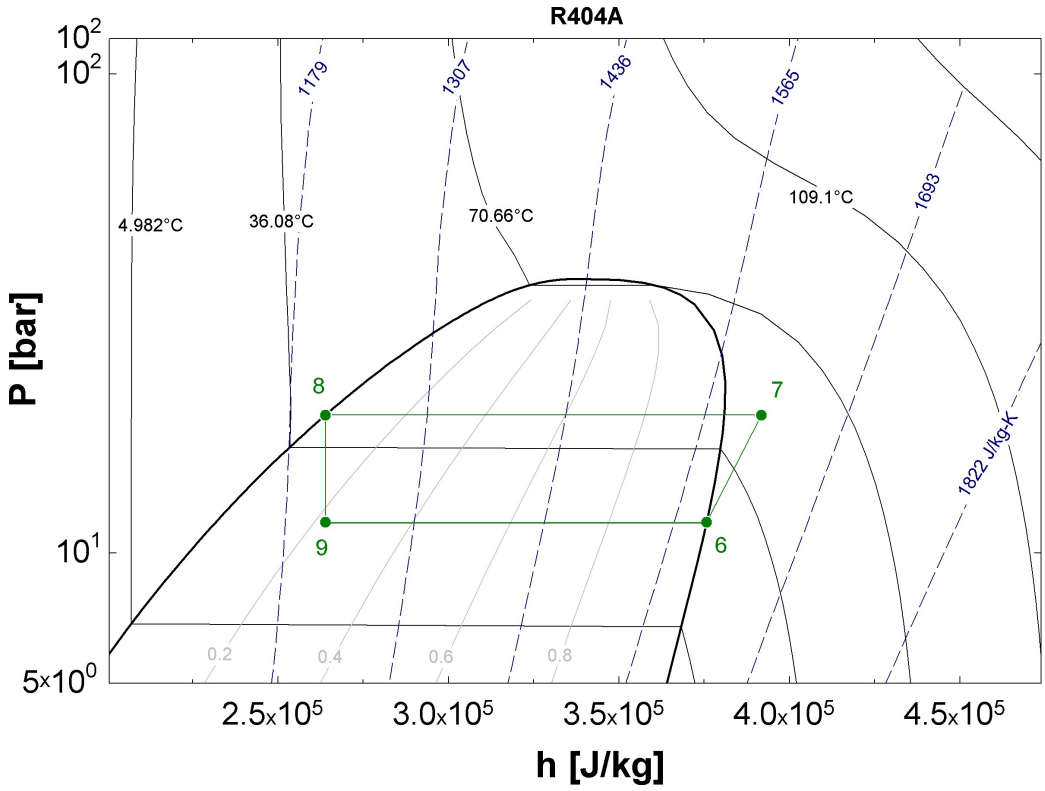

Figure 2.18 – logp-h diagram of the refrigeration system with dedicated mechanical subcooling, secondary cycle (R404a).

part of the project). Like suggested by Llopis et al. [25] to fix the evaporating temperature two criteria can be followed: first, considering a fixed temperature difference between the evaporating temperature and the subcooler outlet temperature. Second, the pressure can be fixed according to the restriction due to the compressor. Even if the second one is the best approximation to the reality, the first one has been chosen to model the cycle, without considering any restrictions for the maximum pressure or the minimum pressure difference. This temperature difference has been set to 5°C. Either in the subcooling cycle the superheat after the compressor is neglected. Fig.2.18 shows the p-h diagram for the secondary cycle (R404a).

It is now possible to write the energy conservation at the subcooler as:

$$\dot{m}_{sc} \cdot q_{0,sec} = \dot{m}_{CO2} \cdot \Delta h_{sec} \tag{2.12}$$

where $\dot{m}_{CO2}$ and $\dot{m}_{sec}$ are respectively the mass flow rate of the primary and secondary cycle,

$q_{0,sec} = h_6 - h_9$ and $\Delta h_{sub} = h_3 - h_4$. The performance of the cycle is given by:

$$COP = \frac{\dot{m}_{CO2} \cdot q_0}{\dot{m}_{CO2} \cdot w_{c,CO2} + \dot{m}_{sec} \cdot w_{c,sec}} \tag{2.13}$$

where $q_0, w_{c,CO2}$ and $w_{c,sec}$ are respectively the specific cooling capacity, the specific work of the primary compressor and the specific work of the secondary compressor. Using the energy conservation at the subcooler [2.12] the overall COP can be expressed as:

$$COP = \frac{q_0}{w_{c,CO2} + \frac{\Delta h_{sub}}{COP_{sec}}} \tag{2.14}$$

Where the performance coefficient of the secondary cycle is:

$$COP_{sec} = \frac{q_{0,sec}}{w_{c,sec}} \tag{2.15}$$

Regarding the subcooling degree it needs to be mentioned that although any value is theoretically possible, there is a practical limit that has to be considered. Mentioning Llopis et al [25]: *"for centralized systems, the maximum subcooling degree would be equal to the approach temperature between gas-cooler outlet and the environment (in this case 5°C), since higher subcooling degrees will be lost due to heat transfer to the environment during the distribution of the refrigerant. For stand-alone systems this subcooling degree can be increased a bit"*. The system will still be studied without any restriction, but in the next chapter the results will be presented considering a reasonable degree of subcooling.

Usually the components of the secondary cycle or subcooling cycle are smaller than those of the main cycle. In order to know how small the secondary cycle is compared to the main one in terms of mass flow and power consumption, two new parameters, the mass ratio and the power ratio, are introduced and defined respectively as:

$$r_m = \frac{\dot{m}_{sec}}{\dot{m}_{CO2}} \tag{2.16}$$

$$r_p = \frac{P_{c,sec}}{P_{c,CO2}} = r_m \cdot \frac{w_{c,sec}}{w_{c,CO2}} \tag{2.17}$$

2.5.2 System analysis

As explain above, the system has been modelled using a determinate temperature difference between the evaporating temperature of the secondary cycle and the outlet subcooler temperature (CO_2 side). In the first part of this section the consequences of varying the temperature difference will be studied. Since the results are similar for all the three secondary fluids only the graphs for the propane will be presented. In next chapter the overall results for all of them will

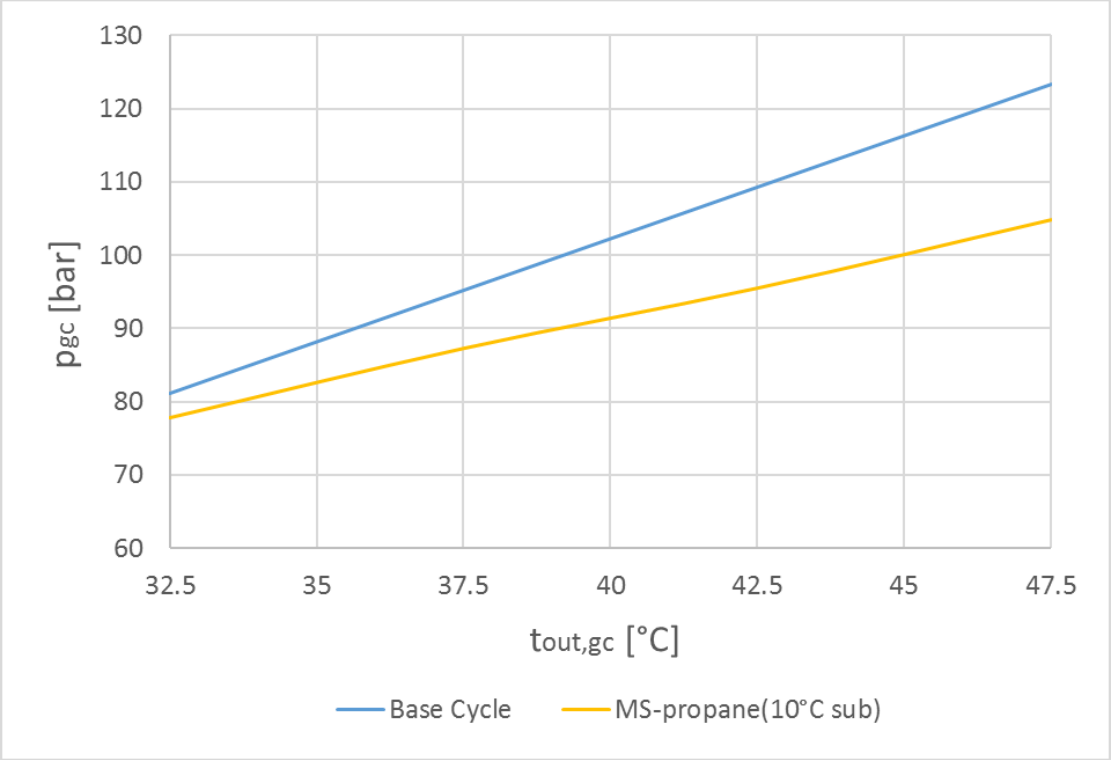

Figure 2.19 – Gas-cooler pressure vs gas-cooler outlet temperature (t_{ev}=-2°C).

be shown. Fig.2.20 show the COP against the Δt_{sub} for different gas-cooler outlet temperature. It can be seen that the best performance is achieved at a certain grade of subcooling, which varies with the temperature at the outlet of the gas-cooler, the higher the ambient temperature is, the higher the temperature difference needed to reach the maximum COP. Fig.2.21 presents how the optimized gas-cooler pressure (the one that permits to have the best performance) varies with the Δt_{sub}. The lines have an U shape, therefore as expected at the begin, the higher the subcooling grade is, the lower the optimal pressure, but after a certain point the pressure starts to increase because of the shape of the isotherms. It is interesting to see that the lower pressure for each gas-cooler outlet temperature does not match with the higher COP condition as seen in the previous graph. The graphs show also that the value of subcooling that achieve the best performance, is always higher than the practical limit.

As done for the other systems fig.2.19 shows the difference between the optimal gas-cooler pressure of the base cycle and the gas-cooler pressure of the cycle with dedicated mechanical subcooling (propane, Δt_{sub}=10°C), the difference increases when the ambient temperature increases.

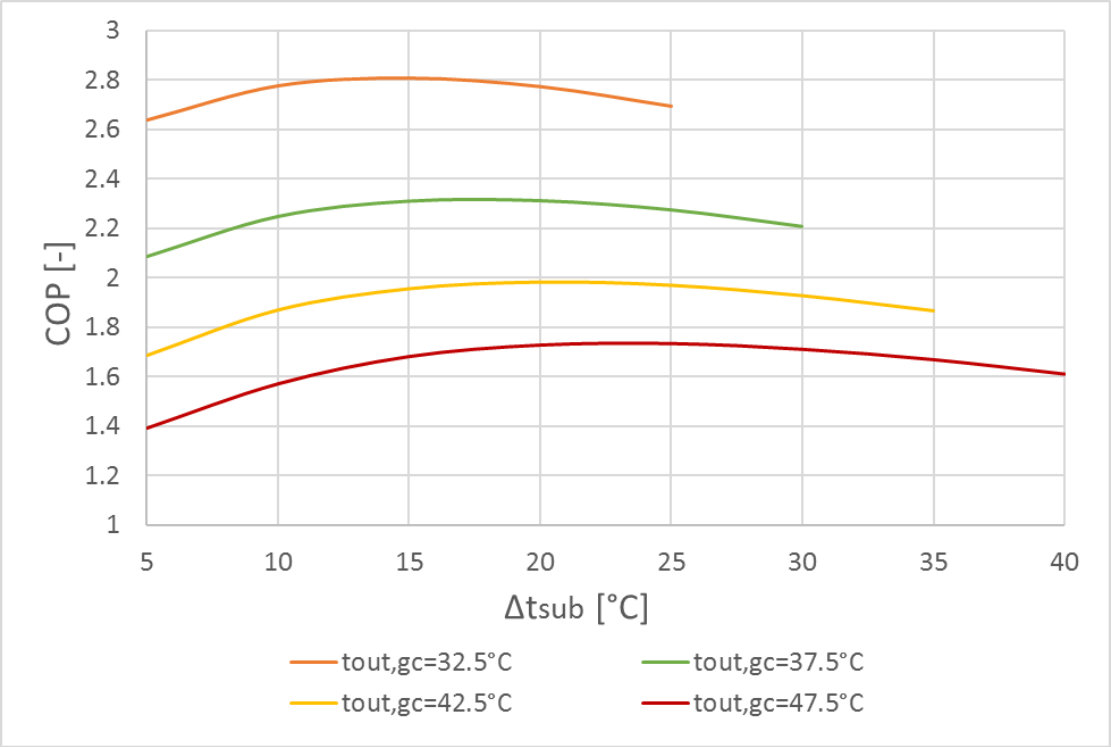

Figure 2.20 – COP vs Δt_{sub} for different gas-cooler outlet temperature (t_{ev}=-2°C, propane).

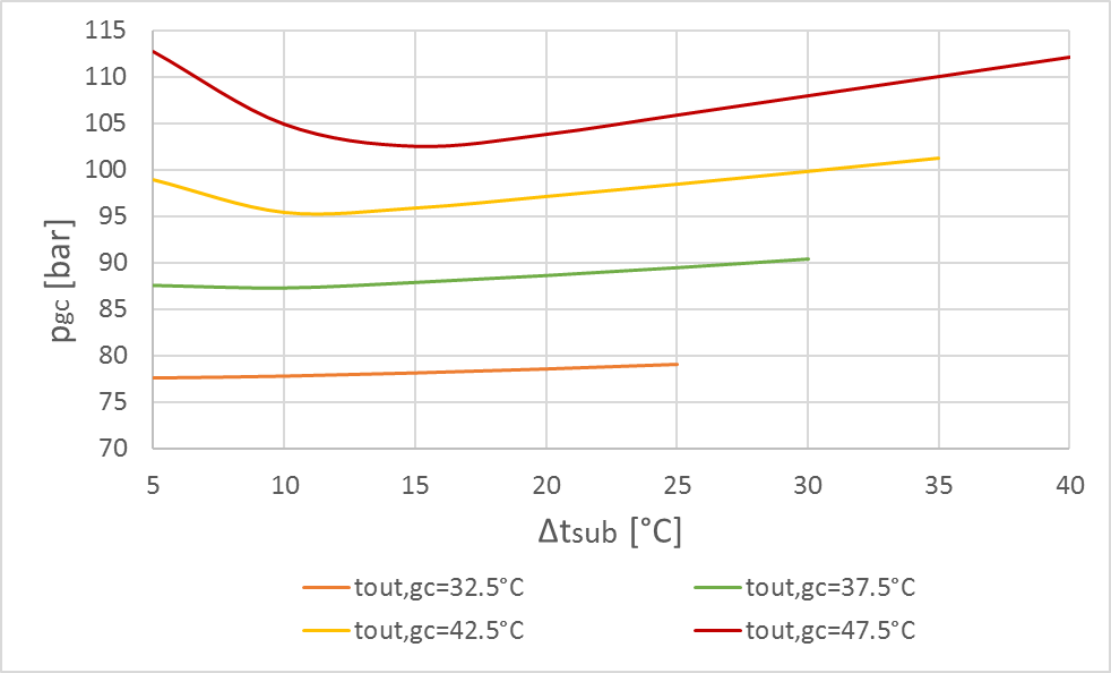

Figure 2.21 – Optimized gas-cooler pressure vs Δt_{sub} for different gas-cooler outlet temperature (t_{ev}=-2°C, propane).

2.5.3 Results

Before presenting the results, the assumptions that have been made are summarized in the following table.

Main cycle	
Evaporative temperature	-2°C
Gas-cooler pressure	optimized
Gas-cooler approach temperature difference	5°C
Δt_{sub}	5°C, 10°C and 15°C
Superheating	0°C
Secondary cycle	
Condenser temperature difference	8°C
Evaporator approach temperature difference	5°C
Subcooling and superheating	0°C
Compressor isentropic efficiency	0.6
Fan power	neglected
Cooling capacity	100 kW

Tables 2.7, 2.8 and 2.9 show the main parameters of the cycle using for secondary fluid propane, R404A and R4134a respectively. It has been chosen to report the results with different value of Δt_{sub} and different ambient temperature to see how these parameters effect the performance together. It can be seen that the highest performance is reached by the R134a, followed by propane and then R404A.

t_{ev}	t_{amb}	Δt_{sub}	$p_{opt,gc}$	y_m	y_p	COP_{sub}	COP	Pc
°C	°C	°C	bar	-	-	-	-	kW
-2	32.5	5	87.55	0.1275	0.05349	10.53	2.084	48.0
		10	87.25	0.2063	0.1183	7.603	2.249	44.5
		15	87.85	0.258	0.1874	5.851	2.312	43.3
-2	42.5	5	112.8	0.08958	0.02667	10.56	1.394	71.7
		10	104.9	0.2116	0.09225	7.618	1.573	63.6
		15	102.5	0.3105	0.1769	5.858	1.683	59.4

Table 2.7 – MS results: propane.

t_{ev}	t_{amb}	Δt_{sub}	$p_{opt,gc}$	y_m	y_p	COP_{sub}	COP	Pc
°C	°C	°C	bar	-	-	-	-	kW
-2	32.5	5	87.77	0.3157	0.05691	9.622	2.075	48.2
		10	87.55	0.51	0.1259	6.943	2.227	44.9
		15	88.2	0.6401	0.2005	5.328	2.277	43.9
-2	42.5	5	113.1	0.24	0.02976	9.353	1.39	71.9
		10	105.8	0.5484	0.09955	6.733	1.556	64.3
		15	104.4	0.7807	0.1849	5.156	1.65	60.6

Table 2.8 – MS results: R404A.

t_{ev}	t_{amb}	Δt_{sub}	$p_{opt,gc}$	y_m	y_p	COP_{sub}	COP	Pc
°C	°C	°C	bar	-	-	-	-	kW
-2	32.5	5	87.49	0.2409	0.05265	10.77	2.087	47.9
		10	87.18	0.3897	0.1165	7.777	2.254	44.4
		15	87.77	0.4866	0.1843	5.983	2.32	43.1
-2	42.5	5	112.7	0.1678	0.02596	10.88	1.395	71.7
		10	104.6	0.3992	0.09058	7.847	1.577	63.4
		15	102	0.5901	0.1756	6.032	1.69	59.2

Table 2.9 – MS results: R134a.

2.6 Cascade system

The cascade system is a refrigeration system working with two different cycles and two different fluids. Like for the system with dedicated mechanical subcooling, the cascade system cannot be properly considered a CO_2 system because of the presence of a different fluid. However the purpose of this study is to understand how to use CO_2 to achieve the best performance in hot climate condition. The best quality of the cascade system is that it makes possible to avoid working in transcritical conditions. This is because the CO_2 is used in the low temperature cycle while another fluid, with higher critical point, is used for the high temperature cycle or secondary cycle. Cascade systems using CO_2 have been widely studied in the past years combined with different fluids, synthetic or natural, as R134a [26], R404A [27] or propane [28]. The common result for all these studies is that a cascade system achieves really good performance when the temperature difference between the hot sink and the cold sink is large.

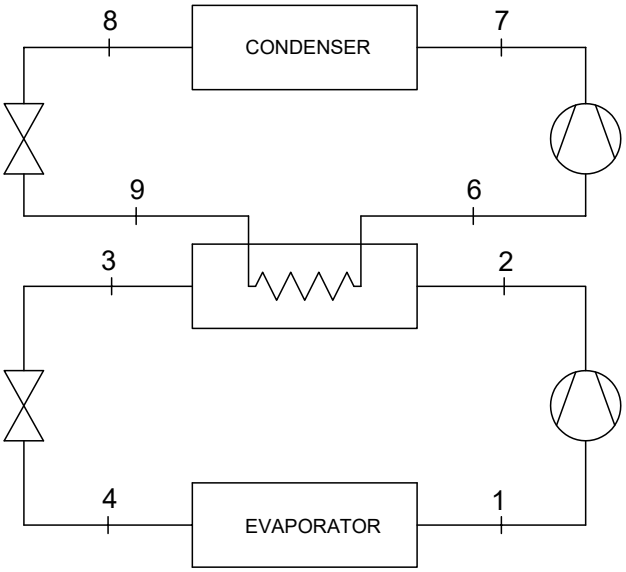

Figure 2.22 – Layout of the refrigeration cascade system.

2.6.1 Description of the system

The flow diagram of the cascade system is shown in Fig.2.6. The system is made by two different 1-stage vapor cycle, the condenser of the low temperature cycle (that work with CO_2) rejects the heat (state 2-3) to the evaporator of the high temperature cycle (state 9-6). The cooling effect is achieved in the low temperature evaporator (state 4-1) while the heat rejection to the environment happens in the high temperature condenser (state 7-8). In order to model the system some new specific boundary conditions have to be specified. The conditions of the refrigerant at the outlet of the condenser and the evaporator, are respectively saturated liquid

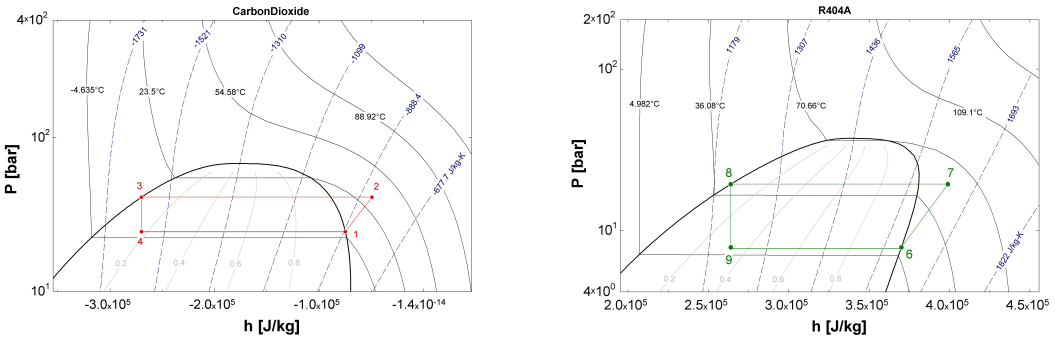

(a) CO_2 (b) R404A

Figure 2.23 – logp-h diagrams of the cascade refrigeration system.

and saturated vapor for both the cycles, superheat is neglected. The isentropic efficiency of both the compressors is assumed to be 0.6 and constant. No restrictions have been taken into consideration concerning the minimum pressure difference. The condensing pressure of the high temperature cycle is chosen considering a temperature different from the environment of 8°C. While the condensing pressure of the low temperature cycle is optimized using the EES min-max function in order to reach the best performance. At the end a constant temperature difference of 5°C is used to find the evaporative temperature of the high-pressure cycle.

Following the same procedure used for the dedicated mechanical subcooling [2.5], i.e. using the energy conservation in the common heat exchanger, makes it possible to write the performance of the cycle as:

$$COP = \frac{q_0}{w_{c,CO2} + \frac{q_{cond,CO2}}{COP_{sec}}} \tag{2.18}$$

Where the performance coefficient of the high temperature cycle is:

$$COP_{sec} = \frac{q_{0,sec}}{w_{c,sec}} \tag{2.19}$$

2.6.2 System analysis

As stated earlier three different fluids have been used as refrigeration fluid in the high-pressure cycle. The choice has been made to understand which one can achieve the best performance. The results have can be seen in fig.2.24. The graph shows that R134a achieves the best COP, followed by propane and then R404A.

Fig.2.25 shows the COP of the secondary cycle and the optimized CO_2 condensing temperature versus the ambient temperature. The first graph is similar to fig.2.24, this mean that the overall COP is mainly influenced by the performance of the high pressure cycle. The second one shows

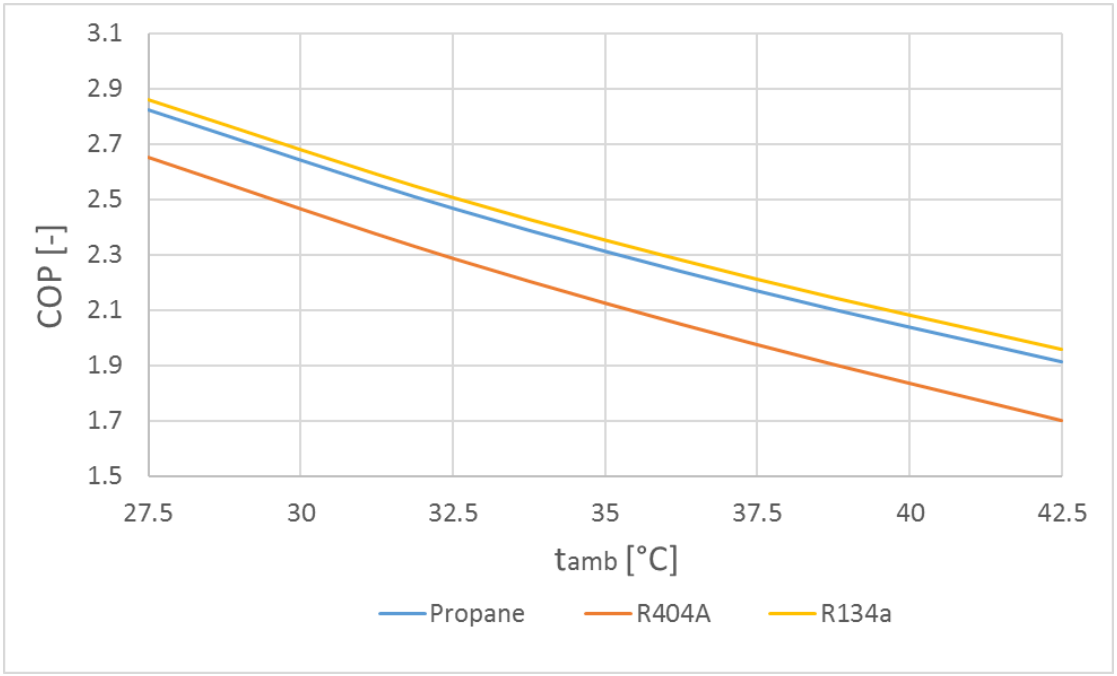

Figure 2.24 – COP vs ambient temperature (t_{ev}=-2°C).

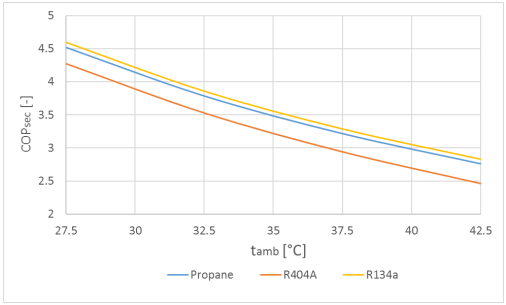

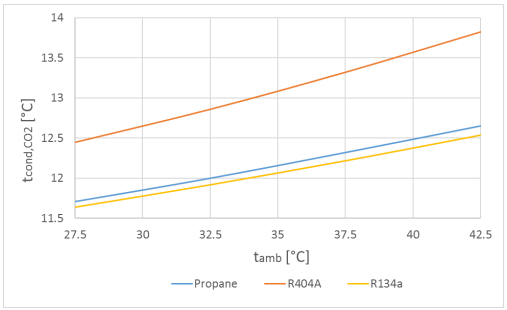

Figure 2.25 – COP of the high pressure cycle and optimized CO_2 condensing temperature vs ambient temperature (t_{ev}=-2°C).

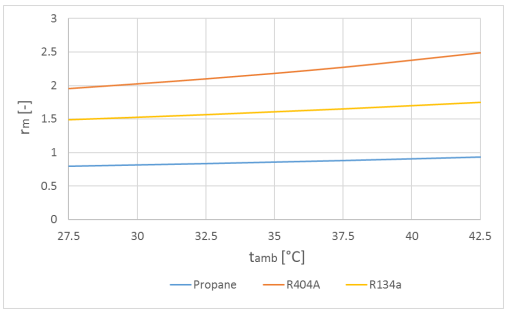

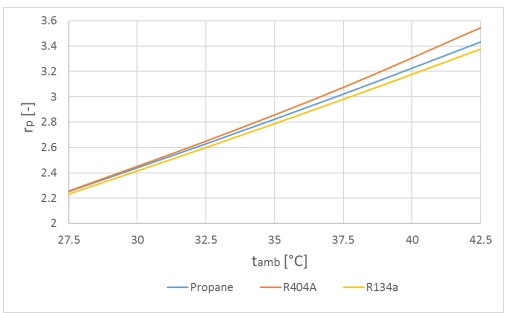

Figure 2.26 – r_m and r_p vs ambient temperature (t_{ev}=-2°C).

the difference between the three fluids concerning the optimal condensing temperature.

In order to understand which amount of power has been used by the two cycles fig.2.26 has been proposed. The graphs show the mass flow ratio and the power ratio in function of the ambient temperature. These two parameter are defined respectively as:

$$r_m = \frac{\dot{m}_{sec}}{\dot{m}_{CO2}} \tag{2.20}$$

$$r_p = \frac{P_{c,sec}}{P_{c,CO2}} = r_m \cdot \frac{w_{c,sec}}{w_{c,CO2}} \tag{2.21}$$

The figure shows that at t_{amb}=42.5°C the amount of power needed by the high pressure cycle is more than three times the power needed by the low pressure cycle for all the refrigerants.

2.6.3 Results

Before presenting the results, the assumptions that have been made are summarized in the following table.

Main cycle	
Evaporative temperature	-2°C
Condenser pressure	optimized
Secondary cycle	
Condenser temperature difference	8°C
Evaporator approach temperature difference	5°C
Subcooling and superheating	0°C
Compressor isentropic efficiency	0.6
Fan power	neglected
Cooling capacity	100 kW

Tables 2.10, 2.11 and 2.11 show the main parameters of the cycle used for secondary fluid propane, R404A and R4134a respectively. The results are reported for the different ambient temperature and the same evaporation temperature (-2°C). It can be seen that as found out for the mechanical subcooling in the previous section, the highest performance is reached by the R134a, followed by propane, then R404A.

t_{ev}	t_{amb}	$p_{cond,CO2,opt}$	$t_{cond,CO2,opt}$	r_m	r_p	COP_{sub}	COP	Pc
°C	°C	bar	°C	-	-	-	-	kW
	27.5	46.97	11.71	0.794	2.253	4.522	2.824	35.4
	32.5	47.3	12	0.8349	2.63	3.789	2.469	40.5
-2	37.5	47.5	12.32	0.8815	3.022	3.221	2.171	46.1
	42.5	48.06	12.65	0.935	3.433	2.765	1.915	52.2

Table 2.10 – Cascade system results: propane.

t_{ev}	t_{amb}	$p_{cond,CO2,opt}$	$t_{cond,CO2,opt}$	r_m	r_p	COP_{sub}	COP	Pc
°C	°C	bar	°C	-	-	-	-	kW
	27.5	47.82	12.45	1.957	2.255	4.272	2.653	37.7
	32.5	48.3	12.86	2.101	2.649	3.529	2.288	43.7
-2	37.5	48.84	13.32	2.273	3.073	2.944	1.976	50.6
	42.5	49.45	13.82	2.487	3.544	2.465	1.702	58.8

Table 2.11 – Cascade system results: R404A.

t_{ev}	t_{amb}	$p_{cond,CO2,opt}$	$t_{cond,CO2,opt}$	r_m	r_p	COP_{sub}	COP	Pc
°C	°C	bar	°C	-	-	-	-	kW
	27.5	46.88	11.64	1.493	2.232	4.593	2.862	34.9
	32.5	47.2	11.92	1.567	2.6	3.858	2.508	39.9
-2	37.5	47.55	12.22	1.651	2.981	3.289	2.212	45.2
	42.5	47.92	12.54	1.746	3.378	2.833	1.958	51.1

Table 2.12 – Cascade system results: R134a.

2.7 Ejector expansion refrigeration cycle

An important field of research for improving the performance of refrigerating systems is the reduction of the losses through the expansion valve. Since the critical temperature of carbon dioxide is usually lower than the heat rejection temperature, the cycle has to work in transcritical conditions. Compared with refrigerating cycle of conventional refrigerants the CO_2 transcritical cycle has a larger pressure difference between the gas-cooler pressure and the evaporating pressure, this means that also the losses through the throttling valve are larger. In order to recover the expansion losses and increase the cycle efficiency, it has been proposed to replace the throttling valve with a different device. There are three kinds of devices that can be used with this purpose:

- Expansion turbine[29]: it is probably the best way to recover the expansion work, but there are some issues that interfere with the development of this device. First of all there is the problem with the cost, especially for small size application, the expansion from transcritical region to the two-phase region is still not theoretically clear and low quality two-phase flow make the device prone to damage.

- Vortex tube[30]: the vortex tube is a device without moving part. Inside it the gas is expanding from the gas-cooler pressure to the evaporation pressure and then divided into three fractions: saturated liquid, saturated vapor, and superheated gas. Some studies regarding it seem promising, but they are at early stage, not enough experimental data is available and the mechanism inside the tube is still not clear.

- Ejector: in literature there can be found a great amount of researches about the device, from the first law standpoint[31] and also from the second law standpoint [32][33]. The results are promising and different companies started to use it in trial plants. Therefore also real data is available[34]. Comparing with the expansion turbine the cost is reduced and the lifetime increased (there is no moving part in this case). Thus the use of an ejector in the CO_2 transcritical cycle seems to be the most promising solution.

In the ejector expansion refrigeration cycle (EERC) an ejector is used instead of the throttling valve to recover the kinetic energy of the expansion process. Using the ejector the compressor suction pressure is higher than it would be normally, this means less compression work and higher performance. Generally the compressor efficiency increases if the pressure ratio is lower. Another beneficial effect is achieved in the evaporator: using an ejector instead of an expansion valve the cycle is provided also with a liquid-vapor separator, which results in the cooling capacity of the cycle to be increased. In this section the EERC will be studied following the model proposed by Kornhauser[35]. The first part is focused just on the ejector with the purpose of understand how it works and what is the best way to model it, followed by the second part where the ejector model will be insert in the system and the whole cycle will be studied.

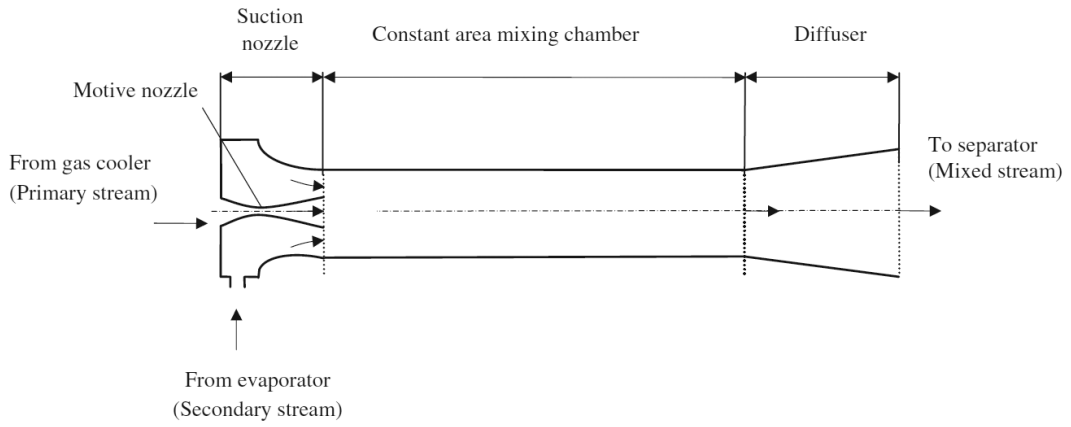

Figure 2.27 – Schematic of constant area ejector flow model[33].

2.7.1 Ejector principle and design

The working principle of the ejector is based on converting the energy otherwise lost in the throttling process into kinetic energy and then again in pressure energy through a diffuser. The ejector can be divided into four different parts: a primary nozzle, a suction chamber, a mixing chamber and a diffuser. Two different flows are entering the ejector: the primary flow and the secondary flow. The primary flow, or nozzle flow, is at high pressure (then coming from the gas-cooler) and the secondary flow, or suction flow, is at low pressure (coming from the evaporator). The basic principle is to use the expansion work of the high-pressure flow to achieve a total flow at the outlet section of the ejector with a pressure higher than the secondary flow. The primary flow expands in the motive nozzle and exits with high velocity and low pressure, usually the velocity is supersonic. The low pressure creates an entrainment effect for the secondary flow that is then entrained in the suction chamber also thanks to high velocity of the primary flow. The two flows are then mixed in the mixing chamber and the momentum is transferred from the primary to the secondary flow. The mixture has a certain velocity that is recovered in order to increase the pressure in the diffuser. Fig.2.27 shows the different parts of the ejector.

The ejector can be described by several dimensionless parameters. The first one is the mass entrainment ratio [2.22] which is defined as the ratio of the secondary mass flow over the primary mass flow, and shows the ability of the ejector sucking the flow from the evaporator. The second one is the pressure lift [2.23] defined as the difference between the diffuser outlet pressure and the suction inlet pressure. In the end the ejector efficiency [2.24], defined to quantify the efficiency of the expansion work recovery. Elbel et al.[36] define the efficiency as the ratio of the compression work obtained over the maximum potential expansion work. The first term is the work recovered by the secondary flow between the suction inlet pressure and

the diffuser outlet pressure. The second one is the ideal expansion work between the nozzle inlet pressure and the diffuser outlet pressure.

$$r = \frac{\dot{m}_s}{\dot{m}_m} \tag{2.22}$$

$$p_{lift} = p_{diff,out} - p_{s,in} \tag{2.23}$$

$$\eta_{ej} = \frac{\dot{m}_s \cdot (h(p_{diff,out}; s_{s,in}) - h_{s,in})}{\dot{m}_m \cdot (h_{m,in} - h(p_{diff,out}; s_{m,in}))} \tag{2.24}$$

2.7.2 Ejector model

In this section the equations used to describe the behavior of the flow in the ejector are presented. Mass, momentum and energy conservation are used to find the outlet conditions of each section supposing that the conditions at the inlet are known. From literature there can be found different kinds of ejector model, the majority refers to two ideal cases: the constant pressure mixing model and the constant area mixing model. However none of these represents properly what happens through the ejector, but are still a sufficient tool when studying the EERC. More complicated models can be used, but their application is limited and the results are always questioned. In this project the model used is the constant pressure model proposed by Kornhauser[35], an *"homogeneous equilibrium model"* for the two phase flow. The analysis assumes that: the flow in the ejector is a one-dimensional homogeneous equilibrium flow, properties and velocities are constant over cross sections. Thus the analysis is one-dimensional, the refrigerant is at all time in thermodynamic quasi-equilibrium, the processes in the motive nozzle, in the suction nozzle and in the diffuser could be expressed in terms of efficiencies. These efficiencies take into account the losses caused by that the process is not reversible and an eventual shock effect. Mixing section process efficiency is supposed unitary, kinetic energy is negligible outside the ejector. About the efficiencies Liu et al. [37] made an important review investigating the literature, finding out that values of 0.7-0.9 are assumed for every part of the ejector. In another study [38] they also proposed three empirical correlations to calculate the efficiencies. Since the purpose of this study is not to study the ejector model, but study the performance of a cycle using an ejector, the efficiencies of the motive nozzle, the suction nozzle and the diffuser have been chosen as constant among the most used in literature and are respectively: $\eta_m = \eta_s = 0.8$ and $\eta_d = 0.75$. Another important assumption that has been made to be able to write the model is that the flows in the motive nozzle and in the suction nozzle at the entrance of the mixing chamber are assumed to have the same pressure. In the constant pressure model this pressure is also the pressure in the

mixing chamber and has to be lower than the evaporative pressure, then: $p_{m,out}$=$p_{s,out}$=p_{mix}. The value to choose for this parameter will be discussed in the next section. The equations used are now presented.

If the inlet conditions are known and the value for the pressure at the outlet of the primary nozzle is assumed, the isentropic enthalpy at the outlet can be found.

$$h_{m,out,is} = h(s_{m,in}; p_{m,out}) \tag{2.25}$$

By using the definition of the motive nozzle's isentropic efficiency the enthalpy at the nozzle outlet is defined.

$$\eta_m = \frac{h_{m,out} - h_{m,in}}{h_{m,out,is} - h_{m,in}} \tag{2.26}$$

Then, the energy conservation is used the outlet velocity assuming that the kinetic energy at the inlet of the nozzle is negligible.

$$h_{m,in} = h_{m,out} + \frac{w_{m,out}^2}{2} \tag{2.27}$$

Similarly to what has been written for the primary nozzle the equations governing the secondary nozzle are presented.

$$h_{s,out,is} = h(s_{s,in}; p_{s,out}) \tag{2.28}$$

$$\eta_s = \frac{h_{s,out} - h_{s,in}}{h_{s,out,is} - h_{s,in}} \tag{2.29}$$

$$h_{s,in} = h_{s,out} + \frac{w_{s,out}^2}{2} \tag{2.30}$$

As said above $p_{s,out}$ and $p_{n,out}$ are given and equal. In the mixing section the mass conservation can be written as:

$$\dot{m}_{tot} = \dot{m}_m + \dot{m}_s \tag{2.31}$$

Using the definition of entrainment ratio[2.22] the momentum conservation and the energy conservation at the exit of the mixing chamber are respectively:

$$w_{mix,out} = \frac{1}{1+r} \cdot w_{m,out} + \frac{r}{1+r} \cdot w_{s,out} \tag{2.32}$$

$$h_{mix,out} = \frac{1}{1+r} \cdot (h_{m,out} + r \cdot h_{s,out}) - \frac{w^2_{mix,out}}{2} \tag{2.33}$$

The enthalpy of the stream at the diffuser exit can be found by applying the principle of energy conservation through the ejector.

$$h_{d,out} = \frac{h_{m,in} + r \cdot h_{s,in}}{1+r} \tag{2.34}$$

By using the definition of the motive nozzle's isentropic efficiency the enthalpy at the nozzle outlet is defined.

$$\eta_d = \frac{h_{d,out,is} - h_{mix,out}}{h_{d,out} - h_{mix,out}} \tag{2.35}$$

Then, the pressure at the outlet of the ejector is found using the isentropic enthalpy.

$$p_{d,out} = p(s_{mix,out}; h_{d,out,is}) \tag{2.36}$$

The quality of the fluid at the exit of the ejector is found by using the diffuser pressure $p_{d,out}$ and the enthalpy $h_{d,out}$. However to ensure the cycle continuity the quality of the stream leaving the ejector should be approved with the follow equation.

$$x_{d,out} = \frac{1}{1+r} \tag{2.37}$$

The equations reported do not allow an accurate investigation of pressure and velocity gradients inside the ejector. The purpose of this project is not to study the inside phenomena of the ejector, but the performance of the entire system. Cross-sectional homogeneity and thermodynamic equilibrium are incorrect assumption.

2.7.3 Description of the system

Now that the ejector has been introduced the overall system can be described. The flow diagram and the corresponding p-h diagram are showed in Fig.2.28 and Fig.2.29 respectively. The high-pressure fluid coming from the gas-cooler (state 1) enters the motive nozzle and expands (state 2). The secondary flow from the evaporator (state 3) enters the suction nozzle and expands (state 4) until the same pressure gets mixed in the mixing chamber with the primary flow at a constant pressure ($p_2 = p_4 = p_5$). The mixed flow enters the diffuser and here its velocity drops until it almost reaches a stagnation state while the pressure increases(state 6). The mixture leaving the ejector enters the separator and separates itself into saturated liquid and saturated vapor. The saturated vapor (state 7) enters the compressor where it has been compressed until the gas-cooler pressure (state 8). After this it enters the gas-cooler where the heat rejection into the environment takes place (state 8-1). The saturated liquid (state 9) then

leaves the separator and enters the throttling valve where it reaches the evaporative pressure (state 10). In the evaporator the cooling effect is performed (state 10-3) and the fluid enters the ejector again.

The equations for the cycle performance are written below. The cooling capacity per unit mixture flow mass is:

$$q_0 = \frac{r}{1+r} \cdot (h_3 - h_{10}) \tag{2.38}$$

The compressor power consumption per unit mixture flow mass is:

$$w_c = \frac{1}{1+r} \cdot (h_8 - h_7) \tag{2.39}$$

The performance of the system can be written as:

$$COP = \frac{q_0}{w_c} \tag{2.40}$$

2.7.4 System analysis

As it has been said above, to solve the model it is necessary to make an assumption regarding the pressure at the outlet of the nozzles and in the mixing chamber ($p_2 = p_4 = p_5$). In literature this value is always chosen considering a certain pressure different between the evaporative pressures. The value used in almost all the studies is $p_3 - p_4 = 0.3bar$. Before using the same value some simulations have been made in order to understand if there is an optimum value for this pressure and how the performance of the cycle varies.

Fig.2.30 and fig.2.31 shows how the COP of the system and the ejector efficiency vary against the pressure difference for different gas-cooler outlet temperatures. It can be seen that the lines concerning the COP are almost constant for each temperature, this means that the value of the pressure difference it not that important when the entire cycle is taken into consideration. However if we are looking at the ejector performance, the second figure shows that the ejector efficiency has a maximum value that is different for each gas-cooler outlet temperature. Considering that the COP is almost constant, it has been decided to follow the literature and use $p_3 - p_4 = 0.3bar$ for modeling the cycle with the purpose to avoid more complications in the ejector model. The optimization of the system was performed determining the gas-cooler pressure that gives the maximum system COP for the given condition. The COP based analysis represent only a first-law investigation. A second law investigation can be made on exergy base to reflect the behavior for each of the single components. Fangtian et al. [32] show in their paper that the exergy losses with an ejector cycle can be reduced by the 25% compared with the base cycle. An important consideration has also been made regarding the minimum value of the p_{lift}. After discussing with Kristian Fredslund[39] from Danfoss, it became clear that the minimum value of this parameter has to be at least 4 bar. This is because of the proper operation of the throttling valve that cannot work if the pressure difference is lower

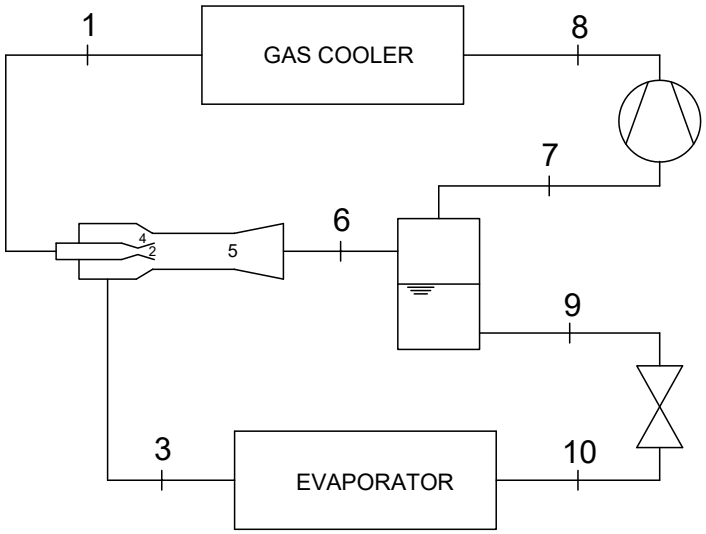

Figure 2.28 – Layout of the EERC.

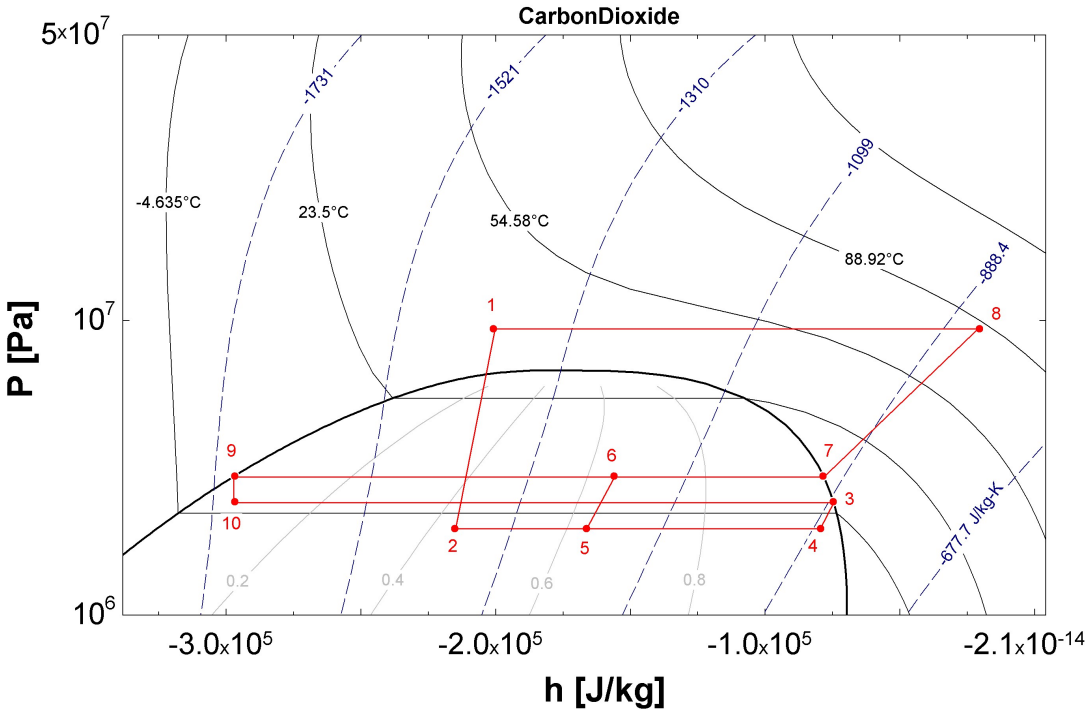

Figure 2.29 – logp-h diagram of the EERC.

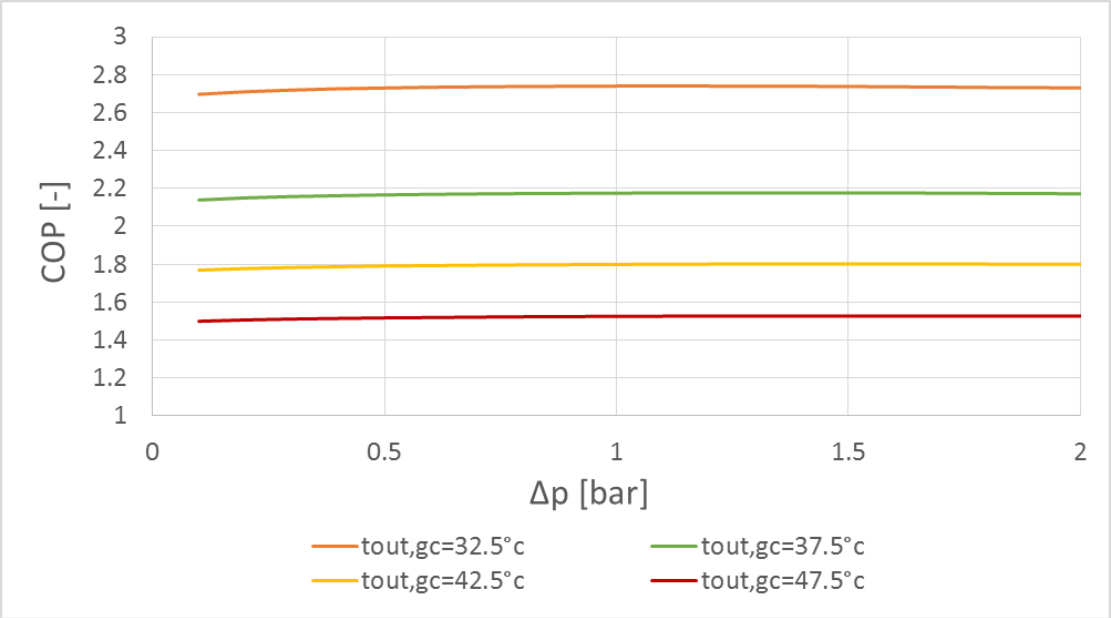

Figure 2.30 – COP vs ($p_3 - p_4$) (t_{ev}=-2°C).

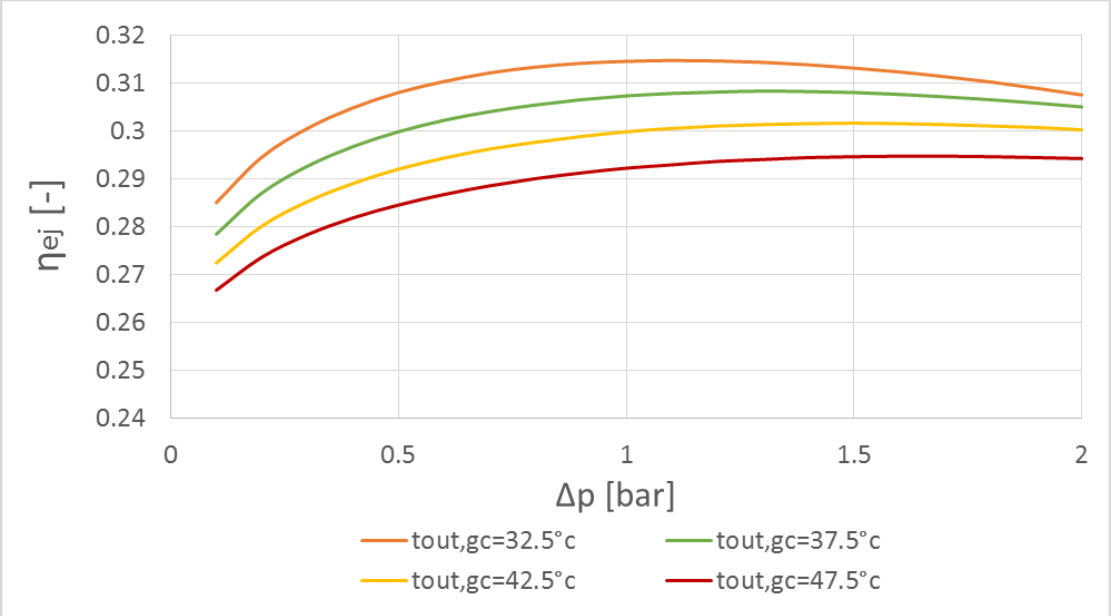

Figure 2.31 – η_{ej} vs ($p_3 - p_4$) (t_{ev}=-2°C).

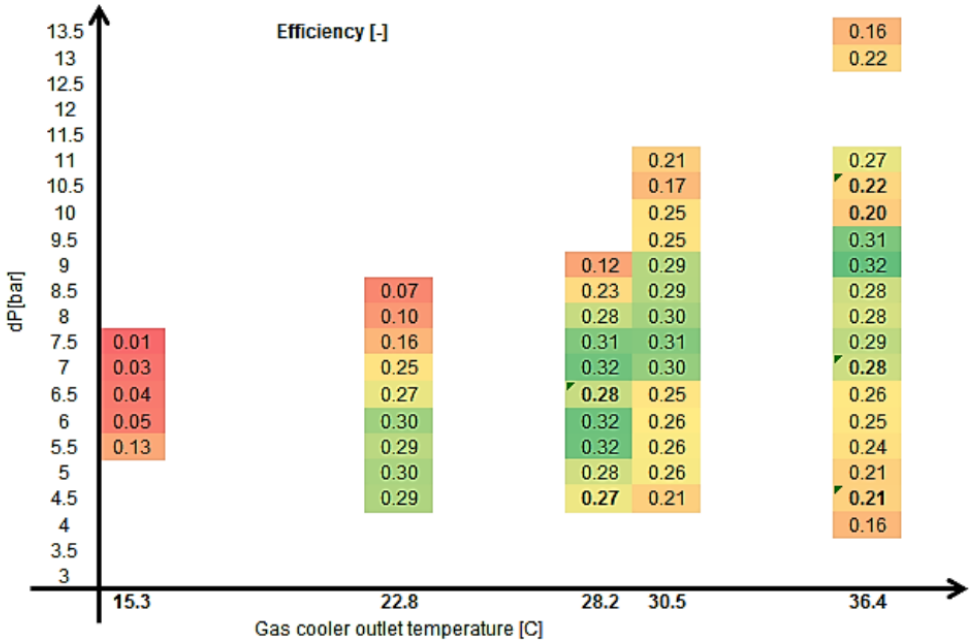

Figure 2.32 – Operation map of the ejectors based on experimental data, numbers represent the ejector efficiency[34].

than this value. It can be seen in the p-h diagram [2.31] that the pressure different through the expansion valve ($p_9 - p_{10}$) is the same pressure different defined as $p_{lift} = (p_6 - p_3)$ in the equation 2.23. Thus, to maintain 4 bar of pressure different, the ejector has to be able to ensure the same lift. Regarding the design conditions with transcritical operation this is not a problem since the gas-cooler pressure is high enough to let the ejector maintain an high pressure lift. The problem starts when the ambient temperature is lower than 25°C, the ejector is not able to ensure 4 bar of pressure lift and therefore has to be by-passed. This problem concerns the off-design condition of the model, it will be further discussed in chapter 4. To conclude this section a comparison of the theoretical ejector efficiency with a real one has been made in order to understand if the ejector model is close to the reality. The experimental data proposed by Kriezi and Fredslund [34] in fig.2.32 has been used (in the y axis dp means p_{lift}).

With these values it has been possible to make an interpolation in order to write the ejector efficiency in function of the p_{lift}. Fig.2.33 shows the results. The orange line is the theoretical ejector efficiency calculates with the equation 2.24, the blue line represent instead the real ejector efficiency calculated using the experimental data. The graph shows that for the values of p_{lift} from 7 bar to 10 bar the two lines are close, meaning that the model is following the real data, for values lower than 7 bar the lines gradually splits up.

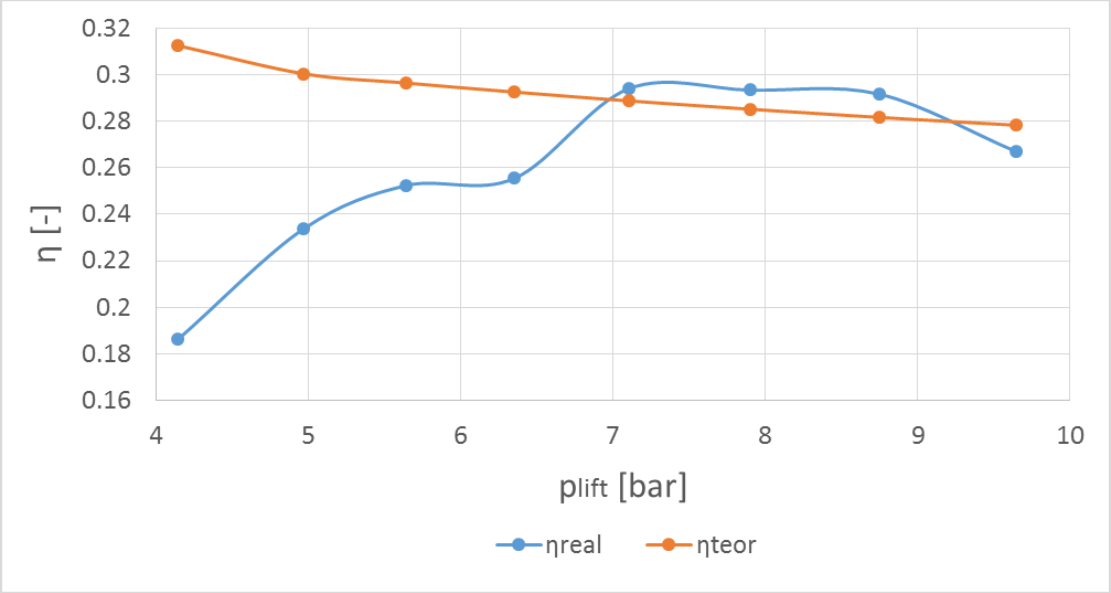

Figure 2.33 – Ejector efficiency vs pressure lift, comparison with the real data.

2.7.5 Results

Before presenting the results, the assumptions that have been made are summarized in the following table.

Evaporative temperature	-2°C
Gas-cooler pressure	optimized
Gas-cooler approach temperature difference	5°C
Ejector model	constant pressure model
Outlet nozzles pressure	0.3 bar less than evaporative pressure
Motive nozzle efficiency	0.8
Suction nozzle efficiency	0.8
Diffuser efficiency	0.75
Subcooling and superheating	0°C
Compressor isentropic efficiency	0.6
Fan power	neglected
Cooling capacity	100 kW

Tables 2.13 and 2.14 shows the main parameters of the cycle for different working conditions. It is important to repeat that the mixing pressure has been fixed at 0.3 bar lower than the evaporation pressure. The choice to fix it and not to optimized it has been made for the reason that the performance are barely affected by this value [2.30].

t_{ev}	t_{amb}	$p_{opt,gc}$	$p_{dis,ej}$	p_{lift}	$\eta_{ej,r}$	$\eta_{ej,t}$	COP	Pc
°C	°C	bar	bar	bar	-	-	-	kW
-2	27.5	81.2	38.01	4.97	0.2338	0.3006	2.719	36.78
	32.5	95.25	39.39	6.35	0.2555	0.2927	2.157	46.36
	37.5	109.3	40.94	7.90	0.2935	0.2853	1.783	56.09
	42.5	123.3	42.69	9.65	0.267	0.2784	1.511	66.18

Table 2.13 – EERC results: different ambient temperature.

t_{amb}	t_{ev}	$p_{opt,gc}$	$p_{dis,ej}$	p_{lift}	$\eta_{ej,r}$	$\eta_{ej,t}$	COP	Pc
°C	°C	bar	bar	bar	-	-	-	kW
42.5	2	121.9	46.53	9.79	0.2513	0.2779	1.647	60.72
	-2	123.3	42.69	9.65	0.267	0.2784	1.511	66.18
	-6	124.8	39.1	9.47	0.2829	0.2786	1.389	71.99
	-10	126.3	35.75	9.26	0.2976	0.2786	1.281	78.06

Table 2.14 – EERC results: different evaporation temperature.

2.8 Ejector expansion refrigeration cycle with two suction groups

In this section the ejector expansion refrigeration cycle will be modified in order to make it possible for a certain fraction of the secondary flow to skip the ejector after the evaporator. This modification has been suggested by Kristian Fredslund [39], with the aim to model a cycle as closer as possible to how a real refrigeration system is made. The basic idea is to use two compressors instead of one so the flow at the exit of the compressor can go through the ejector or can be directly compressed from the evaporative pressure to the gas-cooler pressure. The main purpose of this modification is to make it possible for a reduction of the suction flow when the primary flow is not able to ensure a minimum pressure lift of 4 bar. The real advantage of this cycle compared with the normal one is shown in the second part of the project. However in this part the cycle and the new equations that describe it will be presented. The ejector model is the same as described in section 2.7.

2.8.1 Description of the system

The flow diagram and the corresponding p-h diagram are showed in Fig.2.34 and Fig.2.35. The system is similar to the one seen in the last section. The flow coming from the gas-cooler (state 1) enters the motive nozzle and expands (state 2) until the same pressure of the mixing section ($p_2 = p_4 = p_5$). This pressure is considered constant and 0.3 bar below the evaporative pressure for the reasons explained previously [2.7]. The flow at the outlet from the evaporator (state 11) is divided into two different flows, the first one; the suction flow (state 3) expands in the suction nozzle until the mixing pressure and is then mixed with the primary flow. The second one (state 12) skips the ejector and is compressed until the gas-cooler pressure (state 13) by the secondary compressor. The mixed flow in (state 5) enters the diffuser in the ejector and its velocity decrease until almost a stagnation state while the pressure increase and the pressure lift is achieved (state 6). After this the fluid enters the separator where the vapour part (state 7) is compressed until the gas-cooler pressure by the main compressor (state 8) and then mixed with the flow coming from the secondary compressor. The flow (state 14) enters into the gas-cooler for then to reject the heat into the environment (state 14-1). Going back to the separator, the liquid part (state 9) is expanded in the throttling valve until the evaporative pressure and is then sent into the evaporator to achieve the cooling effect (state 10-11).

It has not been possible to find literature on a model like the one proposed here, all the equations that have been used to describe it have been found and checked by the author. In order to explain the equations describing the system it is necessary to introduce a new parameter, which tell how much of the evaporative flow skips the ejector. The factor is dimensionless and defined as the ratio of the mass flow skipping the ejector on the mass flow through the evaporator.

$$\varphi = \frac{\dot{m}_{12}}{\dot{m}_{11}} \tag{2.41}$$

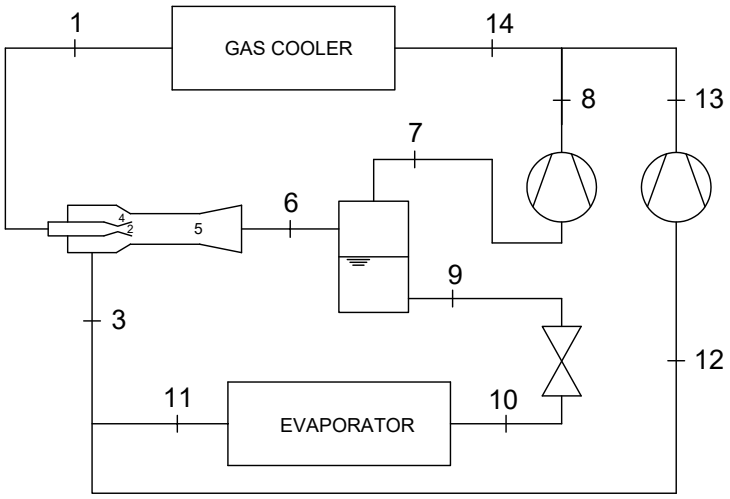

Figure 2.34 – Layout of the EERC with two suction groups.

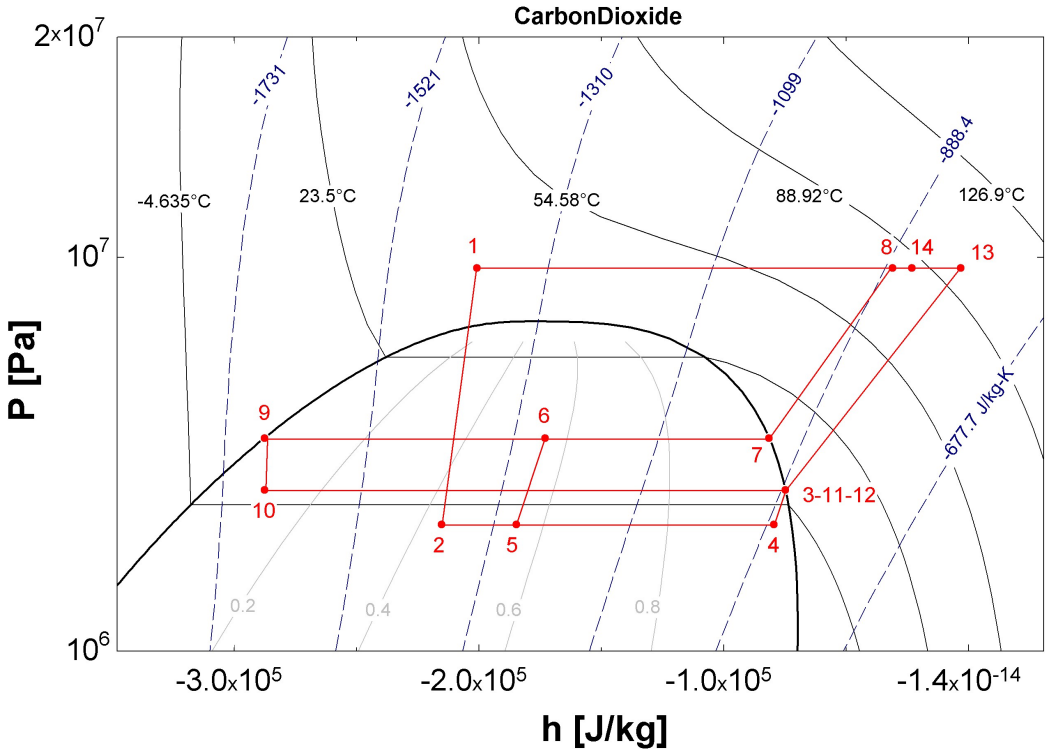

Figure 2.35 – logp-h diagram of the EERC with two suction groups.

The equations used to model the ejector are the same as in the previous section except for the last one, the equation describing the quality of the fluid at the exit of the ejector that ensure the cycle continuity [2.37]. With another flow in the cycle all the mass conservations have to be modified in order to take into consideration also the factor φ. The follow equation can be written.

$$x_{d,out} = x_6 = 1 - \frac{r}{(1+r)\cdot(1-\varphi)} \tag{2.42}$$

Using the definition of φ[2.41] and r[2.22], it is now possible to write all the equations describing the system performance per unit of mixture flow mass (the flow mass leaving the ejector) as followed. The cooling capacity per unit mixture flow mass is:

$$q_0 = \frac{r}{(1+r)\cdot(1-\varphi)} \cdot (h_3 - h_{10}) \tag{2.43}$$

The main compressor power consumption per unit mixture flow mass is:

$$w_{c,main} = \left(1 - \frac{r}{(1+r)\cdot(1-\varphi)}\right) \cdot (h_8 - h_7) \tag{2.44}$$

The secondary compressor power consumption per unit mixture flow mass is:

$$w_{c,sec} = \frac{r\cdot\varphi}{(1+r)\cdot(1-\varphi)} \cdot (h_{13} - h_{12}) \tag{2.45}$$

The heat rejected at the gas-cooler per unit mixture flow mass is:

$$q_0 = \frac{1}{1+r} \cdot (h_{14} - h_1) \tag{2.46}$$

And in the end the performance of the system can be written as:

$$COP = \frac{q_0}{w_{c,main} + w_{c,sec}} \tag{2.47}$$

2.8.2 System analysis

As explained in the previous section the second compressor added to the system makes it possible to skip the ejector, and here the consequences of this modification will be studied. The higher the φ is the lower the mass flow rate going through the ejector is. Fig.2.36 shows how the pressure lift varies against φ for different gas-cooler outlet temperature. It is possible to see that with higher values of φ the ejector ensures higher pressure lift. This is exactly the purpose of having two compressor, this modification will be made possible to be able to use the ejector also with low ambient temperature as will be shown in the chapter regarding the off-design conditions of the system.

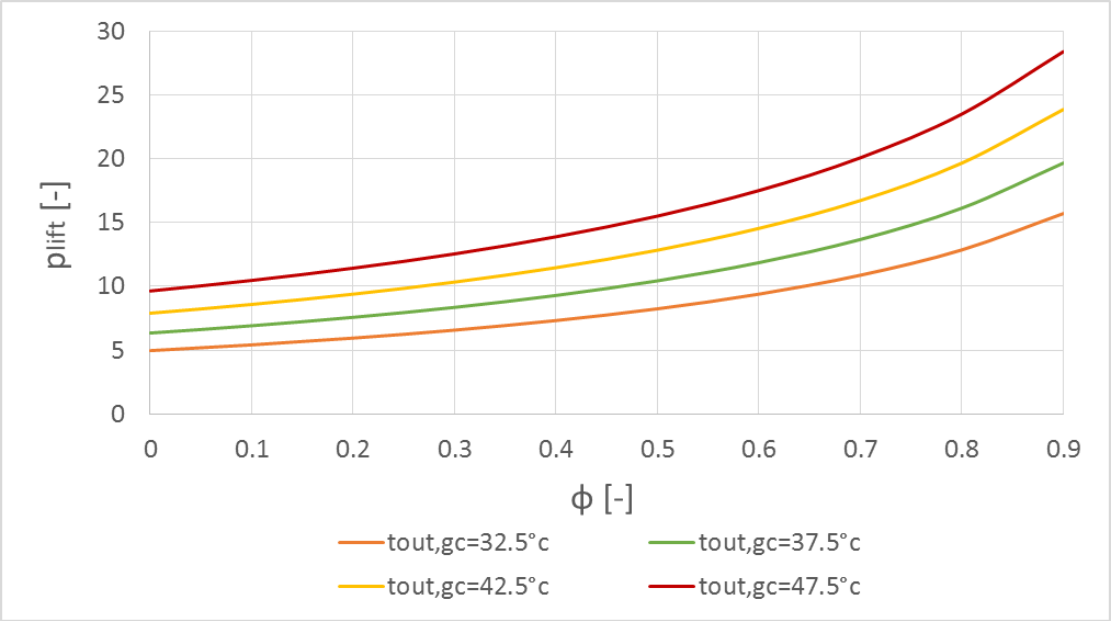

Figure 2.36 – Pressure lift vs φ.

2.8.3 Results

Before presenting the results, the assumptions that have been made are summarized in the following table.

Evaporative temperature	-2°C
Gas-cooler pressure	optimized
Gas-cooler approach temperature difference	5°C
Ejector model	constant pressure model
Outlet nozzles pressure	0.3 bar less than evaporative pressure
Motive nozzle efficiency	0.8
Suction nozzle efficiency	0.8
Diffuser efficiency	0.75
φ	optimized
Subcooling and superheating	0°C
Compressor isentropic efficiency	0.6
Fan power	neglected
Cooling capacity	100 kW

Tables 2.15 and 2.16 show the main parameters of the cycle for different working conditions. From the tables it is possible to see that the performances are similar to the ejector cycle with only one compressor. The real advantage of the modified cycle will be shown in the chapter regarding the yearly analysis.

t_{ev}	t_{amb}	$p_{opt,gc}$	φ_{opt}	$p_{dis,ej}$	p_{lift}	$\eta_{ej,t}$	COP	Pc
°C	°C	bar	-	bar	bar	-	-	kW
-2	27.5	81.2	0.6704	43.44	10.40	0.2586	2.773	36.06
	32.5	95.25	0.6309	45.41	12.37	0.2561	2.197	45.52
	37.5	109.3	0.5803	47.22	14.18	0.2542	1.813	55.16
	42.5	123.3	0.5121	48.77	15.73	0.2533	1.532	65.27

Table 2.15 – EERC with two suction groups results: different ambient temperature.

t_{ev}	t_{amb}	$p_{opt,gc}$	φ_{opt}	$p_{dis,ej}$	p_{lift}	$\eta_{ej,t}$	COP	Pc
°C	°C	bar	-	bar	bar	-	-	kW
42.5	2	121.9	0.4489	45.23	12.19	0.2598	1.664	60.10
	-2	123.3	0.5121	48.77	15.73	0.2533	1.532	65.27
	-6	124.8	0.5617	49.47	16.43	0.2463	1.413	70.77
	-10	126.3	0.6019	49.99	16.95	0.2391	1.306	76.57

Table 2.16 – EERC with two suction groups results: different evaporation temperature.

3 Design conditions: comparison

To conclude the first part of the project, the comparison of the results concerning the design condition operation are here presented. All the results come from computational simulation with the support of the software EES. All the cycles seen in chapter 2 are compared with the 1-stage CO_2 vapour compressor reference cycle under different points of view. All the observations presented in this chapter refer to the chosen operating conditions of the systems. Since the project is about a supermarket installation in Italy, as explained in the previous chapter the design ambient temperature has been chosen for simulate the worst case scenario, a really hot climate conditions with an ambient temperature of 42.5°C. The evaporation temperature and the cooling capacity are -2°C and 100kW respectively and concerning the dedicated mechanical subcooling a value of Δt_{sub}=10° has been chosen. Fig.3.1 shows the optimal gas-cooler pressure for all the cycles, excluding the cascade system since in this case the working condition are subcritical. The mechanical subcooling system is the one that permits the cycle to work with the lowest pressure ratio among the others (-14.9% for propane, -14.2% for R404A and -15.2% for R134a using the base cycle value as comparison), but also the PCE and the PCE with subcooling achieve a useful drop of the gas-cooler pressure, -5.6% and -5.2%. The optimization of the pressure for the ejector cycles gives the same results as the base cycle. Fig.3.2compares the performance for all the systems. At this high ambient temperature the cascade system, no matter which secondary fluid is used, reaches the best performance with a COP of 1.958 if R134a is used. In this case the COP increment is 63.7%, 60.3% for propane and 42.4% for R404a. The increase for the MS cycles is around 30%, 19.5% for the PCE and 28.2% for the ejector cycle with two suction groups. In the end Fig.3.3 compares the power consumption. The result are similar to the COP results, the largest power consumption drop is achieved by the cascade systems, -39% for the R134a, followed from MS cycles, ejector cycles and then the PCE cycle. Tab.3.1 summarizes the values discussed above.

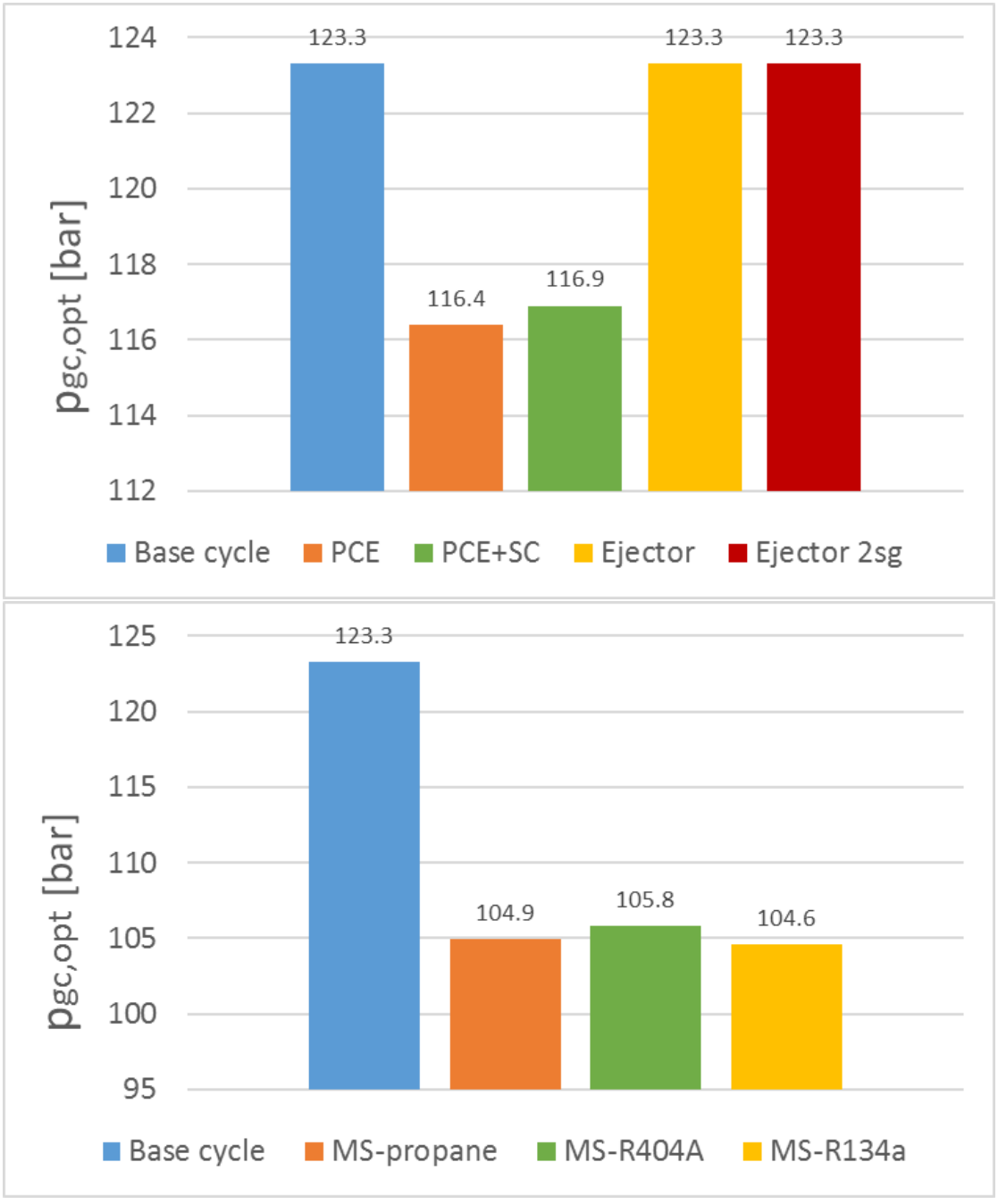

Figure 3.1 – Optimal gas-cooler pressure: comparison.

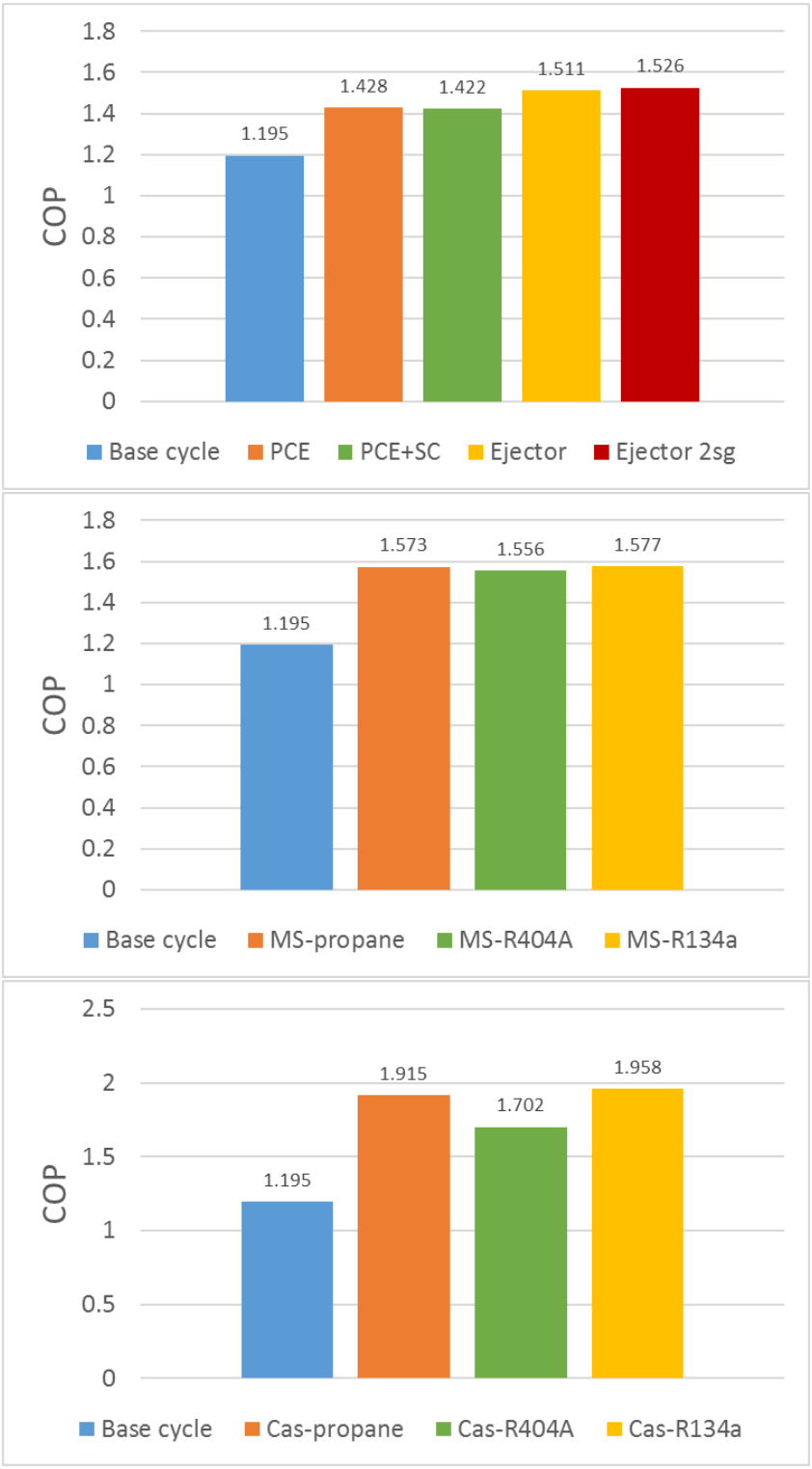

Figure 3.2 – COP: comparison.

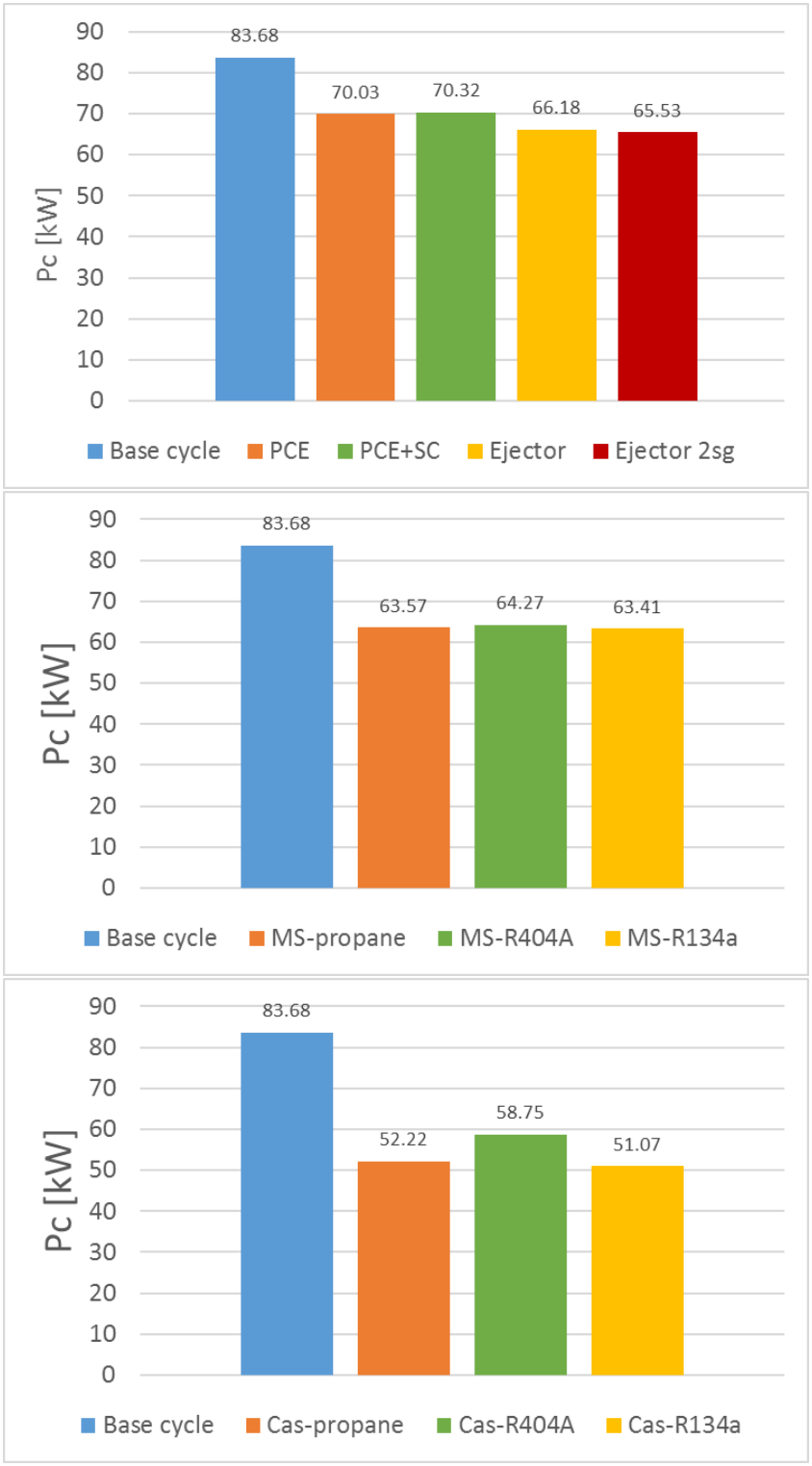

Figure 3.3 – Power consumption: comparison.

	$p_{opt,gc}$	COP	Pc	$p_{opt,gc,var}$	COP_{var}	$P_{c,var}$
	bar	-	kW	%	%	%
Base cycle	123.3	1.195	83.68	0.0%	0.0%	0.0%
PCE	116.4	1.428	70.03	-5.6%	19.5%	-16.3%
PCE sub	116.9	1.422	70.32	-5.2%	19.0%	-16.0%
MS propane	104.9	1.573	63.57	-14.9%	31.6%	-24.0%
MS R404A	105.8	1.556	64.27	-14.2%	30.2%	-23.2%
MS R134a	104.6	1.577	63.41	-15.2%	32.0%	-24.2%
Cas. propane	-	1.915	52.22	-	60.3%	-37.6%
Cas. R404A	-	1.702	58.75	-	42.4%	-29.8%
Cas. R134a	-	1.958	51.07	-	63.8%	-39.0%
Ejctor	123.3	1.511	66.18	0.0%	26.4%	-20.9%
Ejector 2sg	123.3	1.532	65.27	0.0%	28.2%	-22.0%

Table 3.1 – Design condition: comparison (t_{ev}=-2°C, t_{amb}=42.5°C,$\eta_{is,c}$=0.6).

4 Off-design conditions

In the first part of the project the systems were studied and compared for the same operating condition using some simple boundaries. The design operation model of a refrigeration system is an interesting tool to be able to have a preliminary idea of the behaviour of the system. However it is impossible that the cycle could work in the same condition the entire year. The hot sink for a refrigeration system (hot sink means the ambient where the gas-cooler or the condenser rejects the heat at high temperature) is the outdoor environment. The conditions of this environment can be considerably different passing from summer to winter; the performance can therefore change considerably. A refrigeration cycle must be able to deal with this changing and achieve the best performance for all the conditions for which it is subjected to. The purpose of this part of the project is then write a model for all the systems seen in the previous chapters in a way to be able to study the behaviour of them all throughout the year. In the first section the common boundaries conditions are presented. Following the system are described individually. At the end of the chapter (4.9) all the assumptions are summarized in separate tables in order to have a clear view on how all the cycles have been modelled. The models used to perform the analysis are reported in Appendix A.

4.1 Boundary conditions

In order to create a model as close as possible to a real system, some new and more specific boundary conditions have to be introduced and some of the ones that has used before will be changed. As done for the design condition models the entire system has been modelled based on the energy balance of every single component. Steady flow energy equations have been used for each of the different cycle and specific energy quantities are used. Following are the conditions that have not been changed.

- Steady-state processes.
- Isenthalpic expansion.
- Pressure drop and heat losses are neglected.

- The processes in the heat exchangers are considered isobaric.
- The fluid at the outlet of the evaporator is considered saturated vapor.
- Superheat before the compressor is neglected.
- Separation and mixing process are isobaric.

Now all the new and more specific boundaries conditions will be reported and discussed. First of all the compressor efficiency will be discussed. For the design condition investigation the isentropic efficiency of all the compressors was kept constant at a value of 0.6. It has been known that this efficiency varies against the pressure ratio. In order to write a model where the high pressure is continuously changing it is necessary to calculate the efficiency as a function of the pressure ratio. As suggested by Ersoy et al.[33] the CO_2 compressors efficiency could be calculated as followed:

$$\eta_{is} = 1.003 - 0.121 \cdot r_p \tag{4.1}$$

This is obtained by finding the best fit for the experimental data of a Danfoss carbon dioxide compressor. To collect other information about the real compressors the web-program made available by the German company Bitzer [40] was used. Some simulations using the Refprop database [41] linked with Excel have been made. The results are reported in fig.4.1. The blue line fits the results from the Danfoss compressor and the orange one fits the results from the Bitzer compressor. The trend is similar for low pressure ratio and is diverging a bit when this one increases. The results are comparable and for the models the equation proposed by Ersoy et al. has been used. The evaporation temperature has been set to -4°C and kept constant for all the operative conditions. This choice has been made considering a medium temperature load for a supermarket. For a CO_2 evaporator, -2°C is a good value to keep the temperature in the fridges low enough to permit a good conservation of the food. In order to be on the safe side it has been decided to use a temperature a little lower. The ambient temperature is considered a given input for all the cycles and can vary in a wide range. The realistic temperature profiles for Milan and Naples will be discussed more in details in the last chapter of this part of the project. A particular consideration has to be made about the switch from transcritical operation to subcritical operation and vice versa. The cycle has been modelled in order to avoid every kind of step in the power consumptions or in the performance of the system. This decision has been taken after talking with Kristian Fredslund[39], he advised to proceed in this way because the experimental data from real system suggest that there is no kind of rough step in the parameters. The behaviour of the system is different because of the translation from the gas-cooler to the condenser and a certain switch temperature has been set. This temperature is not the same for all the cycles due to the different operative conditions. Concerning the EES models this temperature has been used in an IF-ELSE cycle to switch from transcritical to subcritical operation, however it is not important for the results, but only for the correct operation of the model. Regarding this, appendix B shows how the most important variables of the studied cycles change passing from a subcrtitical working condition to a supercritical

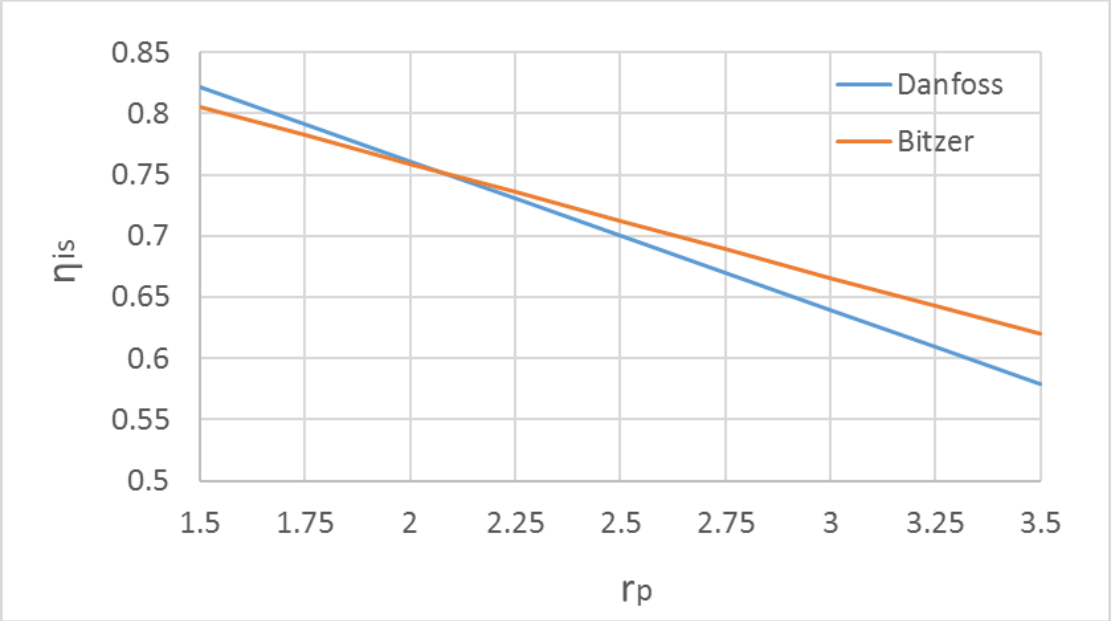

Figure 4.1 – Compressor isentropic efficiency vs pressure ratio.

one. Another change compared to the design condition models regards the gas-cooler outlet temperature. In the design condition chapter a fixed value of temperature difference from the ambient temperature has been used to find the gas-cooler outlet temperature. Now, the same approach will be used for both the gas-cooler and the condenser (while operating in the subcritical region), but with a different value. Some experimental data have been made available by Kristian Fredslund[39]. Fig.4.2 presents the data measured in a real CO_2 plant, the supermarket CCAmort located in Spiazzo, Italy. The graph shows the $\Delta t_{out,gc}$ against the ambient temperature for every minute of the day, from July 2015 to October 2015. Darker is the "cloud", more points are located there. It's possible to see that the most of the point are located between 0°C and 5°C, the orange line is the linear trend. The line is almost constant all along the ambient temperature interval and the corresponding value of $\Delta t_{out,gc}$ is 1.7°C. To be in safety side it has been decided to use a constant value of temperature difference of 3°C. The fan power related to the gas-cooler/condenser heat exchange has been taken into consideration using a simple rule of thumb. It has been supposed that the power needed by the fan is 3% of the thermal flux through the gas-cooler or condenser. In the end, in order to permit the cycle to work also at low ambient temperature, the minimum condensation temperature has been setted to 10°C for all the systems. This value and the associate pressure ensure a minimum pressure difference for the good operation of the throttling valve and the compressor.

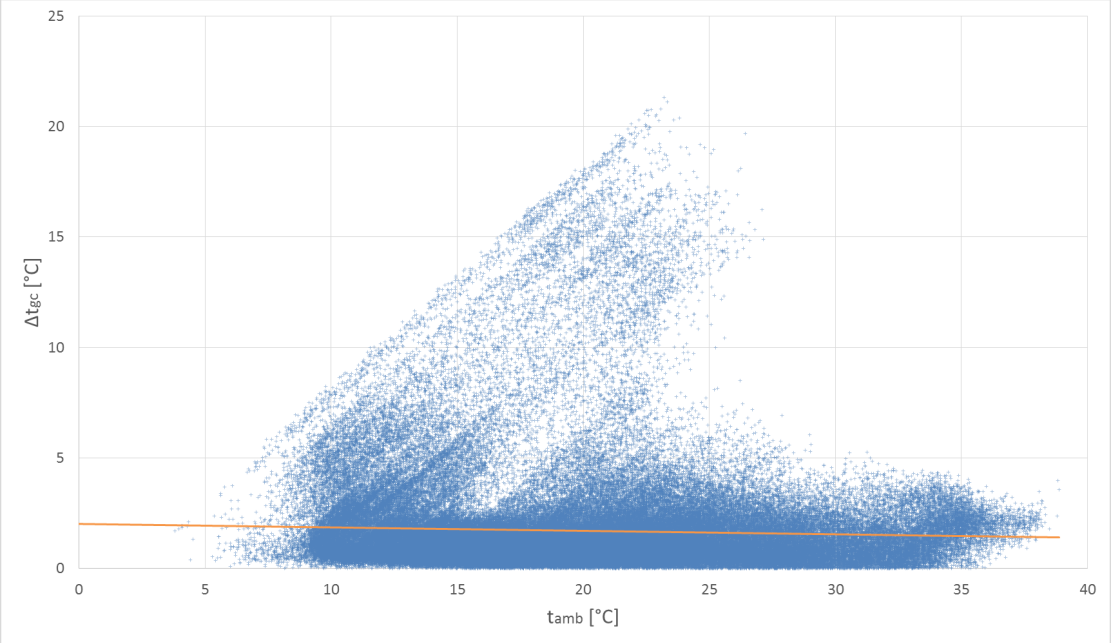

Figure 4.2 – $\Delta t_{out,gc}$ vs t_{amb}: experimental data.

4.2 Base CO_2 refrigeration cycle

The CO_2 1-stage vapour-compression cycle was introduced in chapter 2.2. This cycle is the base cycle and it will be used as a reference also for the yearly analysis of the systems. In this way it will be possible to understand which of the proposed solutions ensure the biggest amount of energy saving. The system has been modelled following the boundary conditions explained in the previous section. As already introduced the system switch automatically from the subcrtitical operation to the supercritical operation at a certain temperature around 25°C. When running transcritical the cycle is provided with a gas-cooler, an expansion valve, an evaporator and a compressor, while when is running subcritical the gas-cooler is replaced by the condenser. During transcritical operation the gas-cooler pressure is optimized every time that the ambient temperature, and consequently the gas-cooler outlet temperature, changes, using a function that permit to found the best value for every condition. This modus operandi will be used for all the systems. Concerning the base cycle the function used was found in literature and is the same equation introduced in section 2.2, eq.2.2, proposed by Liao et al. [16]. For the other systems has not been possible to find a correlation in literature, then a linear equation fitting the optimized results of the design condition has been used for each system. This permits to avoid using of the min/max function in EES and make the model faster. Obviously during subcritcal operation there is no need to optimize the pressure since this one is linked to the condensing temperature.

4.3 Parallel compressor economization

The CO_2 vapour compression cycle with parallel compressor economization (PCE) was introduced in chapter 2.3. The cycle showed promising results for what concern the design condition operation of the system, so it is right to think that it will achieve good performance also during the off-design operation. The cycle, respect to the base one, presents an additional compressor, an additional expansion valve and the separator. The efficiency of both the compressors is calculated in the same way. Obviously for a certain working condition the two efficiencies will be different since they are working between different pressure level(see appendix B). In fact, the main one compresses the fluid from the evaporative pressure to the gas-cooler/condensing pressure while the secondary one from the separator pressure to the gas-cooler/condensing pressure. Thus the second one is working with a lower pressure ratio and then with higher efficiency. During transcritical operation the gas-cooler pressure has been optimized using an equation that is a linear interpolation of the results found with the design model. Obviously no optimization is required when the system runs subcritical. The separator pressure has been calculated in the way to follow the optimization made in the design condition model but also to ensure a minimum pressure difference of 4 bar across the throttling valve for every working condition. This is necessary to have a proper functioning of this device. It has been chosen then to set two limits, 40 bar if the ambient temperature is lower or equal to 10°C and 55 bar if the ambient temperature is higher then 42.5 °C. A linear interpolation has been made between these two values. It's important to say that the upper limit has been setted because of a mechanical resistance problem. In fact this device have a maximum pressure which can stand, over its the separator can broke. The choice of take the value of 55 bar has been made on suggestion of Kristian Fredslund[39] in order to follow the way which this component works in a real system. The last assumption concerning this system regards the swept volume of the secondary compressor. A compressor can not work in every condition, when the volume flow through it is less then 12% of the swept volume it is not able to operate in the right way. The max swept volume required has been taken at the design condition point, with an ambient temperature of 42.5°C. After some simulations has been found out that the minimum temperature which the compressor can work is 15°C. Below this temperature the secondary compressor has to be by-passed. The system become then a base CO_2 cycle when working at low temperature.

4.4 Parallel compressor economization with recooler

The CO_2 vapour-compression cycle with parallel compressor economization and recooler was introduced in chapter 2.4. It has been showed that using an efficiency of 0.7 for the subcooler leads to achieve lower performance than the PCE system without subcooling. This kind of behaviour is expected for all the working conditions, then the performance will be always worse respect to the PCE. To be sure of this fact the cycle has been modelled also for the off-design conditions and the consideration made for the PCE in the previous section are valid. Obviously regarding the gas-cooler pressure a different function has been used. The

subcooler efficiency has been supposed to be constant for all the working conditions. With these assumptions it has been found that the performances of the system are worse than the PCE cycle for every climate conditions. For this reason from now on the PCE cycle with recooler will not be taken into consideration anymore.

4.5 Refrigeration system with mechanical subcooling

The CO_2 vapour-compression cycle with dedicated mechanical subcooling was introduced in chapter 2.5. The behaviour of the system is not different from how it has been showed in the design condition. The subcooling loop provides a further cooling after the gas-cooler or, during the subcritical operation, after the condenser. In order to make the model not too complicated the analysis is based on a fixed temperature difference between the evaporation temperature of the secondary cycle and the gas-cooler outlet temperature, or the condenser temperature, of the primary cycle. This temperature difference has been called Δt_{sub} and it is not constant. In order to have a model similar to a real system the choice to vary this temperature difference from 2.5°C to a maximum of 10°C has been made. More precisely the maximum value is used if the ambient temperature is equal or above 42.5°C, the minimum one, 2.5°C, is used when the ambient temperature is 12.5°C. Between these two temperatures a linear interpolation has been used. In the end, if the ambient temperature is lower than 12.5°C the subcooler is skipped and the system become a normal 1-stage vapour-compression cycle. Moreover, the system when working in transcritical conditions has been optimized finding the optimal gas-cooler pressure every time that the ambient temperature changes. Like said for the other cycles no optimization is required when the system runs subcritical. Regarding the secondary loop, the condenser temperature has been always fixed to be 8°C lower than the ambient temperature. No restrictions have been taken into consideration concerning the minimum pressure difference across the throttling valve and the compressor. This choice has been made to see which are the best results that this system can achieve. The fluids used for the secondary loop are the same seen before: R404A, R134a and propane. Regarding the secondary cycle compressor, an equation to find the isentropic efficiency in function of the pressure ratio has been used. The same equation proposed by Llopis et al.[25] has been used for all the three fluids and is defined as follow:

$$\eta_{is} = 0.95 - 0.1 \cdot r_p \tag{4.2}$$

4.6 Cascade system

The cascade system was previously introduced in chapter 2.6. The off-design model of the system follows the guidelines already explained. The secondary fluids used are the same reported before: R404A, R134a and propane. In this case there is no need to pass from subcritical operation to transcritical since the CO_2 loop, the low temperature cycle, works in subcritical mode whatever the ambient temperatures is. The working principle of the system

is the same, the cooling effect is achieved in the CO_2 cycle, the rejecting heat is transferred from the CO_2 condenser to the secondary cycle evaporator and in the end rejected to the ambient in the condenser of the secondary loop. Also in this case the analysis is based on a fixed temperature difference between the evaporation temperature of the secondary cycle and the condenser temperature of the CO_2 cycle. This temperature difference is fixed to 5°C and kept constant for all the working conditions. The CO_2 condensing temperature has been optimized every time that the ambient temperature changes using a function that give as result the best value for every outdoor condition. The function is a linear interpolation of the optimized values found with the design model. The condensing temperature of the secondary fluid is supposed to be 8°C higher than the ambient temperature. Also in this system no particular restrictions have been taken into account regarding the secondary loop. The only restriction, like done for the CO_2 cycle , was to set a minimum condensing temperature at the value of 15°C in order to maintain the right functioning of the system. Regarding the compressor efficiency the same equations introduced and commented in chapter 4 and 4.5 have been used.

4.7 Ejector expansion refrigeration cycle

The ejector expansion refrigeration cycle was previously presented in chapter 2.7. The components of the system are the same already introduced. Moreover the ejector has been modelled in the same way and the isentorpic efficiencies have been kept constant for all the working conditions. This might be a non-realistic assumption considering that *"the ejectors perform poorly away from their design point"*[35]. Anyway, the purpose of the study is not focused on the ejector model, but in the system model and as seen in the design condition part the theoretical efficiency of the ejector is always comparable with the real one, this mean that the model is not so far from the reality. The gas-cooler pressure has been optimized during transcritical operation, while the mixing pressure has been fixed and kept constant to 0.3 bar lower than the evaporative pressure (see chap.2.7). As explained before the ejector can work only if it is able to ensure a minimum pressure lift of 4 bar. This constriction is due to the throttling valve placed before the evaporator that need at least 4 bar of pressure different to work. Then some simulations have been carried out in order to figure out if it is possible use the ejector for all the ambient temperatures. Fig.4.3 show the trend of the pressure lift against the ambient temperature. It's possible to see that the value of the pressure is lower than 4 bar when the ambient temperature is lower than 25°C. This means that the cycle can't work with the ejector under this value of temperature. Thus, if the ambient temperature is below 25°C the ejector has been by-passed and the system become a normal CO_2 1-stage vapour compression cycle.

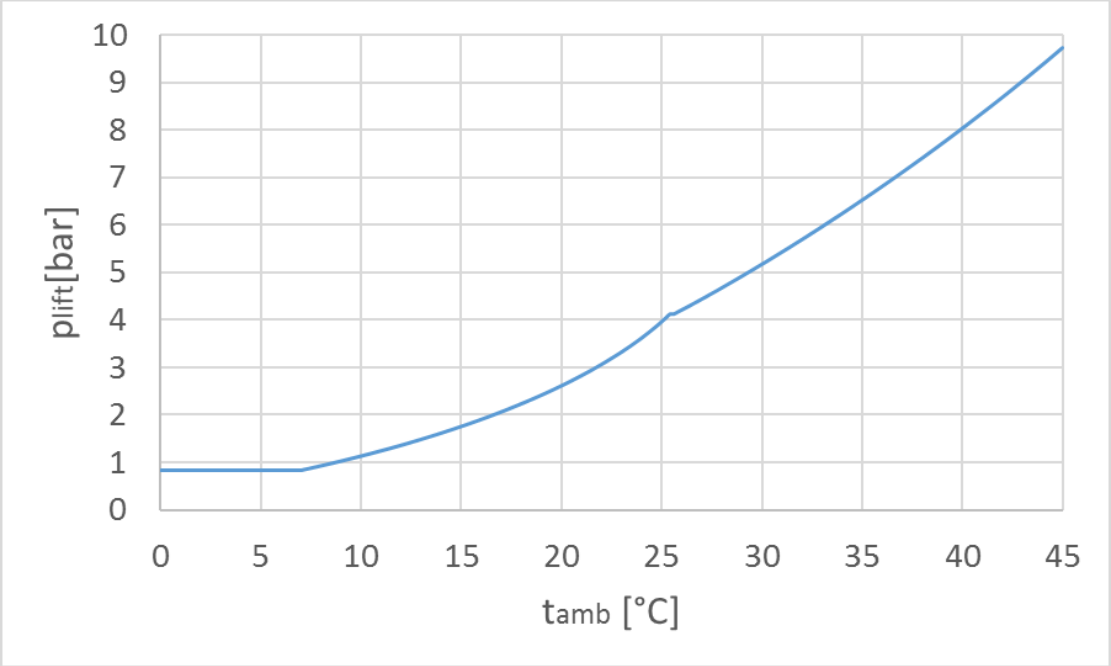

Figure 4.3 – Pressure lift vs ambient temperature.

4.8 Ejector expansion refrigeration cycle with two suction groups

The layout of the ejector expansion refrigeration cycle with two suction groups and all the features about it were presented and commented in chapter 2.8. In the design condition part was explained that the modification of the normal ejector cycle was taken into consideration looking forward to the off-design conditions. Now it will be showed how adding the second compressor improves the performance of the system. Regarding the optimal gas-cooler pressure and the mixing pressure the same considerations made for the base EERC are still valid. The new variable in this cycle is the parameter which tell how much of the evaporative flow skips the ejector. The factor, called φ, is dimensionless and defined as the ratio of the mass flow skipping the ejector on the mass flow through the evaporator(see eq.2.41). An optimization of φ in order to achieve the best performance for every outdoor condition has been carried out and the results are showed in fig.4.4. Rewriting the model in order to follow the optimization of φ, the results showed in 4.5 has been found. It's possible to see that the pressure lift is lower than 4 bar if the ambient temperature is below 16°C. This means that the cycle can't work in this way because of the reason explained in the previous section. Contrary to what has been done for the normal ejector cycle, i.e. skipping the ejector and use a normal expansion valve, in this case is possible to vary the value of φ in order to ensure a minimum pressure lift of 4 bar also if the temperature is below 16°C. The model has then been written optimizing the value of φ but also putting a restriction to the pressure lift. The results achieved are showed in fig.4.6. The graph shows that for temperature below 16°C the value of φ increases, keeping then the pressure lift above the minimum value of 4 bar

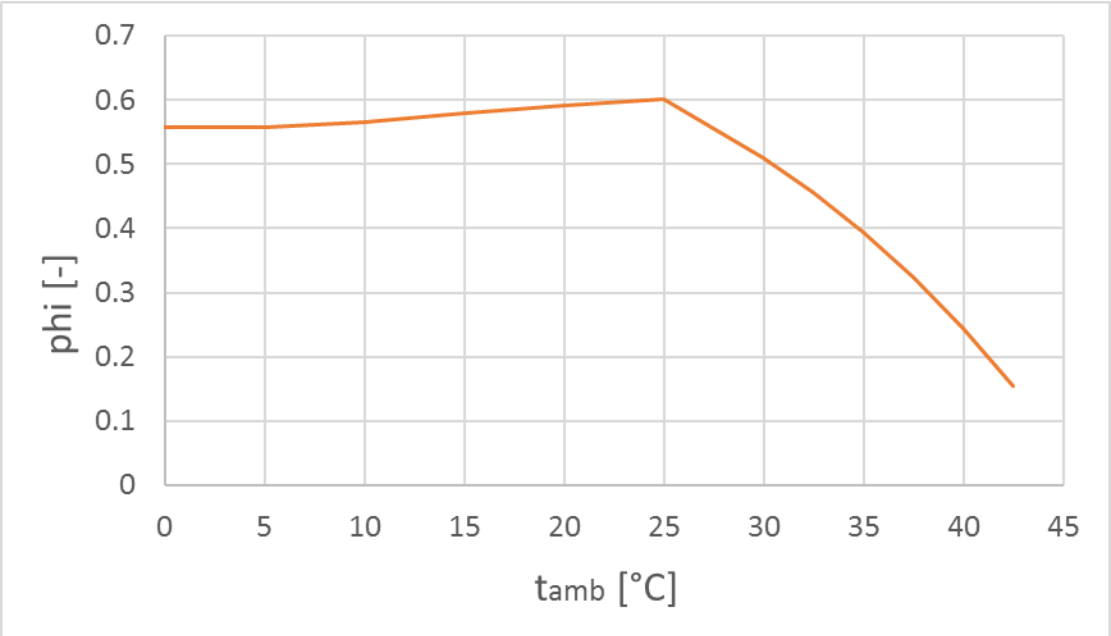

Figure 4.4 – Optimized φ vs ambient temperature.

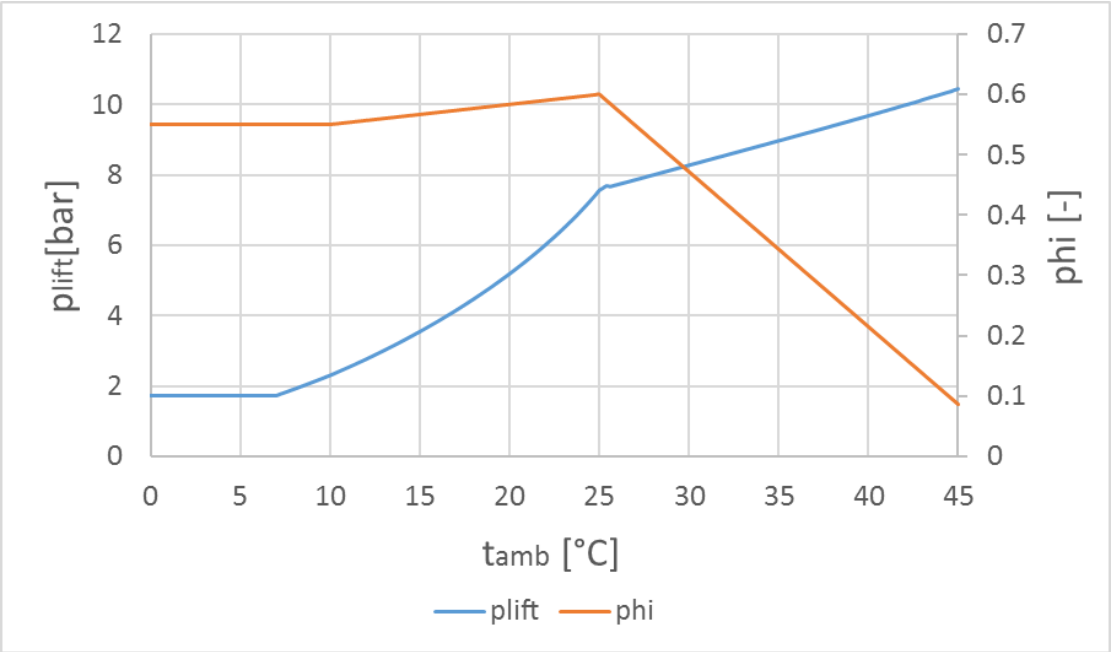

Figure 4.5 – Pressure lift and φ vs ambient temperature (no restriction on p_{lift}).

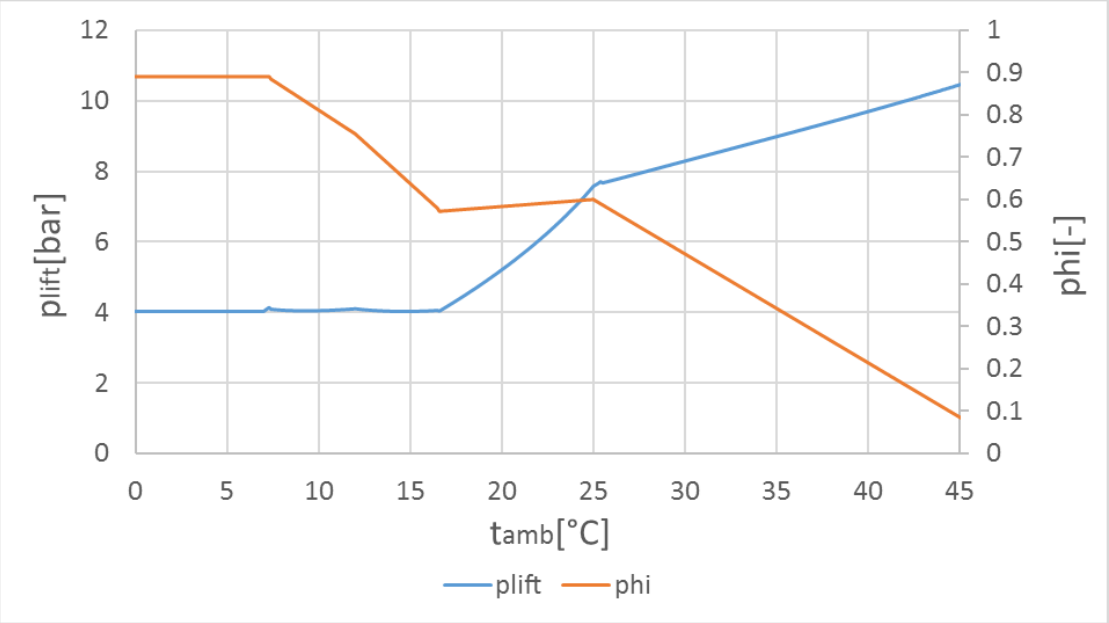

Figure 4.6 – Pressure lift and φ vs ambient temperature (with restriction on p_{lift}).

and ensuring the minimum pressure difference across the throttling valve placed before the evaporator. Like done for the parallel compression economization cycle, a last assumption concerning the swept volume of the secondary compressor has to be taken into consideration. The compressor after the separator can not work in every condition, in fact when the volume flow through it is less then 12% of the swept volume it is not able to ensure the lift. Using the same approach seen before, the max swept volume required has been fixed at the design condition point, when the ambient temperature is 42.5°C. After some simulations has been found out that the minimum temperature which the compressor can work is 11°C. Below this temperature the separator can not be used and has to be by-passed, so the ejector. The system become then a base CO_2 cycle when working at temperature lower than 11°C.

4.9 Assumptions summary

Before proceeding with the comparison of the systems all the boundaries conditions and the assumptions are summarized in the following tables.

Basic cycle	
Evaporative temperature	-4°C
Gas-cooler pressure	optimized
Gas-cooler/condenser approach temperature difference	3°C
Minimum condensing temperature	10°C
Subcooling and superheating	0°C
Compressor isentropic efficiency	polynomial, f(pressure ratio)
Fan power	3% of the rejected heat

Parallel compression economization	
Evaporative temperature	-4°C
Gas-cooler pressure	optimized
Gas-cooler/condenser approach temperature difference	3°C
Economizer pressure	linear interpolation 40 bar @ t_{amb}=10°C and lower 55 bar @ t_{amb}=42.5°C and higher
Secondary compressor	skipped for t_{amb}<15°C
Minimum condensing temperature	10°C
Subcooling and superheating	0°C
Compressor isentropic efficiency	polynomial, f(pressure ratio)
Fan power	3% of the rejected heat

Mechanical subcooling	
Main cycle	
Evaporative temperature	-4°C
Gas-cooler pressure	optimized
Gas-cooler/condenser approach temperature difference	3°C
Δt_{sub}	linear interpolation 2.5°C @ t_{amb}=12.5°C 10°C @ t_{amb}=42.5°C and higher
Subcooler	skipped for t_{amb}<12.5°C
Superheating	0°C
Minimum condensing temperature	10°C
Secondary cycle	
Condenser approach temperature difference	8°C
Evaporator approach temperature difference	5°C
Minimum condensing temperature	15°C
Subcooling and superheating	0°C
Compressor isentropic efficiency	polynomial, f(pressure ratio)
Fan power	3% of the rejected heat

Cascade system	
Main cycle	
Evaporative temperature	-4°C
Condenser pressure	optimized
Secondary cycle	
Condenser approach temperature difference	8°C
Evaporator approach temperature difference	5°C
Minimum condensing temperature	15°C
Subcooling and superheating	0°C
Compressor isentropic efficiency	polynomial, f(pressure ratio)
Fan power	3% of the rejected heat

Ejector cycle	
Evaporative temperature	-4°C
Gas-cooler pressure	optimized
Gas-cooler/cond. approach temperature difference	3°C
Minimum condensing temperature	10°C
Ejector model	constant pressure model
Outlet nozzles pressure	0.3 bar less than evaporative pressure
Motive nozzle efficiency	0.8
Suction nozzle efficiency	0.8
Diffuser efficiency	0.75
Subcooling and superheating	0°C
Compressor isentropic efficiency	polynomial, f(pressure ratio)
Fan power	3% of the rejected heat

Ejector cycle with two suction groups	
Evaporative temperature	-4°C
Gas-cooler pressure	optimized
Gas-cooler/cond. approach temperature difference	3°C
Minimum condensing temperature	10°C
Ejector model	constant pressure model
Outlet nozzles pressure	0.3 bar less than evaporative pressure
Motive nozzle efficiency	0.8
Suction nozzle efficiency	0.8
Diffuser efficiency	0.75
φ	optimized, with limit to granted a minimum Δp of 4 bar through the expansion valve
Secondary compressor	skipped for t_{amb}<11°C
Subcooling and superheating	0°C
Compressor isentropic efficiency	polynomial, f(pressure ratio)
Fan power	3% of the rejected heat

5 Off-design conditions: comparison

This chapter provides a comparison of the CO_2 cycles from the performance coefficient and the power consumption point of view. The COP and the power consumption of the systems will be compared in a wide range of ambient temperature in order to have a preliminary idea of which one can achieve the best results in the yearly analysis. In the previous chapter all the features about the off-design condition models of the studied systems have been presented and commented. New and more specific boundary conditions have been setted in order to make the models closer as possible to the reality. It is important to say that the comparison concerning the power consumption has been made using a constant cooling load of 100kW for every working condition, this approach make the comparison more clear and simpler to understand. A real cooling load will be presented and used in the next chapter, the one concerning the yearly analysis of the system. Fig.5.1 shows how the COP of the studied cycles varies against the ambient temperature. First thing to say it is that from now on, regarding the dedicated mechanical subcooling cycle and the cascade system, only the results about the cycles using propane as secondary fluid will be reported. This choice has been taken in order to make the presentation of the results more clear. The propane has been chosen between the others because of the high performance (higher than the R404A and comparable with the R134a, see chapter 3) and because it is a natural refrigerant like the carbon dioxide. Moreover, in the figure there is not the line concerning the parallel compressor economization cycle with the recooler because, like said before, it has always lower performance than the normal PCE cycle. Then again, to make the results more clear to read and study, the trend of the COP of this system is not reported. Focusing on the high temperatures side of the graphs, it is possible to notice that the COP of the cascade system is higher than all the other, followed by the MS cycle, the ejector cycle, the PCE cycle and in the end the base one. Obviously these results are comparable with those found during the design condition study. More interesting is the lower temperatures range. The cascade system (red line) has very low performance compared with the other systems when the ambient temperature go below 25°C. This happens because of the intermediate heat exchanger that adds irreversibility losses to the cycle. This means that the cascade system worth only if the temperature difference between the hot sink and the cold sink is high. Going down with the ambient temperature it's possible to see that the best results

are achieved by the ejector cycle with two suction groups (green line), since it has the benefits of both the ejector and the parallel compression. This is true until 11°C, below this value the ejector and the separator have to be by-passed because of the constriction on the minimum volume flow across the compressor. The control system make the system switch to the base one if the minimum volume flow is not ensured. The parallel compression economization cycle (orange line) achieves good results until 15°C, then the performance drop for the same reason just explained. The normal ejector cycle (green line) has good performances until 25°C then, like said in the previous chapter, after this value the COP drops because of the by-pass of the ejector. In fact the control system does not allow the separator pressure to be less than 4 bar higher than the evaporation pressure. This regards the already introduced minimum pressure difference across the expansion valve that allows a proper functioning of the device. If this pressure difference is below 4 bar the system switches to the base cycle. Same behaviour is showed for the system with dedicated mechanical subcooling (yellow line), for temperature lower than 12.5°C the subcooler is by-passed and the COP become the same of the base cycle one. Fig.5.2 shows the trends of the power consumption for all the cycle compared with the base one. A constant cooling load of 100kW has been used to built the graphs so the considerations made for the previous figure are still valid. The difference between this figure and the one showed before is that the gaps between the trends are smaller when the ambient temperature is low and bigger when the temperature is high. This means that the improved systems achieve higher COP during transcritical operation compared with the reference cycle and the power consumption saving is even better. This fact is very important since the purpose of the thesis is find how to modify the base CO_2 cycle in order to make it worth also in place with hot climate condition.

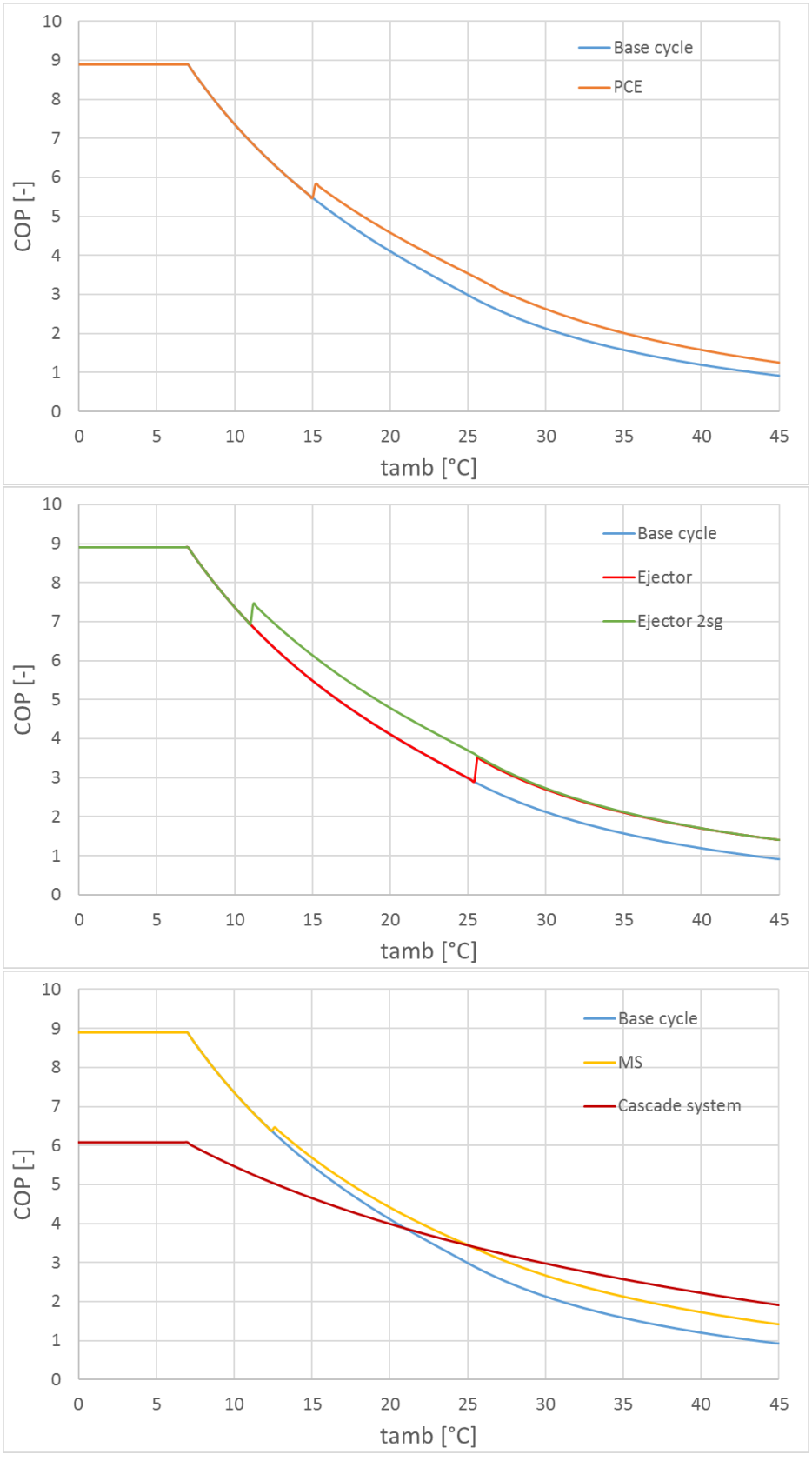

Figure 5.1 – COP vs t_{amb}: comparison.

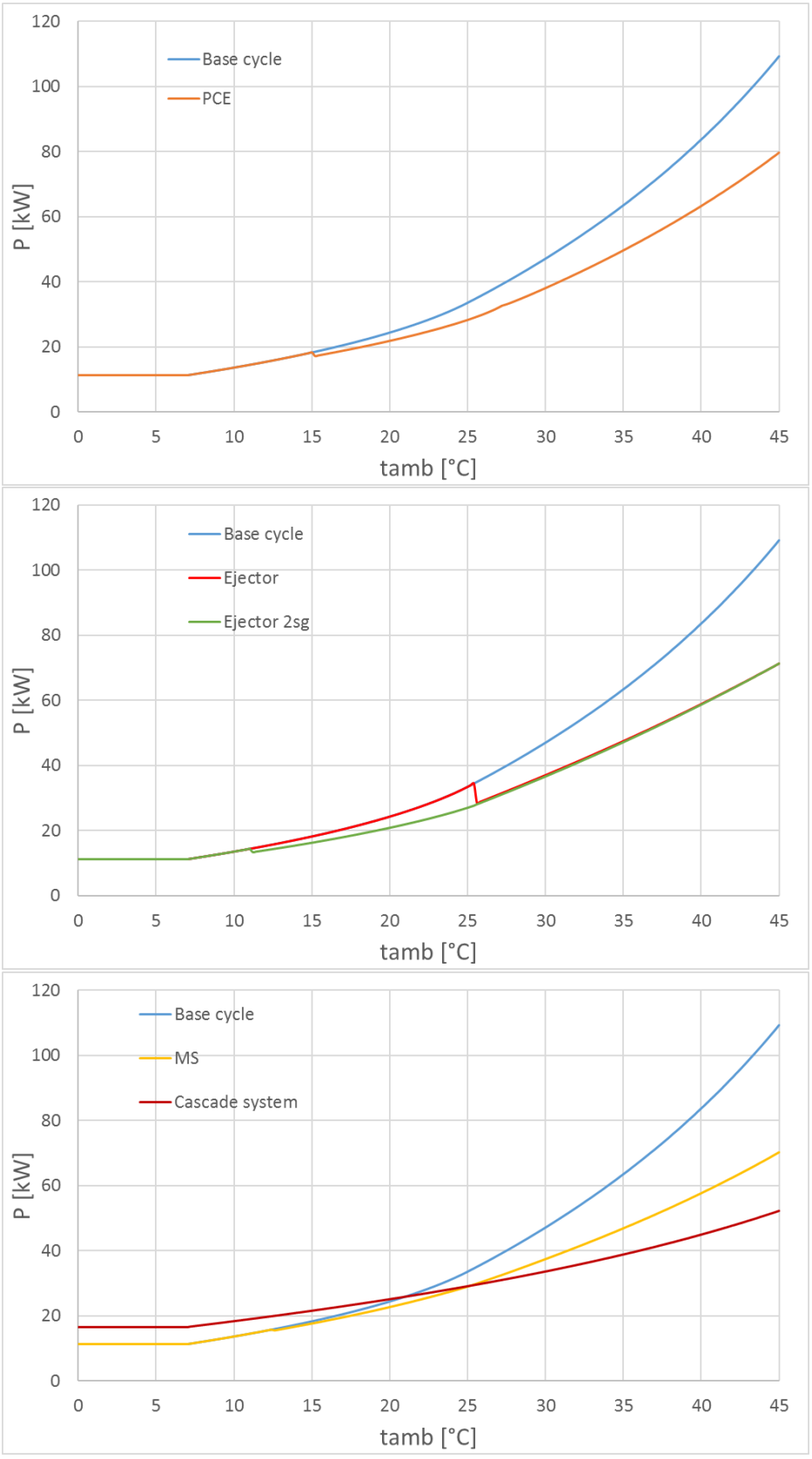

Figure 5.2 – Power consumption vs t_{amb}: comparison (constant cooling load of 100kW).

6 Yearly analysis

This chapter is the main part of the report since the yearly analysis of the systems will be performed. The systems under consideration are meant to bring improvement to the base cycle while operating in hot climates. All the solutions taken into account were proved to have higher performances than the 1-stage vapour compression reference cycle when operating in the design conditions. Moreover, the study of the COP in a wide range of ambient temperature proved that the improved systems are better than the reference cycle also at low temperature, excluding for the cascade system (see chapter 5). Thus, it appears that the considered solutions can achieve good results during all over the year. This chapter will be divided in three sections: in the first and the second one, the real cooling load and and the ambient temperature data will be described and commented, then, in the last one the final results will be reported. The models used for the yearly analysis are proposed in Appendix A. Appendix B shows how the most important variables of the studied cycles change passing from a subcrtitical working condition to a supercritical one.

6.1 Real cooling load

In order to understand how much energy the chosen systems can save during one year of operation, a cooling load has to be used. The purpose is try to follow as good as possible a real cooling load of a supermarket. The cooling capacity is assumed changing during the day following two restriction: the first one it's about the outdoor temperature and the second one it's about the period during the day when the supermarket is open. Regarding the opening hours, the shop is assumed to be open from 8am to 9pm, 12 hours a day and during this hours the cooling capacity is assumed to be 100% of the chosen value; while, during the hours the shop is closed a reduce value of cooling capacity is assumed. In fact during night the refrigerators are not open and closed continuously, consequently the load of the system is lower and the required output from the refrigeration system is lower. The night load is then assumed to be 60% of the day load. This approach is the same used by Minetto et al. in their study [42]. Regarding the outdoor conditions it has been chosen to set two limits: the maximum cooling capacity to 100 kW when the ambient temperature is 42.5°C, and the

minimum to 50 kW if the ambient temperature is equal or below 15°C. A liner interpolation has been used between the two values. This approach has been used in order to take into account the heat gains that the system has to face when the temperature is rising. Obviously if the ambient temperature rises the heat gains will be higher and the cooling capacity will increase. Then, during high ambient temperature operation period, two negative effects are found: the increase of the cooling capacity and the decrease of the COP. It is because of this fact that is important to have a system that can perform good also during transcritical operation. Below 15°C the load is assumed to be constant because the supermarket is supposed to be heated, then the internal temperature is constant and so the cooling capacity. This of course is an approximation, the load of a real supermarket is affected by more factors than the two here considered, anyway is good enough to the purpose of this study.

6.2 Climate conditions

The entire yearly analysis is based on the ambient temperature data here presented. For the study two different Italian cities have been chosen: one in the north with lower ambient temperature, Milan, and one in the south where the climate is surely warmer, Naples. The decision has been taken in order to compare the results not only between different kind of systems but also for cities with different climate conditions. The weather data used is the Test Reference Year (TRY). The definition of test reference year is: *"single year of hourly data (8760 hours), selected to represent the range of weather patterns that would typically be found in a multi-year dataset"*. In other words is a year of hourly data chosen to represent in the best way possible the climate condition of a certain place. This data is available in the U.S. energy department database[43]. In the database is possible to find the values of all the parameters describing the weather of a certain zone, from the quantity of rain to the solar radiation. Anyway, for the purpose of this thesis the only parameter needed was the ambient temperature. Two different parametric table with 8760 rows have been built to recreate the reference year in EES. Thank to that the models were able to optimize the system and calculate all the necessary parameters for every hour of the year. Fig.6.1 shows the number of hours in a year when the ambient temperature is included in a certain interval. This graph is important because permit to have a preliminary idea of how long the system works in a certain conditions. It will be then interesting find out in which city, Milan or Naples, the improve systems achieve the best results. Regarding the working hours in transcritical mode, if 25°C is taken as a theoretical temperature where the switch from subcritical to transcritical happens, a plant installed in Milan will work in transcritical mode for 601 hours in a year, while a plant installed in Naples will work for 1095 hours a year above the critical point. It will be then expected that Naples will have an higher power consumption than Milan but also it should be possible to have an higher energy saving passing from the base cycle to the improved systems.

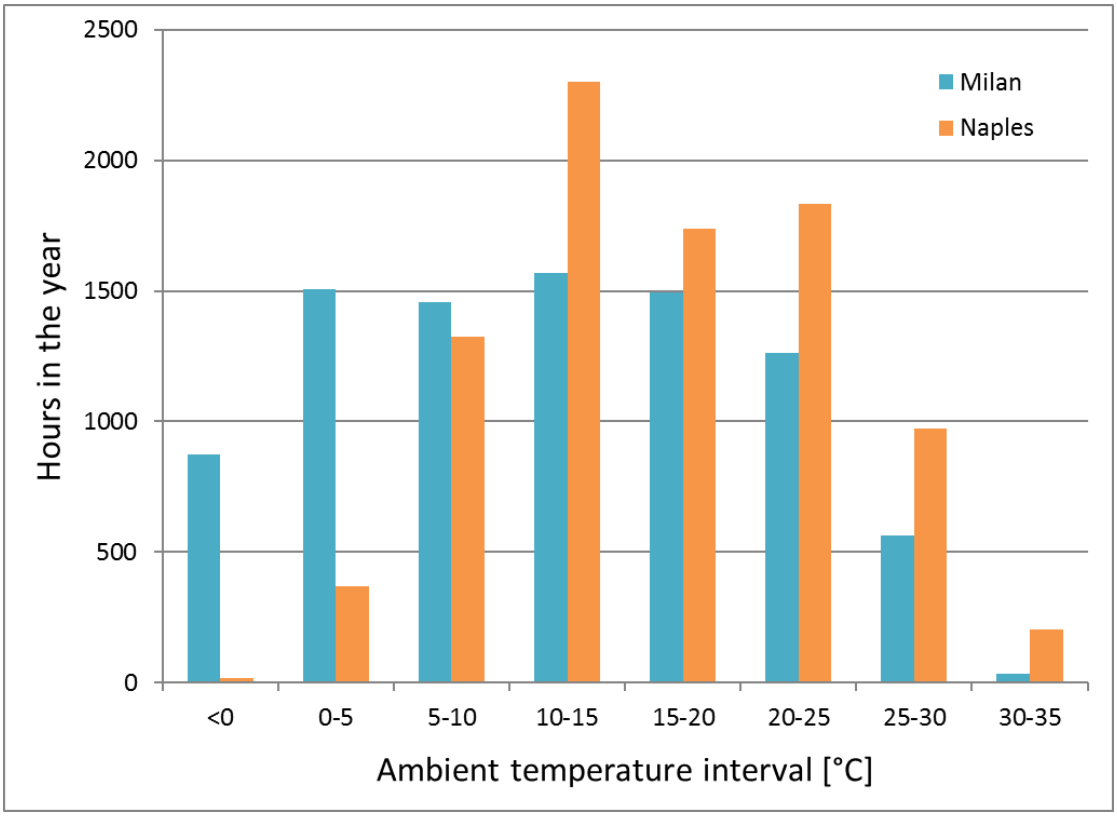

Figure 6.1 – Temperature bins for Milan and Naples.

6.3 Results

In this section the results of the yearly analysis will be presented. In chapter 4 all the assumptions and the boundary conditions necessary to define the systems have been reported and commented. The real cooling load and the climate conditions were the last inputs needed to explain how the models work. Two simulations for each system, one for Milan and one for Naples, have been run to find the final results. A parametric table with 8760 rows has been built for Milan and Naples in order to set the ambient temperature for every hour of the year. Table 6.1 and table 6.2 show the final results for Milan and Naples respectively. The first column shows the average COP weighted on the cooling load during the year, calculated by equation 6.1. COP_i is the coefficient of performance for every hour of the year and $P_{ev,i}$ is the respective cooling load.

$$COP_{av} = \frac{\sum(COP_i \cdot P_{ev,i})}{\sum(P_{ev,i})} \tag{6.1}$$

The second column shows the increment of the COP compared with the reference cycle. These values are useful to have a preliminary idea of the performance of the cycle but they are incomplete because they don't take into consideration the real cooling load. The third and the fourth columns show the maximum power needed in the year by the compressors, the main one and, if present, the secondary one. These values permit to understand how big the compressors have to be installed. The last two columns are the most important since they show the energy consumption of the system all over the year and how much energy it's possible to save compared with the reference cycle. For Milan the best results are achieved by the ejector expander refrigeration cycle with two suction groups, that achieve an energy saving of 12.04%, followed by the parallel compression economization system with 8.78%, the mechanical subcooling with 7.63% and the normal ejector cycle with 3.92%. The cascade system achieves worse performance compared to the reference cycle and it consumes 8.53% more energy. This is because a plant placed in Milan works for many hours during the year in subcritical operation and like seen in chapter 4 the cascade system has bad performance when the ambient temperature is below 25°C. Regarding Naples the systems are placed in the same position. The consumes are higher than Milan but also the energy saving is higher. In fact in this case the ejector cycle with parallel compression achieves an energy savings of 14.78%, followed by the PCE with 11.01%, the MS with 10.09% and the ejector cycle with 6.34%. In this case also the cascade system permits to save some energy (0.64%), this means that probably the cascade system is a very good solution when the ambient temperature are very high or if it's necessary to have the cooling load at lower temperature than -4°C. Regarding the maximum power of the compressors it's possible to see that using the parallel compression, the normal cycle or the cycle with the ejector, permits to reduce considerably the size of the main compressor compared with the base cycle one. This is another good characteristic since the compressor can work closer to its design point.

	COP_{av}	COP_{in}	$P_{max,main}$	$P_{max,sec}$	w_{tot}	w_{saved}	w_{saved}
	-	%	kW	kW	kWh/year	kWh/year	%
BS	6.02	0.00%	41.54	-	77248.71	0.00	0.00%
PCE	6.25	3.80%	25.99	6.52	70468.63	-6780.08	-8.78%
MS	6.21	3.14%	29.73	2.28	71355.57	-5893.14	-7.63%
Cascade	4.82	-19.87%	7.68	18.74	83840.60	6591.88	8.53%
Ejector	6.08	1.00%	31.40	-	74223.94	-3024.78	-3.92%
Ejector 2sg	6.42	6.53%	21.10	10.00	67945.32	-9303.39	-12.04%

Table 6.1 – Yearly analysis results: Milan.

	COP_{av}	COP_{in}	$P_{max,main}$	$P_{max,sec}$	w_{tot}	w_{saved}	w_{saved}
	-	%	kW	kW	kWh/year	kWh/year	%
BS	4.98	0.00%	50.68	-	97018.24	0.00	0.00%
PCE	5.28	6.05%	30.97	8.12	86335.89	-10682.35	-11.01%
MS	5.24	5.28%	35.03	2.68	87225.91	-9792.33	-10.09%
Cascade	4.36	-12.36%	8.18	21.82	96400.72	-617.52	-0.64%
Ejector	5.09	2.15%	37.37	-	90862.82	-6155.42	-6.34%
Ejector 2sg	5.50	10.44%	27.02	10.09	82683.62	-14334.62	-14.78%

Table 6.2 – Yearly analysis results: Naples.

7 Yearly analysis: comparison with an R404A cycle

In this chapter, the last of the thesis, a comparison of the CO_2 systems with a base R404A cycle will be made. Nowadays in the countries of northern Europe several supermarket plants using carbon dioxide as refrigeration fluid have already been installed. As said at the beginning of the thesis the problem of a carbon dioxide cycle is working when the ambient temperature is more then 25°C because of the low critical point. The purpose of this project is understand if a modified system is able to achieve good performance also if is located in a zone with hot climate condition. In the previous chapter it has been seen that the studied cycles can improve considerably the performance compared to a base one. Now the aim is to see if these improved systems can compete also with a system using a synthetic refrigerant. The refrigerant chosen for the comparison is the R404A because is the most used refrigerant in supermarket applications. R404A is a near azeotropic mixture made by 44% of R125, 52% of R143a and 4% of R134a and its critical point is at 72.14°C and 37.35 bar. The ozone depletion potential is zero because all its component are HFC but it has a global warming potential of 3260. Fig.7.1 shows the p-h diagram of the fluid.

7.1 R404A cycle

In this section the R404A cycle will be explain with all its own features. A new model has been built in order to simulate the behaviour of a real R404A refrigeration system. The entire system has been modelled based on energy and mass balance of every single component. Steady flow energy equations and specific energy quantities have been used. The following assumptions have been made in the analysis:

- Steady-state processes.
- Isenthalpic expansion.
- Pressure drop and heat losses are neglected.
- Isentropic efficiency for the compressor is assumed to be function of the pressure ratio

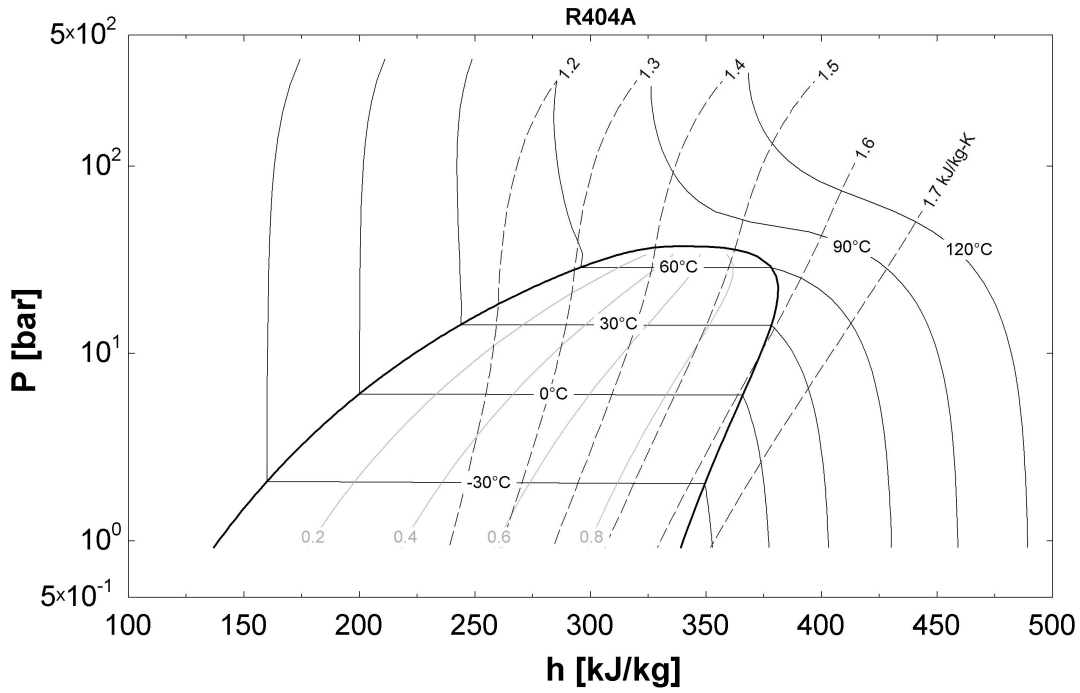

Figure 7.1 – p-h diagram of R404A.

and equation 4.2 has been used.

- The processes in the heat exchangers are considered isobaric.
- The fluid at the outlet of the evaporator is considered saturated vapour.
- The fluid at the outlet of the condenser is considered saturated liquid.
- Superheat and subcooling are neglected.
- The fan power has been calculated as the 3% of the rejected heat at the condenser.

The layout of the system is the same seen in chapter 2 for the base CO_2 cycle and reported in fig.2.1. The only difference is that using R404A there is no gas-cooler but a condenser. In order to make a wider and more accurate comparison a sensibility analysis has been made to study the cycle and compare it with the CO_2 ones. Three different values of evaporation temperature has been chosen for the R404A system, -4°C , -8°C and -12°C. This choice has been made because R404A, differently from the carbon dioxide, needs a larger temperature difference between the evaporator and the cooled environment in order to ensure the adequate temperature. Moreover, three different values of condenser approach temperature difference has been taken int consideration to perform the analysis: 8°C, 6°C, 4°C. This values are higher compared with the CO_2 cycles because the working pressures of R404A is lower and the

temperature is more sensitive to the pressure losses. Since it is more sensitive a certain subcooling out of the condenser is always needed to make sure that these losses will not create flashgas. These facts have been reported by Kim et al.[12], citing their work: *"the minimum heat rejection temperature will be lower in the CO_2 cycle (compared with an 'ordinary' refrigerant) when heat sink inlet temperature and heat exchanger size is given. In addition, the evaporating temperature tends to be higher for a given duty, heat source temperature, and heat exchanger size."* After have run some simulations with the Bitzer software [40] to see the limits of an R404A compressor, the minimum condensing temperature has been setted to 15°C, 12°C and 10°C respectively for the three evaporation temperatures. This minimum temperature fix a minimum pressure difference through the compressor and the throttling valve that ensure a proper functioning of the devices. Regarding the real cooling load and the ambient temperature data, the conditions presented in chapter 6 are still valid and have been used to model the system.

Before proceeding with the comparison of the systems, the boundary conditions and the assumptions are summarized in the following table.

R404A cycle	
Evaporative temperature	-4°C, -8°C, -12°C
Condenser approach temperature difference	8°C, 6°C, 4°C
Minimum condensing temperature	10°C, 12°C, 15°C
Subcooling and superheating	0°C
Compressor isentropic efficiency	polynomial, f(pressure ratio)
Fan power	3% of the rejected heat

7.2 Results

The results are here presented in the following way: for each condenser approach temperature difference two graphs and six tables are reported. The two graphs show a comparison in terms of COP and power consumptions (with constant cooling load) between the base CO_2 cycle and the R404A cycle with different evaporative temperatures. The orange line represents the cycle with an evaporative temperature of -4°C, the green one end the yellow one represent the cycle with an evaporative temperature of -8°C and -12°C respectively. The tables present the comparison in terms of yearly analysis for Milan and Naples. There are then two tables for every combination of evaporative temperature and condenser approach. The assumptions made for the CO_2 systems are the same used for the yearly analysis in chapter 6. The results show that the CO_2 cycles are very promising compared to the R404A one. The higher performances achieved by the carbon dioxide are due to the lower approach temperature different in the gas-cooler/condenser and in the evaporator. The possibility to reduce these two Δt is in fact a great advantage that the carbon dioxide has, thanks to its thermodynamic and transfer properties, respect to the other refrigerants.

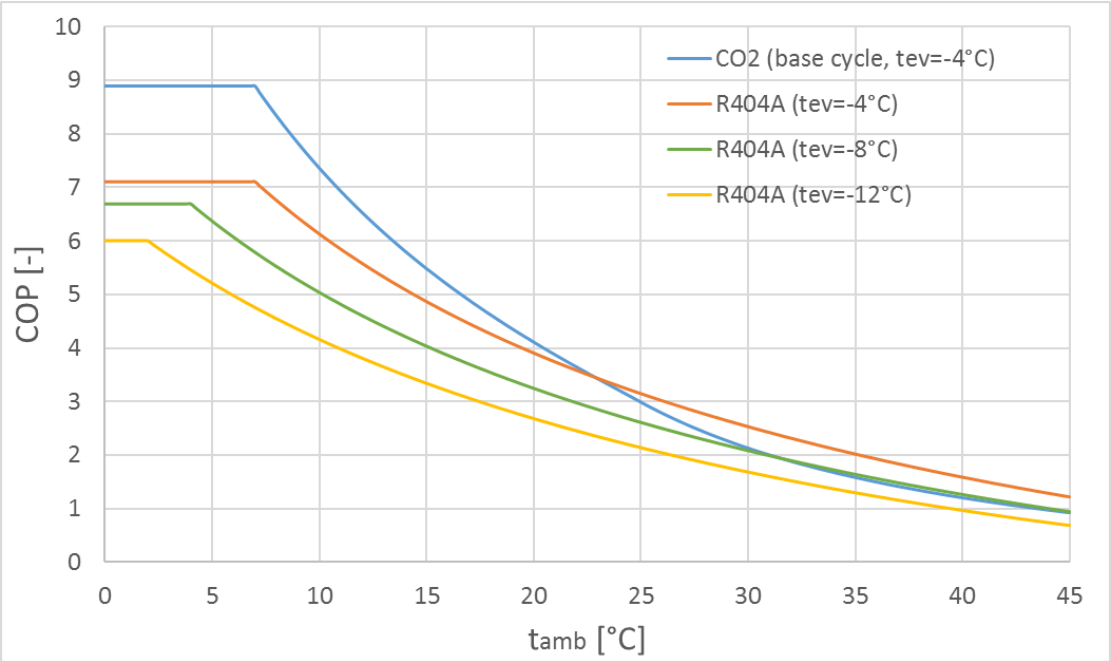

Figure 7.2 – COP vs t_{amb}: comparison ($\Delta t_{cond} = 8°C$).

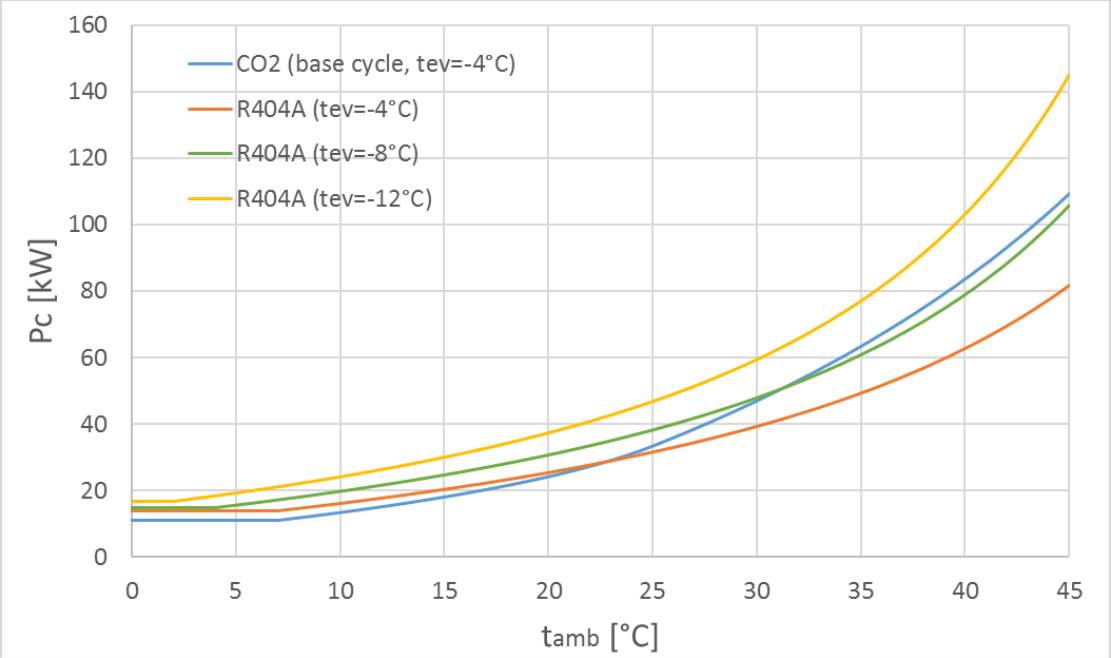

Figure 7.3 – Power consumption vs t_{amb}: comparison (constant cooling load of 100kW, $\Delta t_{cond} = 8°C$).

	COP_{av}	COP_{in}	$P_{max,main}$	$P_{max,sec}$	w_{tot}	w_{saved}	w_{saved}
	-	%	kW	KW	kWh/year	kWh/year	%
R404A	5.48	0.00%	32.87	-	82119.38	0.00	0.00%
BS	6.43	17.38%	41.54	-	77248.71	-4870.66	-5.93%
PCE	6.62	20.79%	25.99	6.52	70468.63	-11650.74	-14.19%
MS	6.59	20.19%	29.73	2.28	71355.57	-10763.81	-13.11%
Cascade	5.01	-8.56%	7.68	18.74	83840.60	1721.22	2.10%
Ejector	6.47	18.06%	31.40	-	74223.94	-7895.44	-9.61%
Ejector 2sg	6.78	23.78%	21.10	10.00	67945.32	-14174.06	-17.26%

Table 7.1 – Yearly analysis comparison: Milan (R404A: $t_{ev} = -4$°C, $\Delta t_{cond} = 8$°C).

	COP_{av}	COP_{in}	$P_{max,main}$	$P_{max,sec}$	w_{tot}	w_{saved}	w_{saved}
	-	%	kW	KW	kWh/year	kWh/year	%
R404A	4.79	0.00%	38.94	-	98295.47	0.00	0.00%
BS	5.39	12.64%	50.68	-	97018.24	-1277.24	-1.30%
PCE	5.65	18.05%	30.97	8.12	86335.89	-11959.58	-12.17%
PCE+SC	5.74	19.86%	32.51	7.46	86724.96	-11570.52	-11.77%
MS	5.62	17.31%	35.03	2.68	87225.91	-11069.56	-11.26%
Cascade	4.56	-4.84%	8.18	21.82	96400.72	-1894.75	-1.93%
Ejector	5.46	14.10%	37.37	-	90862.82	-7432.65	-7.56%
Ejector 2sg	5.88	22.78%	27.02	10.09	82683.62	-15611.85	-15.88%

Table 7.2 – Yearly analysis comparison: Naples (R404A: $t_{ev} = -4$°C, $\Delta t_{cond} = 8$°C).

	COP_{av}	COP_{in}	$P_{max,main}$	$P_{max,sec}$	w_{tot}	w_{saved}	w_{saved}
	-	%	kW	KW	kWh/year	kWh/year	%
R404A	4.75	0.00%	40.71	-	97364.08	0.00	0.00%
BS	6.43	35.30%	41.54	-	77248.71	-20115.37	-20.66%
PCE	6.62	39.25%	25.99	6.52	70468.63	-26895.45	-27.62%
MS	6.59	38.55%	29.73	2.28	71355.57	-26008.51	-26.71%
Cascade	5.01	5.41%	7.68	18.74	83840.60	-13523.48	-13.89%
Ejector	6.47	36.09%	31.40	-	74223.94	-23140.14	-23.77%
Ejector 2sg	6.78	42.69%	21.10	10.00	67945.32	-29418.76	-30.22%

Table 7.3 – Yearly analysis comparison: Milan (R404A: $t_{ev} = -8$°C, $\Delta t_{cond} = 8$°C).

	COP_{av}	COP_{in}	$P_{max,main}$	$P_{max,sec}$	w_{tot}	w_{saved}	w_{saved}
	-	%	kW	KW	kWh/year	kWh/year	%
R404A	4.00	0.00%	48.50	-	118492.35	0.00	0.00%
BS	5.39	34.87%	50.68	-	97018.24	-21474.11	-18.12%
PCE	5.65	41.35%	30.97	8.12	86335.89	-32156.46	-27.14%
MS	5.62	40.46%	35.03	2.68	87225.91	-31266.44	-26.39%
Cascade	4.56	13.94%	8.18	21.82	96400.72	-22091.63	-18.64%
Ejector	5.46	36.62%	37.37	-	90862.82	-27629.53	-23.32%
Ejector 2sg	5.88	47.01%	27.02	10.09	82683.62	-35808.73	-30.22%

Table 7.4 – Yearly analysis comparison: Naples (R404A: $t_{ev} = -8$°C, $\Delta t_{cond} = 8$°C).

	COP_{av}	COP_{in}	$P_{max,main}$	$P_{max,sec}$	w_{tot}	w_{saved}	w_{saved}
	-	%	kW	KW	kWh/year	kWh/year	%
R404A	4.01	0.00%	51.52	-	117532.53	0.00	0.00%
BS	6.43	60.52%	41.54	-	77248.71	-40283.81	-34.27%
PCE	6.62	65.20%	25.99	6.52	70468.63	-47063.89	-40.04%
MS	6.59	64.38%	29.73	2.28	71355.57	-46176.96	-39.29%
Cascade	5.01	25.05%	7.68	18.74	83840.60	-33691.93	-28.67%
Ejector	6.47	61.46%	31.40	-	74223.94	-43308.59	-36.85%
Ejector 2sg	6.78	69.28%	21.10	10.00	67945.32	-49587.21	-42.19%

Table 7.5 – Yearly analysis comparison: Milan (R404A: $t_{ev} = -12$°C, $\Delta t_{cond} = 8$°C).

	COP_{av}	COP_{in}	$P_{max,main}$	$P_{max,sec}$	w_{tot}	w_{saved}	w_{saved}
	-	%	kW	KW	kWh/year	kWh/year	%
R404A	3.30	0.00%	62.03	-	144287.32	0.00	0.00%
BS	5.39	63.30%	50.68	-	97018.24	-47269.08	-32.76%
PCE	5.65	71.14%	30.97	8.12	86335.89	-57951.43	-40.16%
MS	5.62	70.06%	35.03	2.68	87225.91	-57061.41	-39.55%
Cascade	4.56	37.96%	8.18	21.82	96400.72	-47886.60	-33.19%
Ejector	5.46	65.41%	37.37	-	90862.82	-53424.50	-37.03%
Ejector 2sg	5.88	77.99%	27.02	10.09	82683.62	-61603.70	-42.70%

Table 7.6 – Yearly analysis comparison: Naples (R404A: $t_{ev} = -12$°C, $\Delta t_{cond} = 8$°C).

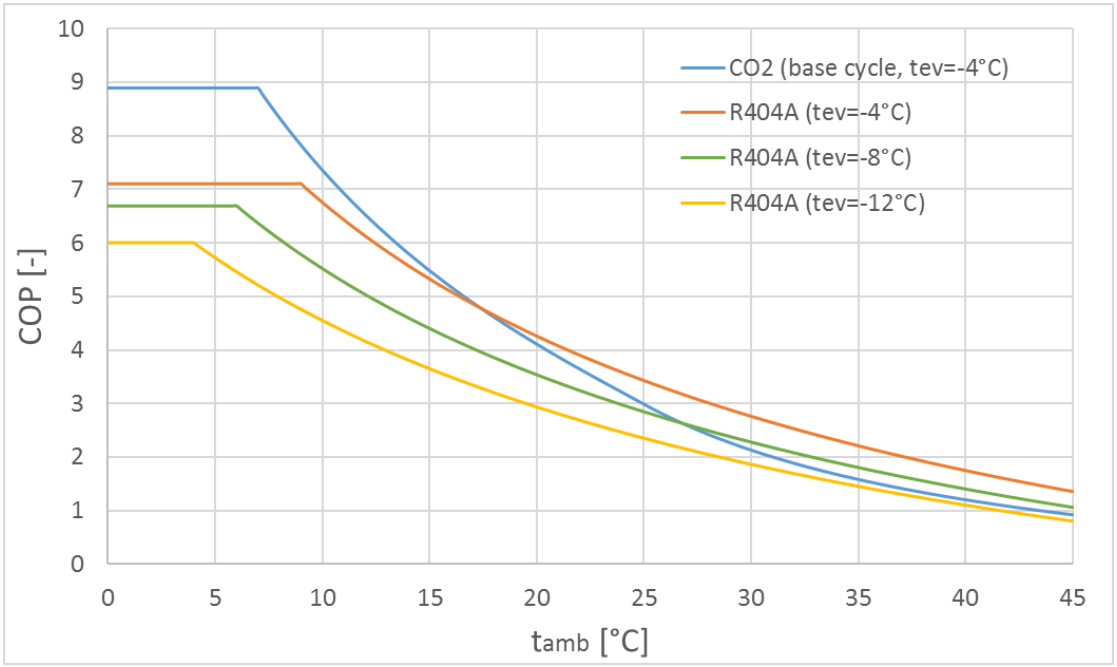

Figure 7.4 – COP vs t_{amb}: comparison ($\Delta t_{cond} = 6°C$).

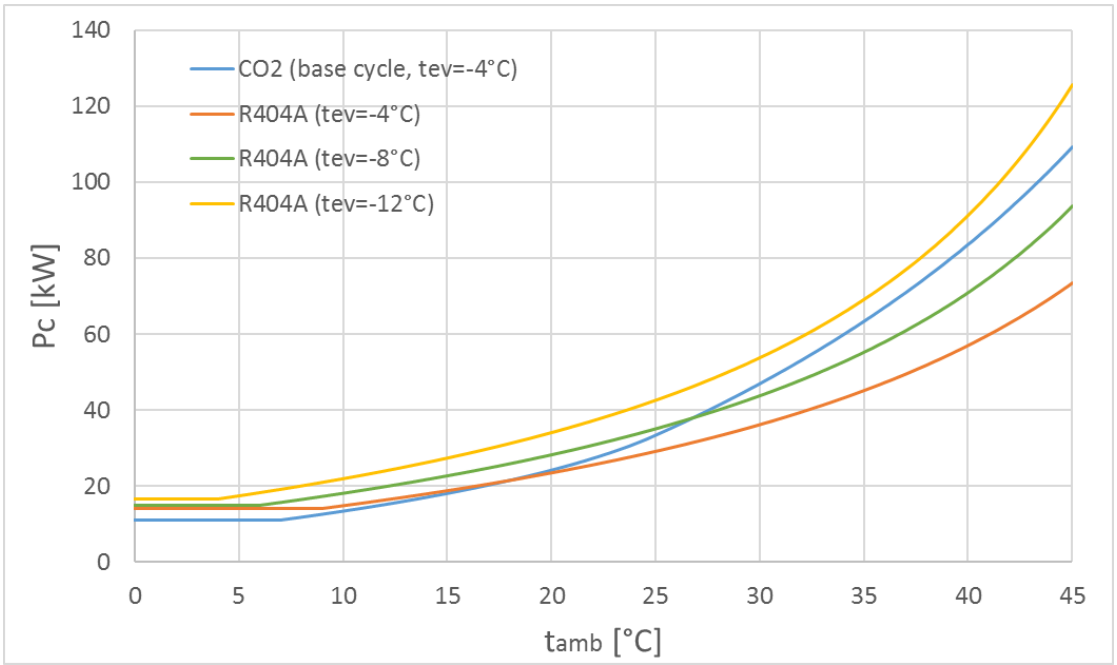

Figure 7.5 – Power consumption vs t_{amb}: comparison (constant cooling load of 100kW, $\Delta t_{cond} = 6°C$).

	COP_{av}	COP_{in}	$P_{max,main}$	$P_{max,sec}$	w_{tot}	w_{saved}	w_{saved}
	-	%	kW	KW	kWh/year	kWh/year	%
R404A	5.48	0.00%	29.85	-	76585.67	0.00	0.00%
BS	6.02	9.81%	41.54	-	77248.71	663.05	0.87%
PCE	6.25	13.98%	25.99	6.52	70468.63	-6117.03	-7.99%
MS	6.21	13.26%	29.73	2.28	71355.57	-5230.10	-6.83%
Cascade	4.82	-12.02%	7.678	18.74	83840.60	7254.93	9.47%
Ejector	6.08	10.90%	31.4	-	74223.94	-2361.73	-3.08%
Ejector 2sg	6.42	16.98%	21.1	10.00	67945.32	-8640.35	-11.28%

Table 7.7 – Yearly analysis comparison: Naples (R404A: $t_{ev} = -4$°C, $\Delta t_{cond} = 6$°C).

	COP_{av}	COP_{in}	$P_{max,main}$	$P_{max,sec}$	w_{tot}	w_{saved}	w_{saved}
	-	%	kW	KW	kWh/year	kWh/year	%
R404A	4.87	0.00%	35.30	-	90420.31	0.00	0.00%
BS	4.98	2.32%	50.68	-	97018.24	6597.92	7.30%
PCE	5.28	8.52%	30.97	8.12	86335.89	-4084.43	-4.52%
MS	5.24	7.72%	35.03	2.68	87225.91	-3194.41	-3.53%
Cascade	4.36	-10.33%	8.182	21.82	96400.72	5980.41	6.61%
Ejector	5.09	4.52%	37.37	-	90862.82	442.51	0.49%
Ejector 2sg	5.50	13.00%	27.02	10.09	82683.62	-7736.69	-8.56%

Table 7.8 – Yearly analysis comparison: Naples (R404A: $t_{ev} = -4$°C, $\Delta t_{cond} = 6$°C).

	COP_{av}	COP_{in}	$P_{max,main}$	$P_{max,sec}$	w_{tot}	w_{saved}	w_{saved}
	-	%	kW	KW	kWh/year	kWh/year	%
R404A	4.77	0.00%	36.84	-	90189.54	0.00	0.00%
BS	6.02	26.18%	41.54	-	77248.71	-12940.83	-14.35%
PCE	6.25	30.97%	25.99	6.52	70468.63	-19720.91	-21.87%
MS	6.21	30.14%	29.73	2.28	71355.57	-18833.97	-20.88%
Cascade	4.82	1.10%	7.678	18.74	83840.60	-6348.94	-7.04%
Ejector	6.08	27.44%	31.4	-	74223.94	-15965.60	-17.70%
Ejector+BP	6.42	34.42%	21.1	10.00	67945.32	-22244.22	-24.66%

Table 7.9 – Yearly analysis comparison: Naples (R404A: $t_{ev} = -8$°C, $\Delta t_{cond} = 6$°C).

	COP_{av}	COP_{in}	$P_{max,main}$	$P_{max,sec}$	w_{tot}	w_{saved}	w_{saved}
	-	%	kW	KW	kWh/year	kWh/year	%
R404A	4.09	0.00%	43.76	-	108593.93	0.00	0.00%
BS	4.98	21.85%	50.68	-	97018.24	-11575.69	-10.66%
PCE	5.28	29.22%	30.97	8.12	86335.89	-22258.04	-20.50%
MS	5.24	28.28%	35.03	2.68	87225.91	-21368.02	-19.68%
Cascade	4.36	6.78%	8.182	21.82	96400.72	-12193.21	-11.23%
Ejector	5.09	24.47%	37.37	-	90862.82	-17731.11	-16.33%
Ejector+BP	5.50	34.57%	27.02	10.09	82683.62	-25910.31	-23.86%

Table 7.10 – Yearly analysis comparison: Naples (R404A: $t_{ev} = -8$°C, $\Delta t_{cond} = 6$°C).

	COP_{av}	COP_{in}	$P_{max,main}$	$P_{max,sec}$	w_{tot}	w_{saved}	w_{saved}
	-	%	kW	KW	kWh/year	kWh/year	%
R404A	4.04	0.00%	46.29	-	108268.02	0.00	0.00%
BS	6.02	49.10%	41.54	-	77248.71	-31019.31	-28.65%
PCE	6.25	54.76%	25.99	6.52	70468.63	-37799.39	-34.91%
MS	6.21	53.78%	29.73	2.28	71355.57	-36912.45	-34.09%
Cascade	4.82	19.47%	7.678	18.74	83840.60	-24427.42	-22.56%
Ejector	6.08	50.59%	31.4	-	74223.94	-34044.08	-31.44%
Ejector+BP	6.42	58.84%	21.1	10.00	67945.32	-40322.70	-37.24%

Table 7.11 – Yearly analysis comparison: Naples (R404A: $t_{ev} = -12$°C, $\Delta t_{cond} = 6$°C).

	COP_{av}	COP_{in}	$P_{max,main}$	$P_{max,sec}$	w_{tot}	w_{saved}	w_{saved}
	-	%	kW	KW	kWh/year	kWh/year	%
R404A	3.38	0.00%	55.46	-	131833.00	0.00	0.00%
BS	4.98	47.24%	50.68	-	97018.24	-34814.76	-26.41%
PCE	5.28	56.15%	30.97	8.12	86335.89	-45497.11	-34.51%
MS	5.24	55.01%	35.03	2.68	87225.91	-44607.09	-33.84%
Cascade	4.36	29.03%	8.182	21.82	96400.72	-35432.28	-26.88%
Ejector	5.09	50.41%	37.37	-	90862.82	-40970.18	-31.08%
Ejector+BP	5.50	62.60%	27.02	10.09	82683.62	-49149.38	-37.28%

Table 7.12 – Yearly analysis comparison: Naples (R404A: $t_{ev} = -12$°C, $\Delta t_{cond} = 6$°C).

	COP_{av}	COP_{in}	$P_{max,main}$	$P_{max,sec}$	w_{tot}	w_{saved}	w_{saved}
	-	%	kW	KW	kWh/year	kWh/year	%
R404A	5.75	0.00%	27.13	-	71782.31	0.00	0.00%
BS	6.02	4.69%	41.54	-	77248.71	5466.41	7.62%
PCE	6.25	8.66%	25.99	6.52	70468.63	-1313.67	-1.83%
MS	6.21	7.98%	29.73	2.28	71355.57	-426.74	-0.59%
Cascade	4.82	-16.12%	7.678	18.74	83840.60	12058.29	16.80%
Ejector	6.08	5.73%	31.4	-	74223.94	2441.63	3.40%
Ejector+BP	6.42	11.53%	21.1	10.00	67945.32	-3836.99	-5.35%

Table 7.13 – Yearly analysis comparison: Naples (R404A: $t_{ev} = -4$°C, $\Delta t_{cond} = 4$°C).

	COP_{av}	COP_{in}	$P_{max,main}$	$P_{max,sec}$	w_{tot}	w_{saved}	w_{saved}
	-	%	kW	KW	kWh/year	kWh/year	%
R404A	5.22	0.00%	32.05	-	83496.26	0.00	0.00%
BS	4.98	-4.62%	50.68	-	97018.24	13521.97	16.19%
PCE	5.28	1.16%	30.97	8.12	86335.89	2839.62	3.40%
MS	5.24	0.42%	35.03	2.68	87225.91	3729.64	4.47%
Cascade	4.36	-16.41%	8.182	21.82	96400.72	12904.46	15.46%
Ejector	5.09	-2.56%	37.37	-	90862.82	7366.56	8.82%
Ejector+BP	5.50	5.34%	27.02	10.09	82683.62	-812.64	-0.97%

Table 7.14 – Yearly analysis comparison: Naples (R404A: $t_{ev} = -4$°C, $\Delta t_{cond} = 4$°C).

	COP_{av}	COP_{in}	$P_{max,main}$	$P_{max,sec}$	w_{tot}	w_{saved}	w_{saved}
	-	%	kW	KW	kWh/year	kWh/year	%
R404A	5.04	0.00%	33.39	-	83925.27	0.00	0.00%
BS	6.02	19.43%	41.54	-	77248.71	-6676.55	-7.96%
PCE	6.25	23.96%	25.99	6.52	70468.63	-13456.64	-16.03%
MS	6.21	23.18%	29.73	2.28	71355.57	-12569.70	-14.98%
Cascade	4.82	-4.31%	7.678	18.74	83840.60	-84.67	-0.10%
Ejector	6.08	20.62%	31.4	-	74223.94	-9701.33	-11.56%
Ejector+BP	6.42	27.23%	21.1	10.00	67945.32	-15979.95	-19.04%

Table 7.15 – Yearly analysis comparison: Naples (R404A: $t_{ev} = -8$°C, $\Delta t_{cond} = 4$°C).

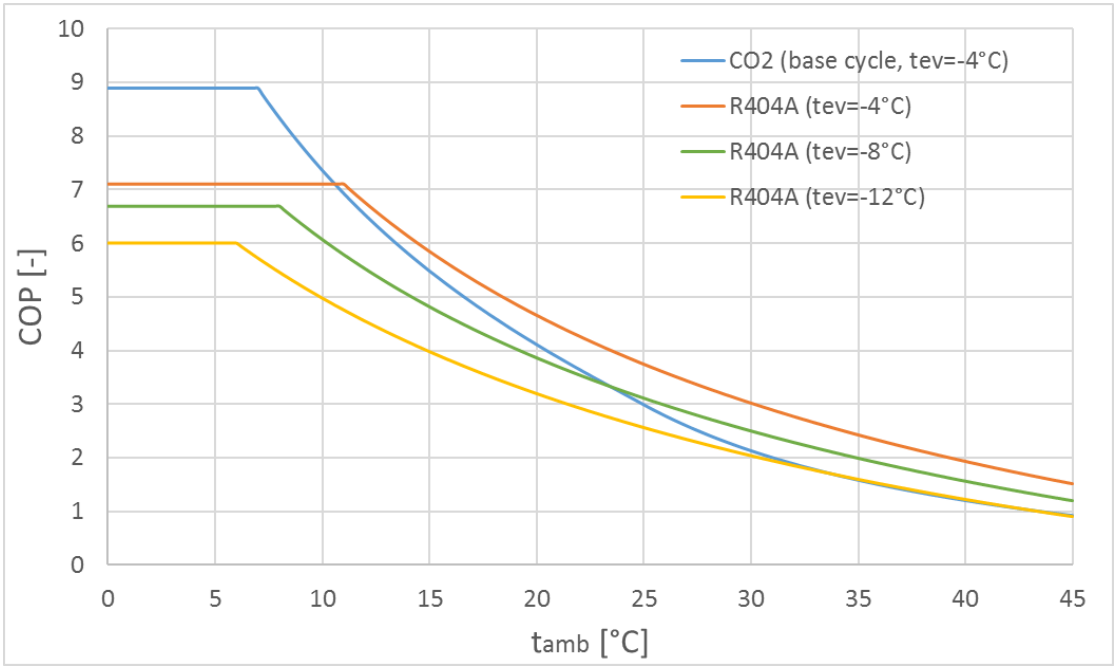

Figure 7.6 – COP vs t_{amb}: comparison ($\Delta t_{cond} = 4°C$).

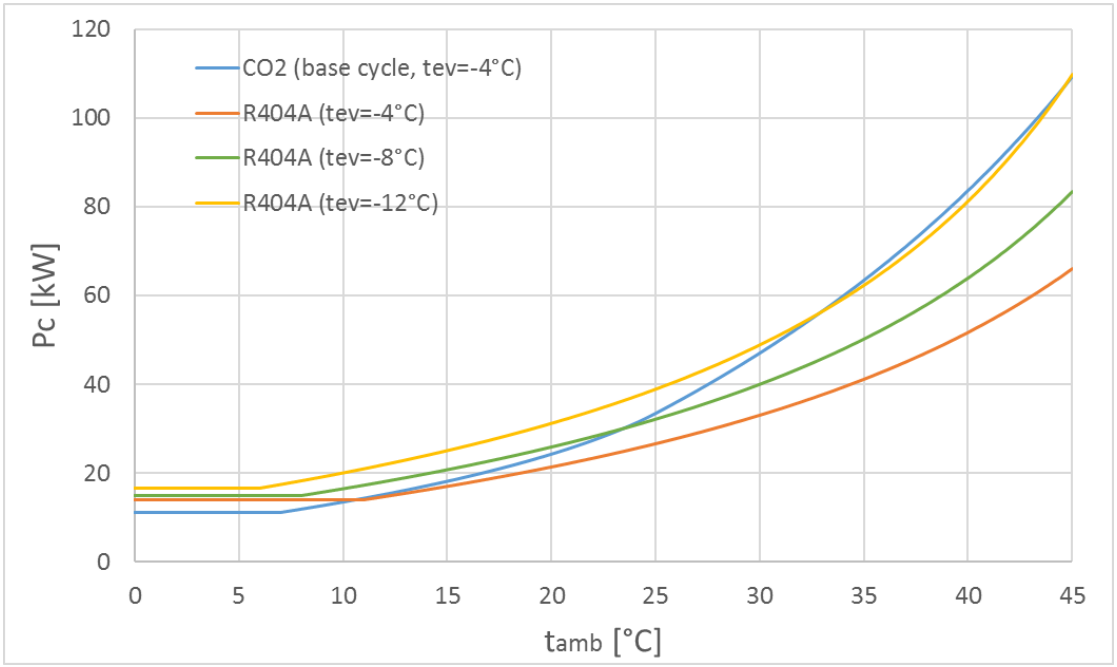

Figure 7.7 – Power consumption vs t_{amb}: comparison (constant cooling load of 100kW, $\Delta t_{cond} = 4°C$).

	COP_{av}	COP_{in}	$P_{max,main}$	$P_{max,sec}$	w_{tot}	w_{saved}	w_{saved}
	-	%	kW	KW	kWh/year	kWh/year	%
R404A	4.43	0.00%	39.58	-	99743.43	0.00	0.00%
BS	4.98	12.53%	50.68	-	97018.24	-2725.19	-2.73%
PCE	5.28	19.34%	30.97	8.12	86335.89	-13407.54	-13.44%
MS	5.24	18.47%	35.03	2.68	87225.91	-12517.52	-12.55%
Cascade	4.36	-1.39%	8.182	21.82	96400.72	-3342.71	-3.35%
Ejector	5.09	14.95%	37.37	-	90862.82	-8880.61	-8.90%
Ejector+BP	5.50	24.27%	27.02	10.09	82683.62	-17059.80	-17.10%

Table 7.16 – Yearly analysis comparison: Naples (R404A: $t_{ev} = -8$°C, $\Delta t_{cond} = 4$°C).

	COP_{av}	COP_{in}	$P_{max,main}$	$P_{max,sec}$	w_{tot}	w_{saved}	w_{saved}
	-	%	kW	KW	kWh/year	kWh/year	%
R404A	4.29	0.00%	41.71	-	100224.10	0.00	0.00%
BS	6.02	40.32%	41.54	-	77248.71	-22975.39	-22.92%
PCE	6.25	45.65%	25.99	6.52	70468.63	-29755.47	-29.69%
MS	6.21	44.73%	29.73	2.28	71355.57	-28868.53	-28.80%
Cascade	4.82	12.43%	7.678	18.74	83840.60	-16383.50	-16.35%
Ejector	6.08	41.72%	31.4	-	74223.94	-26000.16	-25.94%
Ejector+BP	6.42	49.49%	21.1	10.00	67945.32	-32278.78	-32.21%

Table 7.17 – Yearly analysis comparison: Naples (R404A: $t_{ev} = -12$°C, $\Delta t_{cond} = 4$°C).

	COP_{av}	COP_{in}	$P_{max,main}$	$P_{max,sec}$	w_{tot}	w_{saved}	w_{saved}
	-	%	kW	KW	kWh/year	kWh/year	%
R404A	3.68	0.00%	49.79	-	120682.17	0.00	0.00%
BS	4.98	35.33%	50.68	-	97018.24	-23663.93	-19.61%
PCE	5.28	43.52%	30.97	8.12	86335.89	-34346.28	-28.46%
MS	5.24	42.47%	35.03	2.68	87225.91	-33456.26	-27.72%
Cascade	4.36	18.60%	8.182	21.82	96400.72	-24281.45	-20.12%
Ejector	5.09	38.24%	37.37	-	90862.82	-29819.35	-24.71%
Ejector+BP	5.50	49.45%	27.02	10.09	82683.62	-37998.55	-31.49%

Table 7.18 – Yearly analysis comparison: Naples (R404A: $t_{ev} = -12$°C, $\Delta t_{cond} = 4$°C).

8 Conclusions

During the last decades the industry of refrigeration and air-conditioning had to face some radical changes due to the increasing concern about the health of our planet. CFC and HCFC fluids have been discovered to be very harmful and dangerous for the ozone layer and they have been banned already. Even HFCs, introduced as replacements, are now discussion topic because of their impact on the global warming. Regulation (EU) 517/2014 of the European Parliament has been approved with the purpose to put them out of the market in the next years. Natural refrigerants and HFOs, a new type of synthetic fluids, seem now the only solution to reduce the human impact on the environment. Research on natural refrigerants is growing on many parallel ways, including the use of hydrocarbons and ammonia by minimizing charge to avoid safety problem due to their toxicity and flammability. This thesis is focused on carbon dioxide, a natural refrigerant that like most of others has no ozone depletion potential and negligible global warming potential. CO_2 was already used during the end of the 19^{th} century and beginning of the 20^{th} as a refrigerant. From the middle of the 20^{th} century carbon dioxide was completely abandoned due to appearance of CFCs in the market. After the discovery of the damages that these synthetic fluids can do to our planet the reborn of CO_2 started. Thermodynamic and transport properties of carbon dioxide are favourable in terms of heat transfer and pressure drop. It has high working pressure but the main disadvantage is the low critical temperature. Because of this the heat rejection will in most cases take place in supercritical region. This makes the cycle working as transcritical. The higher average temperature of heat rejection and the larger throttling loss penalize the basic CO_2 cycle compared to other refrigerants. Four different solutions have been taken into consideration in order to decrease these losses: parallel compression with and without recooler, mechanical subcooling, cascade system and the use of an ejector to recover the expansion work, with single and parallel compression. From a design condition point of view (a constant and very high ambient temperature has been chosen) it has been proved that all the systems achieve better performances than the base cycle. The cascade system using R134a as secondary fluid permits to reduce the power consumption by 39%, followed by the cycle with mechanical subcooling (24%) and the ejector cycle with parallel compression (22%). These results are interesting and offer a good overview of the adoptable possibilities to improve the base cycle when used

in hot climate. However they do not take into account the fact that a refrigeration system is subject to very different climate conditions during a year of operation. The second and main part of the present study is focused on the yearly analysis of the previously mentioned cycles. Two different Italian cities have been chosen to perform the analysis: Milan and Naples. A Test Reference Year (TRY) dataset has been used to describe the ambient temperature over the year. This choice permitted to study the system under two different climate conditions. A plant installed in Milan works in transcritical mode for 601 hours a year versus 1095 for a plant installed in Naples. Accurate and realistic assumptions have been made to model the cycles. Using an ejector cycle with two suction groups (parallel compression) leads to an energy saving of 12.0% and 14.8% respectively in Milan and Naples compared to the base cycle consumptions. The parallel compression economization system shows satisfying results as well, with an energy saving of 8.8% and 11.0% for the two cities respectively. The cascade system, best cycle when dealing with high ambient temperature, in the yearly analysis is the one with the lowest performances. The last part of the project proposes a simple comparison between the CO_2 systems and a R404A cycle. Results are interesting and show that carbon dioxide can also be competitive where the climate conditions are not favourable. Different trial plants have been installed in southern Europe already. The real data that can be obtained thanks to these systems will be fundamental to understand if the CO_2 can really replace the synthetic refrigerants and finally reduce the impact that the human activity is having on the climate.

Bibliography

[1] International Energy Agency. World Energy Outlook. 2015.

[2] L. Lucas. IIR news. *International Journal of Refrigeration*, 21(2):87–88, 1998.

[3] Regulation (ec) no 2037/2000 of the European Parliament and the council of 29 June 2000 on substances that deplete the ozone layer. *Official Journal of the European Communities*, 244:1–24, 2000.

[4] V. Sharma, B. Fricke, and P. Bansal. Comparative analysis of various CO2 configurations in supermarket refrigeration systems. *International Journal of Refrigeration*, 46:86–99, 2014.

[5] S. Klein and F. Alvarado. Engineering equation solver. F-Chart Software. 2001.

[6] R. Span and W. Wagner. A new equation of state for carbon dioxide covering the fluid region from the triple-point temperature to 1100 K at pressure up to 800 MPa. *Journal of Physical and Chemical Reference Data*, 26:1509–96, 1996.

[7] A. Pearson. Carbon dioxide - New uses for an old refrigerant. *International Journal of Refrigeration*, 28(8):1140–1148, 2005.

[8] J. M. Calm. The next generation of refrigerants - Historical review, considerations, and outlook. *International Journal of Refrigeration*, 31(7):1123–1133, 2008.

[9] G. Lorentzen. Carbon dioxide as a refrigerant. *Journal of the Franklin Institute*, 196(5): 713, 1993.

[10] G. Lorentzen. The use of natural refrigerants : a complete solution to the CFC/HCFC predicament . *International Journal of Refrigeration*, 18(3):190–197, 1995.

[11] G. Lorentzen. Trans-critical vapour compression cycle device, Patent No. WO/07683. 1990.

[12] M. Kim. *Fundamental process and system design issues in CO2 vapor compression systems*, volume 30. 2004.

[13] A. Bredesen, A. Hafner, and J. Pettersen. Heat transfer and pressure drop for in-tube evaporation of CO2. *International Conference on Heat Transfer Issues in Natural Refrigerants, College Park, MD*, pages 1–15, 1997.

[14] S. Girotto, S. Minetto, and P. Neksa. Commercial refrigeration system using CO2 as the refrigerant. *International Journal of Refrigeration*, 27:717–723, 2004.

[15] S. Sawalha, M. Karampour, and J. Rogstam. Field measurements of supermarket refrigeration systems. Part I: Analysis of CO2 trans-critical refrigeration systems. *Applied Thermal Engineering*, 87:633–647, 2015.

[16] S. M. Liao, T. S. Zhao, and A. Jakobsen. Correlation of optimal heat rejection pressures in transcritical carbon dioxide cycles. *Applied Thermal Engineering*, 20(9):831–841, 2000.

[17] Y. T. Ge and S. A. Tassou. Thermodynamic analysis of transcritical CO2 booster refrigeration systems in supermarket. *Energy Conversion and Management*, 52(4):1868–1875, 2011.

[18] J. Sarkar. Performance characteristics of refrigeration cycle with parallel compression economization. *International Journal of Energy Research*, 34(13):1205–1214, 2010.

[19] J. Sarkar and N. Agrawal. Performance optimization of transcritical CO2 cycle with parallel compression economization. *International Journal of Thermal Science*, 49:838–843, 2009.

[20] S. M. Zubair. Improvement of refrigeration/air-conditioning performance with mechanical sub-cooling. *Energy*, 15(5):427–433, 1990.

[21] S. M. Zubair. Thermodynamics of a vapor-compression refrigeration cycle with mechanical subcooling. *Energy*, 19(6):707–715, 1994.

[22] J. Khan and S. Zubair. Design and rating of an integrated mechanical-subcooling vapor-compression refrigeration system. *Energy Conversion and Management*, 41(11):1201–1222, 2000.

[23] J. W. Thornton, S. A. Klein, and J. W. Mitchell. Dedicated mechanical subcoolmg design strategies for supermarket a kations. *International Journal of Refrigeration*, 17(8):508–515, 1994.

[24] J. Khan and S. M. Zubair. Design and rating of dedicated mechanical-subcooling vapour compression refrigeration systems. *Proceedings of the Institution of Mechanical Engineers, Part A: Journal of Power and Energy*, 214(5):455–471, 2000.

[25] R. Llopis, R. Cabello, D. Sánchez, and E. Torrella. Energy improvements of CO2 transcritical refrigeration cycles using dedicated mechanical subcooling. *International Journal of Refrigeration*, 55:129–141, 2015.

[26] C. Sanz-Kock, R. Llopis, D. Sánchez, R. Cabello, and E. Torrella. Experimental evaluation of a R134a/CO2 cascade refrigeration plant. *Applied Thermal Engineering*, 73(1):39–48, 2014.

[27] A. Da Silva, E.P. Bandarra Filho, and A.H.P. Antunes. Comparison of a R744 cascade refrigeration system with R404A and R22 conventional systems for supermarkets. *Applied Thermal Engineering*, 41:30–35, 2012.

[28] S. Bhattacharyya, S. Mukhopadhyay, A. Kumar, R. K. Khurana, and J. Sarkar. Optimization of a CO2-C3H8 cascade system for refrigeration and heating. *International Journal of Refrigeration*, 28(8):1284–1292, 2005.

[29] H. Tian, Y. Ma, M. Li, and W. Wang. Study on expansion power recovery in CO2 transcritical cycle. *Energy Conversion and Management*, 51(12):2516–2522, 2010.

[30] Y.F. Liu and G.Y. Jin. Vortex tube expansion two-stage transcritical CO2 refrigeration cycle. *Advanced Materials Research*, 516:1219–1223, 2012.

[31] D. Li and E.A. Groll. Transcritical CO2 refrigeration cycle with ejector-expansion device. *International Journal of Refrigeration*, 28(5):766–773, 2005.

[32] S. Fangtian and M. Yitai. Thermodynamic analysis of transcritical CO2 refrigeration cycle with an ejector. *Applied Thermal Engineering*, 31(6-7):1184–1189, 2011.

[33] H. K. Ersoy and N. Bilir. Performance characteristics of ejector expander transcritical CO2 refrigeration cycle. *Proceedings of the Institution of Mechanical Engineers, Part A: Journal of Power and Energy*, 226(5):623–635, 2012.

[34] E. Kriezi, K. Fredslund, K. Banasiak, and A. Hafner. Multi ejector and the impact of ejector design on the operation of a CO2 refrigeration System. 2015.

[35] Kornhauser. The Use Of An Ejector In A Geothermal Flash System. *Proceedings of the 25th Intersociety Energy Conversion Engineering Conference*, 5, 1990.

[36] S. Elbel. Historical and present developments of ejector refrigeration systems with emphasis on transcritical carbon dioxide air-conditioning applications. *International Journal of Refrigeration*, 34(7):1545–1561, 2011.

[37] F. Liu and E.A. Groll. Study of ejector efficiencies in refrigeration cycles. *Applied Thermal Engineering*, 52(2):360–370, 2013.

[38] F. Liu, E. Groll, and D. Li. Investigation on performance of variable geometry ejectors for CO 2 refrigeration cycles. *Energy*, 45(1):829–839, 2012.

[39] Private person. Kristian Fredslund, refrigeration specialist, DANFOSS.

[40] BITZER Group. Bitzer compressors database. 2015. URL https://www.bitzer.de/websoftware/.

[41] National Institute of Standards U.S. department of Commerce and Technology. NIST Reference Fluid Thermodynamic and Transport Properties Database, REFPROP. URL http://www.nist.gov/srd/nist23.cfm.

[42] S. Girotto, S. Minetto, and M. Salvatore. Recent installations of CO2 supermarket refrigeration system for warm climates: data from the field. *Science et Technique du Froid*, 2014 (1):78–85, 2014.

[43] U.S. department of Energy. Energy Plus, Italian weather data, 2015. URL https://energyplus.net/weather-region/europe_wmo_region_6/ITA%20%20.

A Appendix A

This appendix collects the models used to perform the yearly analysis for every cycles. The models have been written using the equation solver EES [5]. Every model has been built following some simple steps. The code starts with a procedure that fix the condenser/gas cooler operation, this part is similar for all the cycles except for the equation that optimize the gas cooler pressure. In this procedure the minimum condensing temperature is set using an IF/THEN/ELSE cycle. Another one is used to fix the conditions when to pass from subcritical to transcritical operation. One more procedure have been used to set the load and the respective variation with the ambient temperature and the hour of the day. After this all the boundary conditions are set, except for the ambient temperature and the hour of the day that are the entrance data in the parametric table. The main part of the model is made by all the equations that fix the points and the features of the cycle. At the end the parameters that show the results are calculated. The complete model of the base CO_2 cycle is reported in the appendix. For the other systems only the main parts that differ from the first one are presented. It's important to say that in order to skip the secondary compressor in the parallel compression economization cycle a filter in the results has been used. In this way it was possible to make the code lighter and the compilation faster. The same procedure has been used for the normal ejector cycle and for the ejector cycle with two suction groups.

A.1 Base cycle

```
"CONDENSER/GAS COOLER"
PROCEDURE CONDENSER
"SUBCRITICAL OPERATION"
IF Tamb<7.05 THEN
tcond=10
pc=pressure(R$,t=tcond,x=0)
p[2]=pc
h_is[2]=enthalpy(R$,p=p[2],s=s[1])
"eta_is=((h_is[2]-h[1])/(h[2]-h[1]))"
```

```
h[2]=((h_is[2]-h[1])/eta_is)+h[1]
s[2]=entropy(R$,p=p[2],h=h[2])
t[2]=temperature(R$,p=p[2],h=h[2])
p[3]=p[2]
t[3]=temperature(R$,p=p[3],x=0)
h[3]=enthalpy(R$,p=p[3],x=0)
s[3]=entropy(R$,p=p[3],x=0)
tgc_out=0
ELSE
IF Tamb<25.15 THEN
tcond=tamb+3
pc=pressure(R$,t=tcond,x=0)
p[2]=pc
h_is[2]=enthalpy(R$,p=p[2],s=s[1])
h[2]=((h_is[2]-h[1])/eta_is)+h[1]
s[2]=entropy(R$,p=p[2],h=h[2])
t[2]=temperature(R$,p=p[2],h=h[2])
p[3]=p[2]
t[3]=temperature(R$,p=p[3],x=0)
h[3]=enthalpy(R$,p=p[3],x=0)
s[3]=entropy(R$,p=p[3],x=0)
tgc_out=0
ELSE
"TRANSCRITICAL OPERATION ("Tamb>25.15")"
tgc_out=tamb+3
pc=(2.778-0.0157*te)*tgc_out+(0.381*te-9.34)
p[2]=pc
h_is[2]=enthalpy(R$,p=p[2],s=s[1])
h[2]=((h_is[2]-h[1])/eta_is)+h[1]
t[2]=temperature(R$,p=p[2],h=h[2])
s[2]=entropy(R$,p=p[2],t=t[2])
p[3]=p[2]
t[3]=Tgc_out
h[3]=enthalpy(R$,p=p[3],t=t[3])
s[3]=entropy(R$,p=p[3],t=t[3])
tcond=0
ENDIF
ENDIF
END
"LOAD"
PROCEDURE LOAD
"LOAD IN FUNCTION OF AMBIENT TEMPERATURE"
```

```
IF Tamb>15 THEN
P_ev_real_d=(1/55)*tamb*P_ev+(5/22)*P_ev
P_ev_real_n=0.6*P_ev_real_d
ELSE
P_ev_real_d=0.5*P_ev
P_ev_real_n=0.6*P_ev_real_d
ENDIF
"DAY/NIGHT LOAD"
IF (h>7) AND (h<20) THEN
P_ev_real=P_ev_real_d
ELSE
P_ev_real=P_ev_real_n
ENDIF
END
"CYCLE MODELLING, MAIN PART"
R$='R744'
"BOUNDARY CONDITION"
te=-4
eta_is=1.003-0.121*(pc/pe)
SH=0.00001
P_ev=100 "@ 100% load"
CALL LOAD
"CYCLE ANALYSIS"
t[1]=te
pe=pressure(R$,t=t[1],x=1)
p[1]=pe
h[1]=enthalpy(R$,p=p[1],t=t[1]+SH)
s[1]=entropy(R$,p=p[1],t=t[1]+SH)
CALL CONDENSER
p[4]=p[1]
h[4]=h[3]
s[4]=entropy(R$,p=p[4],h=h[4])
t[4]=t[1]
x[4] = quality(R$,p=p[4],h=h[4])
Q_dot_ev=(h[1]-h[4])
Q_dot_gc=(h[3]-h[2])
W_dot_tot=(h[2]-h[1])
COP=((h[1]-h[4])/((h[2]-h[1])-0.03*(h[3]-h[2])))
COP_p=(h[1]-h[4])/(h[2]-h[1])
m_dot=P_ev_real/Q_dot_ev
P_comp=m_dot*W_dot_tot
P_vent=-0.03*m_dot*(h[3]-h[2])
```

A.2 Parallel compression economization

The equations used to optimize the gas cooler pressure and the economizer pressure are:
pc=2.54*tgc_out-4.25
peco=0.4615*tamb+35.3846

"CYCLE MODELLING, MAIN PART"
eta_is_main=1.003-0.121*(pc/pe)
eta_is_sec=1.003-0.121*(pc/peco)
t[1]=te
pe=pressure(R$,t=t[1],x=1)
p[1]=pe
h[1]=enthalpy(R$,p=p[1],t=t[1]+SH)
s[1]=entropy(R$,p=p[1],t=t[1]+SH)
CALL CONDENSER p[4]=peco
h[4]=h[3]
s[4]=entropy(R$,p=p[4],h=h[4])
teco=temperature(R$,p=p[4],h=h[4])
t[4]=teco
x[4] = quality(R$,p=p[4],h=h[4])
x[4]=y_flash
(1-x[4])=y_ev
p[5]=p[4]
t[5]=t[4]
h[5]=enthalpy(R$,p=p[5],x=0)
s[5]=entropy(R$,p=p[5],x=0)
p[6]=pe
h[6]=h[5]
x[6] = quality(R$,p=p[6],h=h[6])
s[6]=entropy(R$,p=p[6],h=h[6])
t[6]=te
p[7]=peco
t[7]=t[4]
h[7]=enthalpy(R$,p=p[7],t=t[7]+SH)
s[7]=entropy(R$,p=p[7],t=t[7]+SH)
v[7]=volume(R$,p=p[7],t=t[7]+SH)
p[8]=pc
h_is[8]=enthalpy(R$,p=p[8],s=s[7])
eta_is_sec=((h_is[8]-h[7])/(h[8]-h[7]))

t[8]=temperature(R$,p=p[8],h=h[8])
s[8]=entropy(R$,p=p[8],t=t[8])
y_flash*h[8]+y_ev*h[2]=h[9]
p[9]=pc
t[9]=temperature(R$,p=p[9],h=h[9])
s[9]=entropy(R$,p=p[9],h=h[9])
Q_dot_ev=y_ev*(h[1]-h[6])
Q_dot_gc=(h[3]-h[9])
W_dot_tot=y_ev*(h[2]-h[1])+y_flash*(h[8]-h[7])
COP=Q_dot_ev/(W_dot_tot-0.03*Q_dot_gc)
COP_p=P_ev_real/P_comp
m_dot_tot=P_ev_real/Q_dot_ev
P_comp=m_dot_tot*W_dot_tot
P_comp_main=m_dot_tot*y_ev*(h[2]-h[1])
P_comp_sec=m_dot_tot*y_flash*(h[8]-h[7])
m_vol=m_dot_tot*y_flash*v[7]
P_vent=-0.03*m_dot_tot*(h[3]-h[9])

A.3 Parallel compression economization with recooler

The equations used to optimize the gas cooler pressure and the subcooler pressure are:
psc=0.4615*tamb+35.3846
pc=2.58*tgc_out-5.71

"CYCLE MODELLING, MAIN PART"
eta_is_main=1.003-0.121*(pc/pe)
eta_is_sec=1.003-0.121*(pc/psc)
y=1
eta_sc=0.7
t[1]=te
pe=pressure(R$,t=t[1],x=1)
p[1]=pe
h[1]=enthalpy(R$,p=p[1],t=t[1]+SH)
s[1]=entropy(R$,p=p[1],t=t[1]+SH)
CALL CONDENSER
p[4]=psc
h[4]=h[3]
s[4]=entropy(R$,p=p[4],h=h[4])
tsc=temperature(R$,p=p[4],h=h[4])
t[4]=tsc

```
x[4] = quality(R$,p=p[4],h=h[4])
p[5]=psc
t[5]=t[4]
h[5]=enthalpy(R$,p=p[5],t=t[5]+SH)
s[5]=entropy(R$,p=p[5],t=t[5]+SH)
p[6]=pc
h_is[6]=enthalpy(R$,p=p[6],s=s[5])
eta_is_sec=((h_is[6]-h[5])/(h[6]-h[5]))
t[6]=temperature(R$,p=p[6],h=h[6])
s[6]=entropy(R$,p=p[6],t=t[6])
y=y_sc+y_ev
y_sc*h[6]+y_ev*h[2]=y*h[7]
p[7]=pc
t[7]=temperature(R$,p=p[7],h=h[7])
s[7]=entropy(R$,p=p[7],h=h[7])
eta_sc=(t[3]-t[8])/(t[3]-t[4])
p[8]=pc
h[8]=enthalpy(R$,p=p[8],t=t[8])
s[8]=entropy(R$,p=p[8],t=t[8])
p[9]=pe
h[9]=h[8]
x[9]=quality(R$,p=p[9],h=h[9])
s[9]=entropy(R$,p=p[9],h=h[9])
t[9]=te
Q_dot_sc=(h[3]-h[8])*y_ev
Q_dot_sc=(h[5]-h[4])*y_sc
Q_dot_ev=y_ev*(h[1]-h[9])
Q_dot_gc=y*(h[3]-h[7])
W_dot_tot=y_ev*(h[2]-h[1])+y_sc*(h[6]-h[5])
COP=Q_dot_ev/(W_dot_tot-0.03*Q_dot_gc)
m_dot_tot=P_ev_real/Q_dot_ev
P_comp=m_dot_tot*W_dot_tot
P_comp_main=m_dot_tot*y_ev*(h[2]-h[1])
P_comp_sec=m_dot_tot*y_sc*(h[6]-h[5])
P_vent=-0.03*m_dot_tot*Q_dot_gc
COP_p=P_ev_real/P_comp
```

A.4 Refrigeration cycle with mechanical subcooling

In this model two more procedures have been used: the first one is needed to define the secondary loop and the second one to calculate the results with or without the secondary loop.

The equation used to optimize the gas cooler pressure is:
pc=1.8666667*tgc_out+16.666667

```
"SECONDARY LOOP"
PROCEDURE SECLOOP
"assumption on t_cond"
tcond_sec=tamb+8
t[8]=tcond_sec
p[8]=pressure(R$,t=t[8],x=0)
h[8]=enthalpy(R$,p=p[8],x=0)
s[8]=entropy(R$,p=p[8],x=0)
"assumption on tev_sub"
tev_sec=t[4]-5
t[6]=tev_sec
p[6]=pressure(R$,t=t[6],x=1)
h[6]=enthalpy(R$,p=p[6],x=1)
s[6]=entropy(R$,p=p[6],x=1)
t[9]=t[6]
h[9]=h[8]
p[9]=p[6]
s[9]=entropy(R$,h=h[9],p=p[9])
x[9]=quality(R$,p=p[9],h=h[9])
"eta_is_sec=1.003-0.121*(p[8]/p[6])"
eta_is_sec=0.95-0.1*(p[8]/p[6])
p[7]=p[8]
h_is[7]=enthalpy(R$,p=p[7],s=s[6])
"eta_is=((h_is[7]-h[6])/(h[7]-h[6]))"
h[7]=((h_is[7]-h[6])/eta_is_sec)+h[6]
s[7]=entropy(R$,p=p[7],h=h[7])
t[7]=temperature(R$,p=p[7],h=h[7])
END

"RESULTS"
PROCEDURE RESULTS
IF Tamb<12.45 THEN
qev_main=h[1]-h[5]
```

```
qcond_main=h[3]-h[2]
DELTAh_sub=0
qev_sec=0
w_main=h[2]-h[1]
w_sec=0
y_m=0
y_p=0
COP_sec=0
COP=qev_main/(w_main-0.03*qcond_main)
m_dot_main=P_ev_real/qev_main
m_dot_sec=0
P_comp_main=m_dot_main*w_main
P_comp_sec=0
P_vent=-0.03*m_dot_main*qcond_main
COP_p=(P_ev_real/(P_comp_main+P_comp_sec))
ELSE "tamb>12.45"
qev_main=h[1]-h[5]
qcond_main=h[3]-h[2]
DELTAh_sub=h[3]-h[4]
qev_sec=h[6]-h[9]
w_main=h[2]-h[1]
w_sec=h[7]-h[6]
y_m=DELTAh_sub/qev_sec
y_p=y_m*w_sec/w_main
m_dot_main=P_ev_real/qev_main
m_dot_sec=m_dot_main*y_m
COP_sec=qev_sec/w_sec
P_comp_sec=m_dot_sec*w_sec
P_comp_main=m_dot_main*w_main
P_vent=-0.03*m_dot_main*qcond_main
COP=qev_main/(w_main+(DELTAh_sub/COP_sec)-(0.03*qcond_main))
COP_p=(P_ev_real/(P_comp_main+P_comp_sec))
ENDIF
END

"CYCLE MODELLING, MAIN PART"
"R$='R404a'"
R$='propane'
"R$='R134a'"
eta_is_main=1.003-0.121*(pc/pe)
CALL LOAD
SUB_max=10
```

```
SUB=0.025*tamb*SUB_max-(1/16)*SUB_max
t[1]=te
pe=pressure(R744,t=t[1],x=1)
p[1]=pe
h[1]=enthalpy(R744,p=p[1],t=t[1]+SH)
s[1]=entropy(R744,p=p[1],t=t[1]+SH)
CALL CONDENSER
p[5]=p[1]
t[5]=t[1]
h[5]=h[4]
s[5]=entropy(R744,p=p[5],h=h[5])
x[5]=quality(R744,p=p[5],h=h[5])
CALL RESULTS
```

A.5 Cascade system

The cascade system model is a bit different from the other ones since there are no supercritical working condition. The model start with two procedures that are used to fix the condensation temperature of the the secondary cycle and the CO_2 cycle.

```
PROCEDURE TCONDSEC
IF tamb>7 THEN
t_cond_sec=tamb+8
ELSE
t_cond_sec=15
ENDIF
END

PROCEDURE TCONDCO2
IF tamb>7 THEN
p_cond_co2=0.0691*Tamb+44.864propane
"p_cond_co2=0.1011*Tamb+44.954 R404a"
"p_cond_co2=0.0665*Tamb+44.832 R134a"
t_cond_co2=temperature(R744,p=p_cond_co2,x=0)
ELSE
t_cond_co2=10
p_cond_co2=pressure(R744,t=t_cond_co2,x=0)
ENDIF
END

"CYCLE MODELLING, MAIN PART"
```

```
eta_is_main=1.003-0.121*(p_cond_co2/pe)
eta_is_sec=0.95-0.1*(p_cond_sec/p_ev_sec)
t[1]=te
pe=pressure(R744,t=t[1],x=1)
p[1]=pe
h[1]=enthalpy(R744,p=p[1],t=t[1]+SH)
s[1]=entropy(R744,p=p[1],t=t[1]+SH)
CALL LOAD
R$='propane'
"R$='R404a'"
"R$='R134a'"
CALL TCONDCO2
p[2]=p_cond_co2
h_is[2]=enthalpy(R744,p=p[2],s=s[1])
h[2]=((h_is[2]-h[1])/eta_is_main)+h[1]
t[2]=temperature(R744,p=p[2],h=h[2])
s[2]=entropy(R744,p=p[2],t=t[2])
p[3]=p[2]
t[3]=temperature(R744,p=p[3],x=0)
h[3]=enthalpy(R744,p=p[3],x=0)
s[3]=entropy(R744,p=p[3],x=0)
p[4]=p[1]
t[4]=t[1]
h[4]=h[3]
s[4]=entropy(R744,p=p[4],h=h[4])
x[4]=quality(R744,p=p[4],h=h[4])
CALL TCONDSEC
t[8]=t_cond_sec
p[8]=pressure(R$,t=t[8],x=0)
h[8]=enthalpy(R$,p=p[8],x=0)
s[8]=entropy(R$,p=p[8],x=0)
p[8]=p_cond_sec
"assumption on tev_sub"
t_ev_sec=t_cond_co2-5
t[6]=t_ev_sec
p[6]=pressure(R$,t=t[6],x=1)
h[6]=enthalpy(R$,p=p[6],t=t[6]+SH)
s[6]=entropy(R$,p=p[6],t=t[6]+SH)
p_ev_sec=p[6]
t[9]=t[6]
h[9]=h[8]
p[9]=p[6]
```

```
s[9]=entropy(R$,h=h[9],p=p[9])
x[9]=quality(R$,p=p[9],h=h[9])
p[7]=p[8]
h_is[7]=enthalpy(R$,p=p[7],s=s[6])
"eta_is=((h_is[7]-h[6])/(h[7]-h[6]))"
h[7]=((h_is[7]-h[6])/eta_is_sec)+h[6]
s[7]=entropy(R$,p=p[7],h=h[7])
t[7]=temperature(R$,p=p[7],h=h[7])
q_ev_main=h[1]-h[4]
q_cond_main=h[2]-h[3]
q_ev_sec=h[6]-h[9]
q_cond_sec=h[7]-h[8]
w_main=h[2]-h[1]
w_sec=h[7]-h[6]
y_m=q_cond_main/q_ev_sec
y_p=y_m*w_sec/w_main
m_dot_main=P_ev_real/q_ev_main
m_dot_sec=m_dot_main*y_m
P_comp_sec=m_dot_sec*w_sec
P_comp_main=m_dot_main*w_main
P_vent=0.03*m_dot_sec*q_cond_sec
COP_sec=q_ev_sec/w_sec
COP_p=(P_ev_real/(P_comp_main+P_comp_sec))
COP=q_ev_main/(w_main+(q_cond_main/COP_sec)+(y_m*0.03*q_cond_sec))
```

A.6 Ejector expansion refrigeration cycle

In this model the equation used to optimize the gas cooler pressure is the same reported in the base CO_2 cycle since the optimal pressure is almost the same. In order to describe the behaviour of the ejector a constant pressure model has been used.

```
pe=pressure(CarbonDioxide,t=te,x=1)
eta_is=1.003-0.121*(pc/p[7])
CALL LOAD
CALL CONDENSER

"EJECTOR MODEL"
eta_m=0.8
eta_s=0.8
eta_d=0.75
"DELTAp is the difference between the evaporator pressure and the prssure at the oytlet of the
```

```
nozzle and suction chamber"
p_is[2]=p[3]-DELTAp
DELTAp=0.3e5
"MOTIVE NOZZLE"
s_is[2]=s[1]
h_is[2]=enthalpy(CarbonDioxide,p=p_is[2],s=s_is[2])
t_is[2]=temperature(CarbonDioxide,p=p_is[2],h=h_is[2])
eta_m=(h[2]-h[1])/(h_is[2]-h[1])
p[2]=p_is[2]
s[2]=entropy(CarbonDioxide,p=p[2],h=h[2])
t[2]=temperature(CarbonDioxide,p=p[2],h=h[2])
v[2]=volume(CarbonDioxide,p=p[2],h=h[2])
u[2]=sqrt(2*(h[1]-h[2]))
"SUCTION NOZZLE"
p[3]=pe
t[3]=te
h[3]=enthalpy(CarbonDioxide,p=p[3],x=1)
s[3]=entropy(CarbonDioxide,p=p[3],x=1)
p_is[4]=p_is[2]
s_is[4]=s[3]
h_is[4]=enthalpy(CarbonDioxide,p=p_is[4],s=s_is[4])
t_is[4]=temperature(CarbonDioxide,p=p_is[4],h=h_is[4])
eta_s=(h[4]-h[3])/(h_is[4]-h[3])
p[4]=p_is[4]
s[4]=entropy(CarbonDioxide,p=p[4],h=h[4])
v[4]=volume(CarbonDioxide,p=p[4],h=h[4])
u[4]=sqrt(2*(h[3]-h[4]))
"MIXING SECTION"
p[5]=p_is[2]
u[5]=u[2]*(1/(1+r))+u[4]*(r/(1+r))
(h[1]+r*h[3])=(1+r)*(h[5]+0.5*((u[5])^2))
v[5]=volume(CarbonDioxide,p=p[5],h=h[5])
s[5]=entropy(CarbonDioxide,p=p[5],h=h[5])
"DIFFUSER"
s_is[6]=s[5]
h[6]=(h[1]+r*h[3])/(1+r)
h_is[6]=eta_d*(h[6]-h[5])+h[5]
p[6]=pressure(CarbonDioxide,h=h_is[6],s=s_is[6])
s[6]=entropy(CarbonDioxide,p=p[6],h=h[6])
x[6]=quality(CarbonDioxide,p=p[6],h=h[6])
(1+r)*x[6]=1
```

```
"SEPARATOR"
p[7]=p[6]
h[7]=enthalpy(CarbonDioxide,p=p[6],x=1)
t[7]=temperature(CarbonDioxide,p=p[6],x=1)
s[7]=entropy(CarbonDioxide,p=p[6],t=t[7]+SH)
p[9]=p[6]
h[9]=enthalpy(CarbonDioxide,p=p[6],x=0)
s[9]=entropy(CarbonDioxide,p=p[9],x=0)
p[8]=pc
h_is[8]=enthalpy(CarbonDioxide,p=p[8],s=s[7])
eta_is=((h_is[8]-h[7])/(h[8]-h[7]))
t[8]=temperature(CarbonDioxide,p=p[8],h=h[8])
s[8]=entropy(CarbonDioxide,p=p[8],t=t[8])
p[10]=pe
h[10]=h[9]
s[10]=entropy(CarbonDioxide,p=p[10],h=h[10])
x[10]=quality(CarbonDioxide,p=p[10],h=h[10])
Q_dot_ev=(r/(1+r))*(h[3]-h[10])
Q_dot_gc=(1/(1+r))*(h[1]-h[8])
W_dot_tot=(1/(1+r))*(h[8]-h[7])
p_lift=p[6]-p[3]
h_p6s3=enthalpy(CarbonDioxide,p=p[6],s=s[3])
h_p6s1=enthalpy(CarbonDioxide,p=p[6],s=s[1])
eta_ej_teor=((r/(1+r))*(h_p6s3-h[3]))/((1/(1+r))*(h[1]-h_p6s1))
COP=Q_dot_ev/(W_dot_tot-0.03*Q_dot_gc)
m_dot_tot=P_ev_real/Q_dot_ev
P_comp=m_dot_tot*W_dot_tot
P_vent=-0.03*m_dot_tot*Q_dot_gc
COP_p=P_ev_real/P_comp
```

A.7 Ejector expansion refrigeration cycle with two suction groups

For this system one more procedure is needed compared with the normal ejector cycle in order to optimize the factor 'phi', the factor that describe how much of the evaporator outlet flow enters the ejector and how much skips it. The equations of the ejector are not reported since are the same of the previous cycle.

```
"BY-PASS"
PROCEDURE BP
IF tamb<7.3 THEN
phi=0.89
```

```
ELSE
IF tamb<12 THEN
phi=-0.02813*tamb+1.0925
ELSE
IF tamb<16.6 THEN
phi=-0.03913*tamb+1.224565
ELSE
IF tamb<25 THEN
phi=0.003333*tamb+0.51667
ELSE "tamb>25"
phi=-0.02571*tamb+1.242857
ENDIF
ENDIF
ENDIF
ENDIF
END

eta_is_c=1.003-0.121*(pc/p[7])
eta_is_bp=1.003-0.121*(pc/pe)
CALL LOAD
CALL CONDENSER
CALL BP

"SEPARATOR"
x[6]=1-r/((1+r)*(1-phi))
p[7]=p[6]
h[7]=enthalpy(CarbonDioxide,p=p[6],x=1)
t[7]=temperature(CarbonDioxide,p=p[6],x=1)
s[7]=entropy(CarbonDioxide,p=p[6],x=1)
v[7]=volume(CarbonDioxide,p=p[6],x=1)
p[9]=p[6]
h[9]=enthalpy(CarbonDioxide,p=p[6],x=0)
s[9]=entropy(CarbonDioxide,p=p[9],x=0)
p[8]=pc
h_is[8]=enthalpy(CarbonDioxide,p=p[8],s=s[7])
eta_is_c=((h_is[8]-h[7])/(h[8]-h[7]))
t[8]=temperature(CarbonDioxide,p=p[8],h=h[8])
s[8]=entropy(CarbonDioxide,p=p[8],t=t[8])
p[10]=pe
h[10]=h[9]
s[10]=entropy(CarbonDioxide,p=p[10],h=h[10])
x[10]=quality(CarbonDioxide,p=p[10],h=h[10])
```

"gas-cooler inlet"
(1-r/((1+r)*(1-phi)))*h[8]+(r*phi/((1+r)*(1-phi)))*h[13]=(1/(1+r))*h[14]
p[14]=pc
t[14]=temperature(CarbonDioxide,p=p[14],h=h[14])
s[14]=entropy(CarbonDioxide,p=p[14],h=h[14])
"evaporator outlet"
p[11]=pe
t[11]=te
h[11]=enthalpy(CarbonDioxide,p=p[11],x=1)
s[11]=entropy(CarbonDioxide,p=p[11],x=1)
p[12]=p[11]
s[12]=entropy(CarbonDioxide,p=p[12],x=1)
h[12]=h[11]
v[12]=volume(CarbonDioxide,p=p[12],x=1)
"secondary compressor"
p[13]=pc
h_is[13]=enthalpy(CarbonDioxide,p=p[13],s=s[12])
eta_is_bp=((h_is[13]-h[12])/(h[13]-h[12]))
t[13]=temperature(CarbonDioxide,p=p[13],h=h[13])
s[13]=entropy(CarbonDioxide,p=p[13],t=t[13])

Q_dot_ev=(r/((1+r)*(1-phi)))*(h[3]-h[10])
Q_dot_gc=(1/(1+r))*(h[1]-h[14])
W_dot_c=(1-(r/((1+r)*(1-phi))))*(h[8]-h[7])
W_dot_bp=((phi*r)/((1+r)*(1-phi)))*(h[13]-h[12])
W_dot_tot=W_dot_c+W_dot_bp
m_vol_bp=((phi*r)/((1+r)*(1-phi)))*m_dot_tot*v[12]
m_vol_sep=(1-(r/((1+r)*(1-phi))))*m_dot_tot*v[7]
p_lift=p[6]-p[3]
h_p6s3=enthalpy(CarbonDioxide,p=p[6],s=s[3])
h_p6s1=enthalpy(CarbonDioxide,p=p[6],s=s[1])
eta_ej_teor=((r/(1+r))*(h_p6s3-h[3]))/((1/(1+r))*(h[1]-h_p6s1))
COP=Q_dot_ev/(W_dot_tot-0.03*Q_dot_gc)
m_dot_tot=P_ev_real/Q_dot_ev
P_comp_c=m_dot_tot*W_dot_c
P_comp_bp=m_dot_tot*W_dot_bp
P_comp=m_dot_tot*W_dot_tot
P_vent=-0.03*m_dot_tot*Q_dot_gc
COP_p=P_ev_real/P_comp

B Appendix B

This appendix collects some schemes of the solutions studied during the project. The figures present the diagram of the systems with all the most important variables. It has been chosen to report two different working condition for each cycle: the first one shows the system working in subcritical mode, while the second one shows the system during transcritical operation. The purpose is to show how the variables of the cycle change passing from a low ambient temperature to a very high ambient temperature, 40°C. For the base cycle [B.1], the mechanical subcooling [B.3] and the cascade system [B.4] the low ambient temperature has been fixed to 5°C, while for the parallel compression economization cycle [B.2] and the ejector cycle with two suction groups [B.5] has been fixed to 15°C. This choice has been made because of the secondary compressor problem that imposes to skip the parallel compression under a certain ambient temperature (see chapter 4). The PCE cycle with recooler and the normal ejector cycle have not been reported.

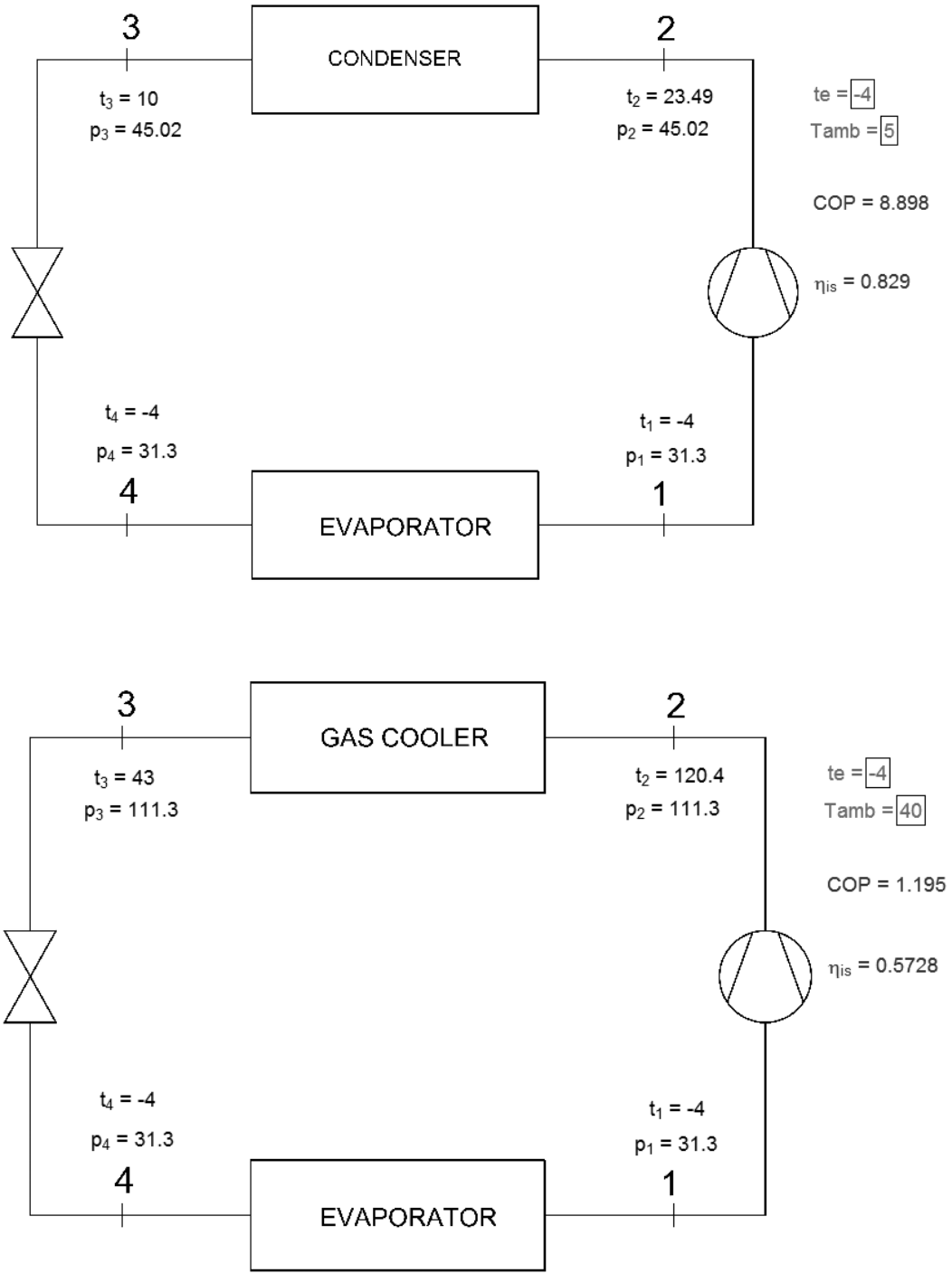

Figure B.1 – Base cycle: variables comparison (temperatures in °C, pressures in bar).

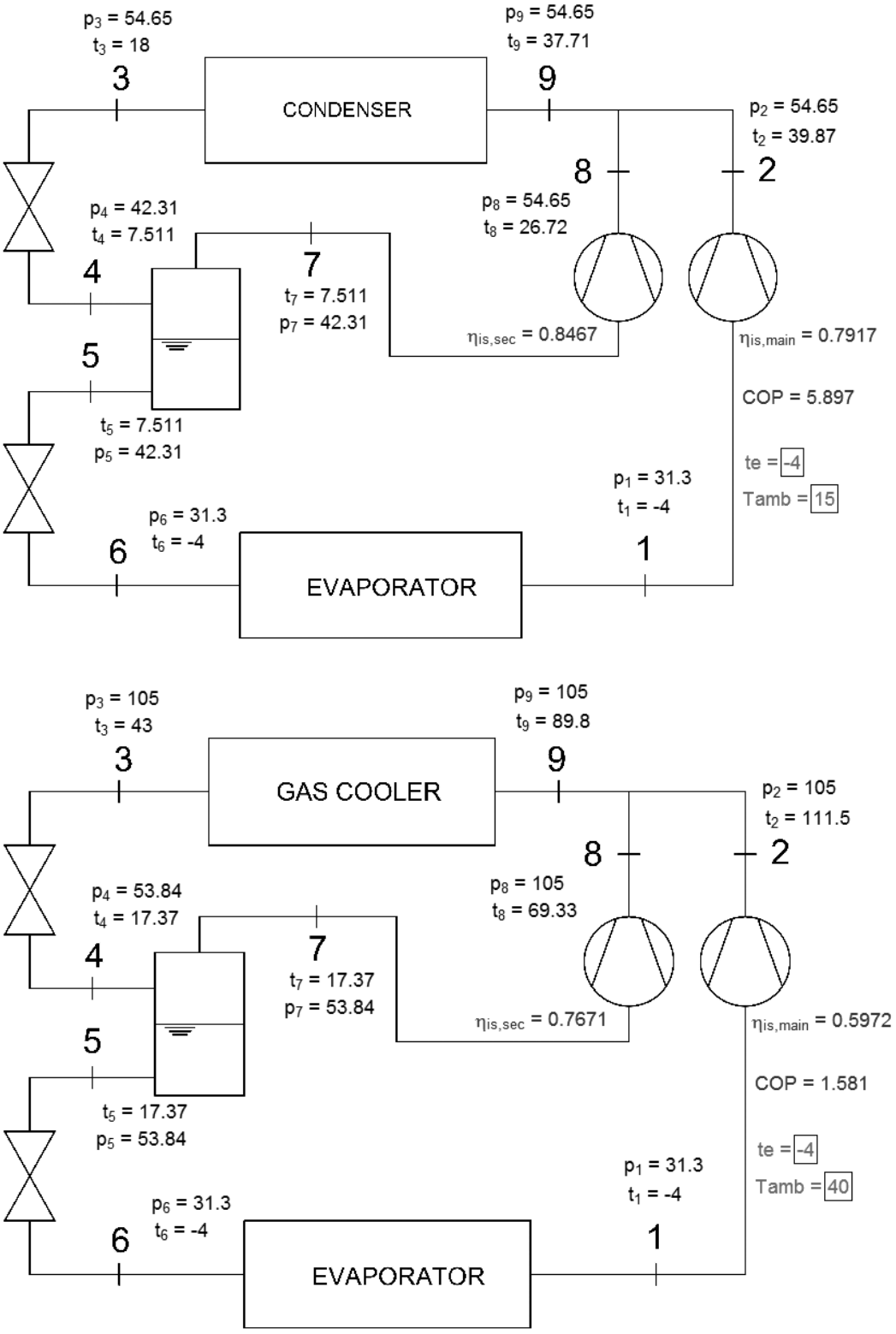

Figure B.2 – PCE: variables comparison (temperatures in °C, pressures in bar).

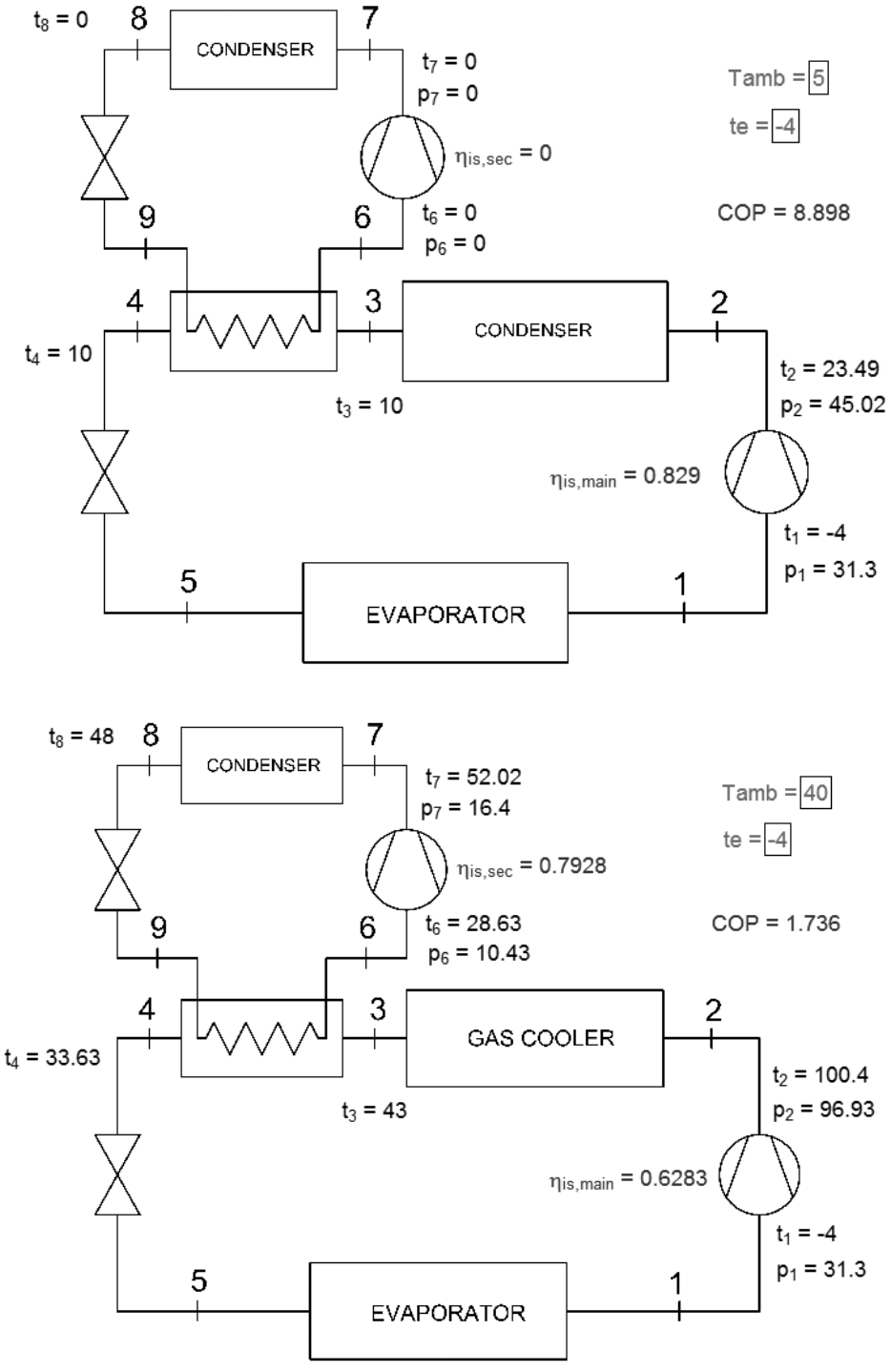

Figure B.3 – MS: variables comparison (temperatures in °C, pressures in bar).

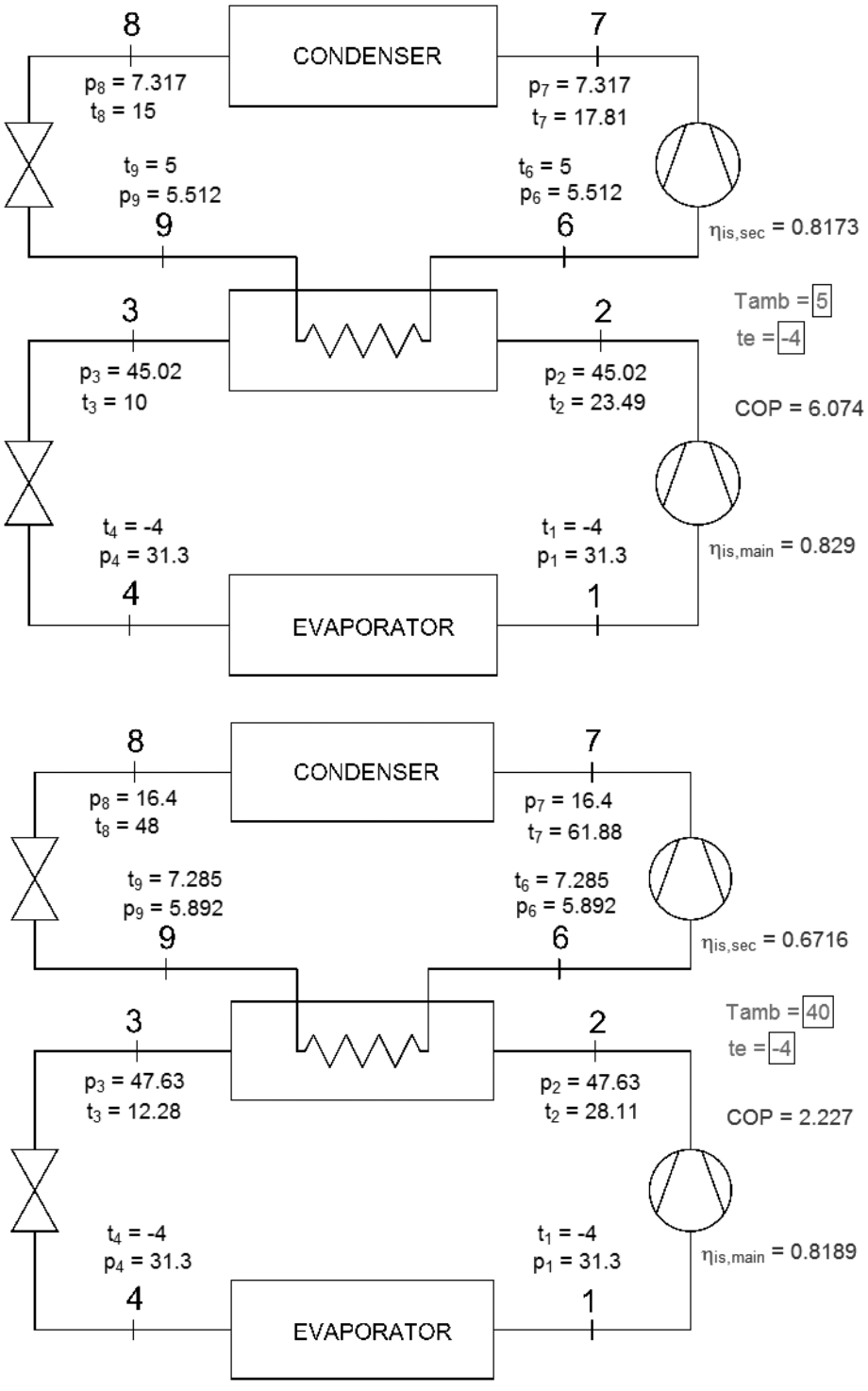

Figure B.4 – Cascade system: variables comparison (temperatures in °C, pressures in bar).

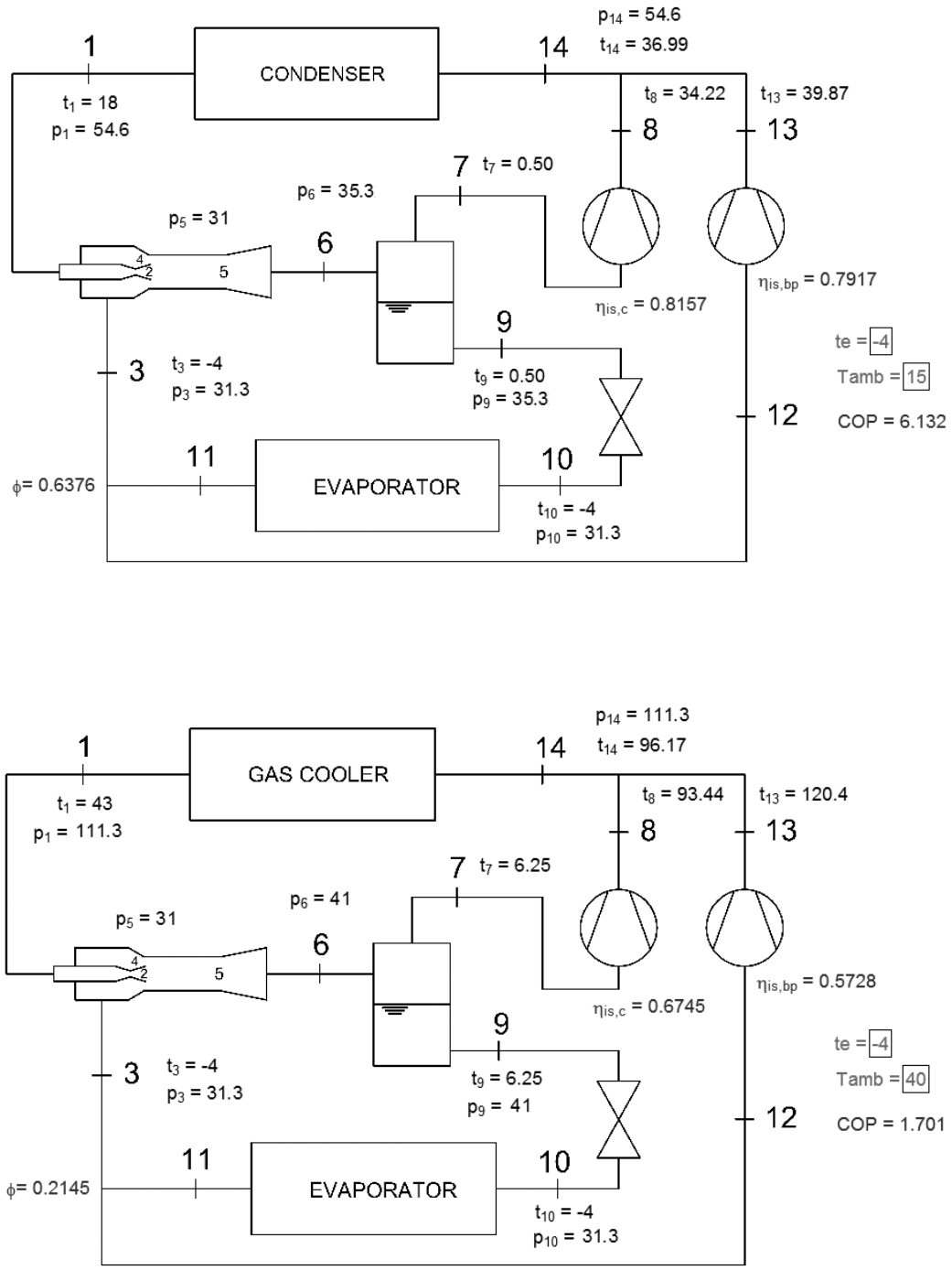

Figure B.5 – Ejector cycle with two suction groups: variables comparison (temperatures in °C, pressures in bar).